

NOT FOR QUOTATION
WITHOUT PERMISSION
OF THE AUTHOR

MODELING WIND-DRIVEN CIRCULATION
IN LAKE BALATON

Peter Shanahan
Donald R.F. Harleman
László Somlyódy

March 1981
CP-81-7

Collaborative Papers report work which has not been performed solely at the International Institute for Applied Systems Analysis and which has received only limited review. Views or opinions expressed herein do not necessarily represent those of the Institute, its National Member Organizations, or other organizations supporting the work.

INTERNATIONAL INSTITUTE FOR APPLIED SYSTEMS ANALYSIS
A-2361 Laxenburg, Austria

AUTHORS

Peter Shanahan is a graduate research assistant at the Ralph M. Parsons Laboratory for Water Resources and Hydrodynamics, Department of Civil Engineering, Massachusetts Institute of Technology.

Donald R.F. Harleman is a Ford professor of Engineering and Director at the Ralph M. Parsons Laboratory for Water Resources and Hydrodynamics, Department of Civil Engineering, Massachusetts Institute of Technology.

László Somlyódy is a research scholar and the leader of Lake Balaton Case Study at the International Institute for Applied Systems Analysis, Laxenburg (he is a scientific adviser and is on leave from the Research Center for Water Resources Development (VITUKI), Budapest, Hungary).

PREFACE

One of the principal themes of the Task on Environmental Quality Control and Management in IIASA's Resources and Environment Area is a case study of eutrophication management for Lake Balaton, Hungary. The case study is a collaborative project involving a number of scientists from several Hungarian institutions and IIASA (for details see WP-80-187).

As part of the case study three different biochemical models of the lake's behavior are under development (results for two of these models have already been described in earlier working papers WP-80-139 and WP-80-149). All of these approaches describe the role of spatial mass exchange resulting from wind-induced water motion in a very simplified manner. This paper presents the development of a transient, three-dimensional hydrodynamic model and its application to Lake Balaton. Another paper (to appear) illustrates the application of a much simpler one-dimensional model which has been developed jointly and in parallel with the present approach. It is believed that as a result of these efforts a better balance will be achieved between the relative complexities of the biochemical and hydrophysical modeling studies as components in the development of an overall lake ecological model. This balance should reflect also the relative importance of the different subprocesses being modeled.



Table of Contents

1	ABSTRACT.....	1-1
2	INTRODUCTION.....	2-1
	2.1 Background of the Study.....	2-1
	2.2 Introduction to the Report.....	2-3
	2.3 Summary of the Report.....	2-5
3	OVERVIEW OF LAKE CIRCULATION MODELS.....	3-1
	3.1 Mathematical Formulation of Lake Circulation..	3-1
	3.2 Modeling Strategies.....	3-8
	3.2.1 Single Layer Models.....	3-8
	3.2.2 Multi-layer Models.....	3-8
	3.2.3 Ekman-type Models.....	3-9
4	MAJOR MODEL ASSUMPTIONS.....	4-1
	4.1 Vertical Variability.....	4-1
	4.2 Convective Accelerations.....	4-2
	4.3 Free Surface Effects.....	4-3
	4.4 Horizontal Shear Effects.....	4-5
5	MODEL PARAMETERS.....	5-1
	5.1 Vertical Eddy Viscosity.....	5-1
	5.1.1 Published Formulae.....	5-1
	5.1.2 Comparison with Observations.....	5-4
	5.2 Wind Stress on the Water Surface.....	5-6
	5.3 Bottom Friction.....	5-9
6	LAKE BALATON: MODELING BACKGROUND.....	6-1
	6.1 General Characteristics of Lake Balaton.....	6-1
	6.2 Circulation in Lake Balaton.....	6-3
	6.2.1 Hydrologic Flow.....	6-3
	6.2.2 Wind-Driven Flows.....	6-3
	6.2.3 Seiches.....	6-5

7	A MODEL OF WIND-DRIVEN CIRCULATION IN SHALLOW LAKES.....	7-1
7.1	Brief Description of the Model.....	7-1
7.2	Galerkin Model Formulation.....	7-2
7.2.1	Governing Equations.....	7-2
7.2.2	Galerkin Formulation.....	7-3
7.3	Modeling Considerations.....	7-6
7.3.1	Coupled Circulation and Water Quality Models.....	7-6
7.3.2	Circulation Model Applicability.....	7-10
7.3.3	Conclusions.....	7-12
8	MODEL APPLICATION TO LAKE BALATON.....	8-1
8.1	Model Input Data.....	8-1
8.2	Parameter Sensitivity Studies.....	8-3
8.2.1	General Description.....	8-3
8.2.2	Study Results.....	8-5
8.2.3	Conclusions.....	8-8
8.3	Grid and Wind Field Sensitivity.....	8-15
8.3.1	Wind Effects.....	8-15
8.3.2	Grid Size Effects.....	8-17
8.4	Simulation of Historical Events.....	8-25
8.4.1	Event of July 4 and 5, 1961.....	8-25
8.4.2	Event of July 8 and 9, 1963.....	8-26
8.4.3	Event of October 5, 1963.....	8-26
8.5	Analysis and Conclusions.....	8-33
8.5.1	Conclusions.....	8-33
8.5.2	Analysis of an Event Simulation.....	8-34
9	CONCLUSION.....	9-1
9.1	Summary of Findings.....	9-1
9.2	Utility of the Galerkin Model for Lake Balaton.....	9-2
9.3	Extending the Capability to Model Lake Balaton's Water Quality.....	9-4
9.4	Recommendations for Further Research.....	9-9

APPENDICES

A FIELD STUDIES OF LAKE BALATON CURRENTS.....A-1
A.1 Introduction.....A-1
A.2 Measurement Results.....A-2
A.3 Conclusions.....A-4

B A GALERKIN MODEL OF WIND-DRIVEN CIRCULATIONB-1
B.1 Formulation of the Galerkin Equations.....B-1
B.2 Derivation of Nelson's Model.....B-3
B.3 Solution of the Equations.....B-8
B.3.1 Finite Difference Solution Scheme.....B-8
B.3.2 Stability Criteria.....B-10
B.3.3 Modification of the Solution
Procedure.....B-11

REFERENCES

List of Tables

3.1 Published single-layer circulation models.....3-10
3.2 Published multi-layer circulation models.....3-11
3.3 Published Ekman-type circulation models.....3-12

5.1 Wind stress drag coefficients.....5-7

7.1 Volume transports between the Balaton basins.....7-9
7.2 Physical parameters for Lake Balaton.....7-11

8.1 Estimates of vertical eddy viscosity
 in Lake Balaton.....8-4
8.2 Summary of sensitivity run results.....8-14

A.1 Collected current data.....A-12



List of Figures

3.1	Definition sketch for mathematical formulation....	3-3
3.2	Non-dimensional form of the governing equations...	3-6
5.1	Representations of the vertical eddy viscosity....	5-2
5.2	Surface drag coefficients as a function of wind speed.....	5-8
6.1	Map of Lake Balaton.....	6-2
6.2	Comparison of observed daily average wind speeds at Keszthely, Siofok and Balatonszemes...	6-4
6.3	Circulation from physical hydraulic model.....	6-6
6.4	Theoretical wind-induced velocity profile.....	6-6
6.5	Typical water surface elevation records showing seiche motions.....	6-8
6.6	Example of Muszkalay's seiche observations.....	6-9
7.1	Piecewise-linear form of the vertical eddy viscosity.....	7-4
7.2	Finite difference solution procedure.....	7-5
7.3	Approximate length and time scales in Lake Balaton.....	7-7
8.1	Coarse finite difference grid for Lake Balaton....	8-2
8.2	Fine finite difference grid for Lake Balaton.....	8-2
8.3	Eddy viscosity functions used in the simulations..	8-7
8.4	Sensitivity of seiche to constant eddy viscosity..	8-10
8.5	Sensitivity of seiche to bottom friction coefficient with constant eddy viscosity.....	8-10
8.6	Sensitivity of seiche to bi-linear eddy viscosity.....	8-11
8.7	Sensitivity of seiche to bottom friction coefficient with bi-linear eddy viscosity.....	8-11
8.8	Sensitivity of seiche to bi-linear eddy viscosity inflection point.....	8-12
8.9	Sensitivity of seiche to various eddy viscosity forms.....	8-12
8.10	Summary of sensitivity simulation results.....	8-13
8.11	Effect of wind shear formula on seiche simulation.....	8-19
8.12	Effect of wind direction on seiche simulation.....	8-19
8.13	Hypothetical spatially varying wind field.....	8-20
8.14	Effect of wind field variation on seiche simulation.....	8-20
8.15	Steady state horizontal circulation under uniform wind field.....	8-21
8.16	Steady state horizontal circulation under spatially varying wind field.....	8-22
8.17	Steady state depth average circulation under spatially varying wind field.....	8-23

8.18	Steady state vertical velocity profiles at Szemes basin mid-point.....	8-23
8.19	Effect of grid size on seiche simulation.....	8-23
8.20	Steady state horizontal circulation with fine grid under uniform wind field.....	8-24
8.21	Observation data for event of July 4 and 5, 1981.....	8-28
8.22	Comparison of simulation results and observations for event of July 4 and 5, 1961.....	8-28
8.23	Observation data for event of July 8 and 9, 1963.....	8-29
8.24	Comparison of simulation results and observations for event of July 8 and 9, 1963.....	8-30
8.25	Observation data for event of October 5, 1963.....	8-31
8.26	Comparison of simulation results and observations for event of October 5, 1963.....	8-32
8.27	Correspondence of the Lake Balaton basins with the circulation model finite difference grid.....	8-34
8.28	Net transport fluxes between the Lake Balaton basins, Simulation of July 8, 1963.....	8-37
8.29	Lateral variation and vertical structure of longitudinal velocity from the Keszthely to Szigliget basin, Simulation of July 8, 1963.....	8-38
8.30	Lateral variation and vertical structure of longitudinal velocity from the Szigliget to Szemes basin, Simulation of July 8, 1963.....	8-39
8.31	Vertical profile of longitudinal velocity from the Szemes to Siofok basin, Simulation of July 8, 1963.....	8-40
8.32	Longitudinal variation and vertical structure of transverse velocity within the Szemes basin, Simulation of July 8, 1963.....	8-41
9.1	Water quality models possible for Lake Balaton....	9-4
A.1	Approximate location of measuring stations.....	A-1
A.2	Current measurements at Station 1, 11 July 1980...	A-5
A.3	Current measurements at Station 2, 11 July 1980...	A-5
A.4	Current measurements at Station 3, 11 July 1980...	A-6
A.5	Current measurements at Station 4, 11 July 1980...	A-6
A.6	Current measurements at Station 1, 11 August 1980.....	A-7
A.7	Current measurements at Station 3, 11 August 1980.....	A-8
A.8	Continuous measurements at Station 1, 11 August 1980.....	A-9
A.9	Temporal statistics of continuous measurements at Station 1, 11 August 1980.....	A-9
A.10	Current measurements at Station 3, 12 August 1980.....	A-10
A.11	Current measurements at Station 5, 15 August 1980.....	A-11
A.12	Current measurements at Station 5, 15 August 1980.....	A-11

1 ABSTRACT

This paper reports the results achieved to date in a program of research to develop and apply mathematical computer models of water quality in shallow lakes. The portion of the research which is the specific topic of this paper is the development, testing and trial application of a transient three-dimensional model of wind-driven circulation. The results are presented in the context of an application to Lake Balaton in Hungary, a large yet very shallow lake.

The paper presents a review of the mathematical formulation of the circulation problem and the major methods used in computer models of wind-driven circulation. Detailed examinations of the model assumptions and parameters are also included. A description of the application lake follows and a three-dimensional model appropriate to shallow lakes is proposed and derived. This model is examined for consistency with Lake Balaton's characteristics, and the important need for congruence with an eventual coupled biogeochemical model of the water quality is described and investigated. The requirement that the length and time scales of the hydrodynamic model and the biogeochemical model be consistent with each other and with the processes of interest in the lake is stressed.

The proposed circulation model employs a Galerkin technique to compute the vertical velocity profile using a depth-dependent vertical eddy viscosity. The parameters for this model are determined by calibration using simple hypothetical seiche simulations as a standard. It is found that the function specified for the vertical eddy viscosity is a crucial determinant of the model response. The resulting model and calibration are then successfully verified with historical events on Lake Balaton. A detailed examination of the results of one of these event simulations explores aspects of the model predictions pertinent to the mass transport of water quality constituents. Conclusions of the paper include identification of the need to improve the representation of mass transport in existing models of Balaton's water quality and an agenda for future development of a coupled hydrodynamic-biogeochemical water quality model.



2 INTRODUCTION

2.1 Background of the Study

The deterioration of lake water quality is being faced throughout the world. Increasing population and development, and changing agricultural practices have created pressures from which few water bodies escape. And, although society can take steps to prevent or correct water quality degradation, such actions are invariably costly and prior knowledge of their effectiveness is often impossible. The people and agencies charged with planning water quality control thus face a very difficult set of problems indeed. Not only must they develop methods and strategies to control water pollution, but they must also forecast the cost and effectiveness of these strategies to guarantee that the controls used insure the best water quality at the least expense.

Mathematical computer models of water quality have arisen in response to the needs of water pollution control planning. Clearly, society cannot afford to test expensive control strategies by trial and error; a less costly means to develop and evaluate control alternatives is required. Water quality models contribute in two ways. First, by describing the physical, biological and chemical processes affecting water quality, models increase understanding and suggest control methods. And secondly, predictive models can forecast future water quality and permit trials of possible strategies at very reasonable expense. Accurate and efficient water quality models can thus play a valuable role in the management of environmental water quality.

This paper is a report from a program of research to develop and apply mathematical computer models of water quality in a particular, important environment: the shallow fresh water lake. Although shallow lakes as large as the application lake in this report, Lake Balaton in Hungary, are rare, small shallow lakes and ponds are perhaps the most common of water bodies. Relatively little attention has been paid in the past to the special problems of modeling such environments and even less attention has been directed to the particular interest of our research: the influence of hydrodynamics upon shallow lake water quality, and the proper linkage of hydrodynamic transport models with biogeochemical water quality models.

Our attention to the linkage of hydrodynamic models and biogeochemical water quality models addresses a weakness in current water quality modeling practice. This weakness arises when the modeler fails to consider the dominant length and time scales of the lake processes of interest. The complete water quality model must match these dominant scales in its representation of both hydrodynamics and biological dynamics. This is seldom done in practice. As a result, one finds highly sophisticated models of lake water quality chemistry and biology compromised by inadequate, or even inaccurate, models of water motion and mass transport. Similarly, there are models which attempt to determine hydrodynamics and mass transport with high accuracy, but then simply lump all biochemical transformations into a single first-order loss term. In this report, and in our continuing research, we seek to demonstrate the necessity to consider both hydrodynamics and biochemistry in a compatible and even-handed fashion. Our hypothesis is that the proper linkage of hydrodynamic and biogeochemical models will create a more accurate and complete picture of lake water quality dynamics.

2.2 Introduction to the Report

This paper reports the results achieved in the first part of a program of research to develop and apply mathematical computer models of eutrophication in shallow lakes. This first portion of the research concerns the modeling of lake circulation and, particularly, the application of a three-dimensional model of wind-driven circulation to Lake Balaton in Hungary.

The purposes of the report are:

to survey the published literature on lake circulation modeling, the assumptions of those models, and the various parameters important to the models

to report on the suitability of a three-dimensional circulation model with depth-variable vertical eddy viscosity developed for shallow lakes

to show the results of preliminary applications of the model to Lake Balaton

The organization of the report is to first present the literature review as background to the model development and application. The review attempts to provide a brief introduction to general aspects of circulation modeling and then to concentrate on two particular issues which are significant to the application to shallow lakes. The first of these issues concerns the possible assumptions made in circulation models, and the conditions under which these assumptions are appropriate. The second, and perhaps most critical issue for practical application, is the nature and magnitude of various model parameters.

With the background of the literature review, the report turns to the specific case of Lake Balaton and the circulation model employed in these studies. Following a general description of the lake and a more detailed look at what is known about its circulation, the applicability of the Galerkin model is examined in light of the criteria developed in the literature review. The model is then used to simulate circulation in Lake Balaton using a range of parameter values and hypothetical wind conditions. These sensitivity studies are intended to supplement the limited information to be found in the literature regarding parameters.

The report closes with a set of conclusions and recommendations for further work. Particular attention is paid in these closing remarks to the development of a coupled hydrodynamic and biogeochemical water quality model for practical application to Lake Balaton.

The work leading to this report was carried out at the Ralph M. Parsons Laboratory for Water Resources and Hydrodynamics at the Massachusetts Institute of Technology, Cambridge, Massachusetts, U.S.A., and at the International Institute of Applied Systems Analysis, Laxenburg, Austria. The work reported herein represents a portion of the doctoral thesis research of the first author completed under the supervision of the second author. Research funds for the work completed at M.I.T. were supplied by the United States National Science Foundation under their Water Resources and Environmental Engineering Program. The research at IIASA was undertaken during a two month appointment of the first author under the supervision of the third author of IIASA's Resources and Environment Area. In addition, Prof. Keith D. Stolzenbach of the Parsons Laboratory supplied considerable aid and advice during the course of the work. His help is gratefully acknowledged.

The report text was prepared on the M.I.T. Information Processing Center IBM 370/168 using the University of Waterloo Script text editing system. We thank Mrs. Beth Quivey for completing the text with her expertly typed equations. The circulation model computations were also performed at the M.I.T. Information Processing Center.

2.3 Summary of the Report

A successful predictive model of the eutrophication process in a lake or reservoir requires attention to not only water quality biology and chemistry, but to hydrodynamics as well. This report investigates the hydrodynamic component for eventual incorporation into a eutrophication model of Lake Balaton, Hungary. The report consists of two main parts: a review of the theory and practice of wind-driven circulation modeling, and a description of a transient three-dimensional model and its application to Lake Balaton.

The review of wind-driven circulation modeling proceeds along three subject lines: an overview of the common modeling approaches, an examination of the limitations imposed by typical model assumptions, and a look at the important parameters to be employed as model input.

The numerous approaches to circulation modeling all seek to solve the equations of momentum and continuity in some simplified form. The variations on these simplifications and solution methods fall into three categories of models: single-layer models, which assume a vertically homogeneous lake; multi-layer models, which presume the lake to be divisible in two or more essentially homogeneous layers; and, the Ekman models, which neglect certain forces and accelerations in order to partially solve the problem by analytical methods.

Simplifying assumptions and approximations are a necessary part of any circulation model, and are quite acceptable where conditions permit. A number of assumptions in wide use are examined in this report, and conditions under which the assumptions are appropriate are given. For example, if the water body is shallow, one may neglect dynamic pressure forces, vertical velocities and density inhomogeneities. In a similar way, other assumptions may be made if permitted by the characteristics of the water body, the practice being to employ dimensionless force ratios to represent those characteristics mathematically. The common assumptions include neglect of convective accelerations, permitted if the Rossby number (inertial to Coriolis force ratio) is small; neglect of horizontal shear forces, allowed where the horizontal Ekman number (shear to Coriolis force ratio) is small; and imposition of a rigid lid to eliminate free surface gravity waves, an assumption appropriate when the Coriolis to gravity force ratio is small. All of the approximation criteria, however, include the very important caveat that they may be inapplicable in nearshore or other local regions where bathymetry changes

abruptly.

Circulation models also depend upon the selection of values and formulae for various input parameters. Particularly important parameters are the vertical eddy viscosity and the stresses at the water surface and bottom. The eddy viscosity, though it significantly impacts the velocity profiles predicted by a model, is a subject of considerable disagreement in the literature. Many representations of this parameter as a function of depth have been proposed, but there is virtually no information with which to identify the superior alternative. Luckily, there is greater coherence in the literature addressing the stress produced by wind on the water surface. The formulae of Wu (1969) are found to be widely accepted, although preliminary results by some researchers indicate that these formulae may not be accurate in very shallow water. Bottom stresses are represented in a greater variety of methods than surface stress, though this is due more to computational constraints than to a lack of understanding or agreement. Three basic bottom stress formulae may be identified: the linear law, which is computationally simple but lacks accuracy; the non-linear or quadratic law, which is considered accurate, but requires extensive iterative computation; and the quasi-linear law, which lies intermediate to these two. Though it is less true for the bottom stress as a parameter than for the surface stress or vertical viscosity, we can nevertheless make the following summary observation: Although the form and value of these parameters significantly affects model results, selection of parameters is made difficult by the lack of unified theory or adequate experimental data. Thus, the model results inevitably reflect the considerable uncertainty of these parameters.

Following the review of the literature of circulation modeling, the report turns to a description of the circulation model developed in these studies and applied to Lake Balaton. Balaton is a large, but unusually shallow lake (3.2 meters deep, on average, and 75 kilometers long). Hydrologic flows into and out of the lake are minor compared to the dominating wind-driven flows and seiching. Wind-driven flows are influential due to the lake's shallowness, however their complexity defies a simple generalization of their dynamics. Non-uniformities in wind speed and direction, as well as the confines of the lake shoreline, influence the horizontal flow patterns. The vertical flow profile is shown by field measurements to be non-uniform, and additionally highly transient. Superimposed upon this motion is a very prominent seiche, with both longitudinal and transverse modes, as well as various secondary modes. Comprehensive field studies by Hungarian scientists over more than a decade have defined the characteristics of these

seiche motions in some detail. The shallowness of the lake significantly influences the longitudinal seiche by lengthening its period and causing it to damp out after a few cycles.

The three-dimensional transient circulation model for the Balaton application is based upon a model developed by Cooper and Pearce (1977) and modified by Nelson (1979). The model may be classified as an Ekman-type by virtue of its use of the simplified equations of motion. It is made more powerful than the usual Ekman model, however, by the use of a Galerkin solution method to determine the vertical velocity profile as the weighted sum of a series of analytic solutions. This technique permits additional complexity in the model boundary conditions and parameters. In particular, the vertical eddy viscosity may be defined as a function of depth. The model has been programmed to solve the equations of motion on a finite-difference grid, determining the three-dimensional structure of the horizontal currents.

To be considered in selecting this model for application to Lake Balaton are its consistency with the biological and chemical aspects of the lake's water quality, and the suitability of the mathematical formulation for this lake. The first consideration addresses the requirements that the model be able to capture those aspects of the lake hydrodynamics which significantly affect water quality. An analysis of the length and time scales of the major physical and biochemical processes in the lake, as well as estimates of the seiche-related transport, illustrate the appropriateness of the model. A point-by-point examination of the major model assumptions further demonstrates the model validity for Lake Balaton, but with the caution that predictions may be poor at isolated localities where geometry and bathymetry change abruptly, for example, around Tihany Peninsula and Strait.

Application of the Galerkin model to Lake Balaton proceeded in three stages: calibration, sensitivity testing and verification. First, the model parameters were calibrated in order to produce a model response generally similar to that observed in the lake itself. The calibration was judged on a number of specific criteria, including the magnitude of set-up, the seiche period and dissipation, the form of the vertical velocity profile, and the magnitude of the surface current in simulations of a simple hypothetical seiche event. These simulations afforded the opportunity to test the sensitivity of the model to its calibration parameters, an investigation continued with other input data as well. The model showed relative insensitivity to the bottom friction factor and the finite difference grid spacing, but considerable sensitivity

to the vertical eddy viscosity and to spatial variations in the wind field.

Following calibration and testing, the model was verified by comparison with collected field data. Using wind speed and direction recorded on the lake, the model simulated three different historical events. Longitudinal seiches characterized two of these events, and were well duplicated by model results. A third event, which caused a large transverse seiche, was less well represented. This was probably due to the magnification of small errors in wind direction when the wind is directed transverse to the lake. Despite these problems, we were encouraged by the model's overall ability to reproduce historical events and felt the verification to be a success.

In the closing sections of the report, we use the circulation model to examine the character of transport fluxes in time and space, and propose the role of the three-dimensional transient circulation model in future study of Lake Balaton's water quality. The complexity and expense of the three-dimensional model preclude its use in a direct coupling with biogeochemical water quality models. Rather, the model is more appropriate as a means to develop and calibrate more simple and practical models of the lake's hydrodynamics. A demonstration of the model used in such a role is an analysis of the mass transports computed in our simulation of the July 8 and 9, 1963 wind event. The model results show the longitudinal fluxes, due mainly to seiche motion, to be very strong and highly transient. These flows are generally uni-directional over the lake cross section, though they are occasionally interrupted by flow reversals within the lake depth. Temporal variations are considerably more important than vertical and lateral spatial non-uniformities, however. An examination of transverse fluxes across a longitudinal plane within the lake reveals considerable flows which would tend to eliminate lateral concentration gradients. In summary, the analysis shows that temporal variations of the longitudinal fluxes are the dominant dynamics to be evaluated for water quality modeling. The hydrologic flows, which have been used in the water quality models to date, are dwarfed by the magnitude of the seiche-related currents.

In the continuing phases of this research, the three-dimensional model will be simplified to a two-dimensional longitudinal-vertical model. This modification, which effectively integrates the velocity over the lake's lateral dimension, will yield a model sufficiently simple to be coupled with a biogeochemical model of the lake water quality. A number of proposals for the form of this coupling are proposed and these will be evaluated in the research to be continued.

3 OVERVIEW OF LAKE CIRCULATION MODELING

3.1 Mathematical Formulation of Lake Circulation

The equations of fluid motion in a lake are the departure point from which all mathematical circulation models must begin. These equations include the equations of conservation of mass (or the continuity equation), and the equation of conservation of momentum in each of the three coordinate directions. For an incompressible fluid, the continuity equation is:

$$\frac{\partial u}{\partial x} + \frac{\partial v}{\partial y} + \frac{\partial w}{\partial z} = 0 \quad (3.1)$$

where, x and y are the horizontal direction components, as shown in Figure 3.1;
 z is the vertical direction component, measured downwards from the mean water surface elevation; and,
 u, v, and w are the fluid velocity components in the x, y and z directions respectively.

The momentum equations express the acceleration of the fluid resulting from various forces. The equations in the horizontal plane are given as Equations 3.2 and 3.3. For clarity, the correspondence between the terms in the equations and the physical accelerations and forces which they represent is shown:

$$\frac{\partial u}{\partial t} + \left\{ u \frac{\partial u}{\partial x} + v \frac{\partial u}{\partial y} + w \frac{\partial u}{\partial z} \right\} = f_v - \frac{1}{\rho} \frac{\partial p}{\partial x} + A_H \left\{ \frac{\partial^2 u}{\partial x^2} + \frac{\partial^2 u}{\partial y^2} \right\} + \frac{\partial}{\partial z} \left(A_V \frac{\partial u}{\partial z} \right) \quad (3.2)$$

(a) (b) (c) (d) (e) (f)

$$\begin{aligned}
& \frac{\partial v}{\partial t} + \left\{ u \frac{\partial v}{\partial x} + v \frac{\partial v}{\partial y} + w \frac{\partial v}{\partial z} \right\} = \\
& \text{(a)} \qquad \qquad \qquad \text{(b)} \\
& \qquad \qquad \qquad -fu - \frac{1}{\rho} \frac{\partial p}{\partial y} + A_H \left\{ \frac{\partial^2 v}{\partial x^2} + \frac{\partial^2 v}{\partial y^2} \right\} + \frac{\partial}{\partial z} (A_V \frac{\partial v}{\partial z}) \qquad (3.3) \\
& \qquad \qquad \qquad \text{(c)} \qquad \text{(d)} \qquad \qquad \qquad \text{(e)} \qquad \qquad \qquad \text{(f)}
\end{aligned}$$

where, t is the time variable;
 f is the Coriolis parameter;
 p is the fluid pressure;
 ρ is the fluid density;
 A_H is the horizontal eddy viscosity; and,
 A_V is the vertical eddy viscosity.

The terms of these equations have the following meanings:

- a - the instantaneous or local acceleration of the fluid at a point
- b - the convective acceleration, caused when fluid is transported from one point to another of different fluid velocity
- c - the Coriolis force due to the earth's rotation
- d - the horizontal pressure force
- e - the horizontal transport of momentum due to shear stresses
- f - the vertical transport of momentum due to shear stresses

The momentum equation in the vertical direction is entirely similar to those above, but includes an additional term on the right hand side to represent the force due to the gravitational acceleration, represented by g . The equation is considerably simplified by the realization that the pressure and gravitational forces dominate all others.

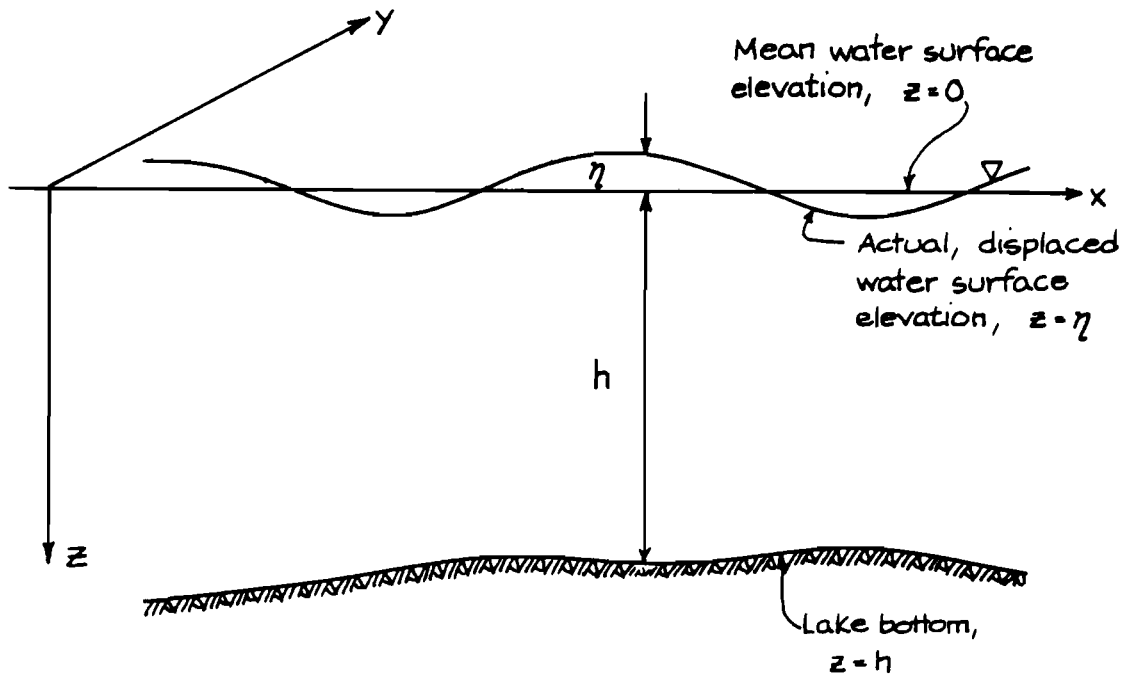


Figure 3.1

Definition sketch for mathematical formulation

Neglect of these lesser terms is known as the hydrostatic approximation, and leads to the equation:

$$\frac{1}{\rho} \frac{\partial p}{\partial z} = -g \quad (3.4)$$

The boundary conditions for these equations are specified at the free surface, the lake bottom, and the lake shoreline. At the free surface, the kinematic boundary condition specifies that continuity be maintained:

$$\frac{\partial \eta}{\partial t} + u \frac{\partial \eta}{\partial x} + v \frac{\partial \eta}{\partial y} = w \quad \text{at } z = \eta \quad (3.5)$$

where, η is the free surface displacement.

An additional condition at the free surface represents the shear stress due to the wind:

$$\rho A_v \frac{\partial u}{\partial z} = \tau_s^x \quad \rho A_v \frac{\partial v}{\partial z} = \tau_s^y \quad \text{at } z = \eta \quad (3.6)$$

where, τ_s^x is the x-component of the shear stress on the surface; and τ_s^y is the y-component.

At the lake bottom, a no-slip boundary condition specifies that the fluid in direct contact with the rough bottom cannot move:

$$u = v = 0 \quad \text{at } z = h \quad (3.7)$$

where, h is the lake depth.

Alternatively, a shear stress condition similar to that at the surface may instead be specified:

$$\rho A_v \frac{\partial u}{\partial z} = \tau_b^x \quad \rho A_v \frac{\partial v}{\partial z} = \tau_b^y \quad \text{at } z = h \quad (3.8)$$

where, τ_b^x is the x-component of the bottom shear stress; and τ_b^y is the y-component.

At the lake perimeter, a no-flow no-slip boundary condition applies:

$$u = v = 0 \quad \text{at the } x \text{ and } y \text{ boundaries} \quad (3.9)$$

The equations and boundary conditions presented above are complex and their solution is difficult; the non-linear convective terms and boundary conditions being particularly troublesome. As a consequence, most solution methods depend

upon simplification of the equations by averaging to reduce the problem dimensions, or by neglecting the less important terms in the equations. We can gain insight into the relative importance of the various terms by transforming the equations to a non-dimensional form. This is done in Figure 3.2, where typical scales of length, depth, time and velocity have been used to normalize the dimensional variables. The scales employed are length, L ; depth, h ; time, $1/f$; and velocity, U . As seen in Figure 3.2, this process gives rise to the Rossby number, Ekman numbers and Froude number as dimensionless parameters which indicate the relative magnitude of the terms in the equations. We will refer to these parameters in the following discussions of modeling strategies, assumptions and parameters.

Definition of Dimensionless Parameters

$$Fr = \text{Froude Number} = \frac{U}{\sqrt{gH}} \quad (3.10)$$

$$Ro = \text{Rossby Number} = \frac{U}{fL} \quad (3.11)$$

$$E_H = \text{Horizontal Ekman Number} = \frac{A_H}{fL^2} \quad (3.12)$$

$$E_V = \text{Vertical Ekman Number} = \frac{A_V}{fL^2} \quad (3.13)$$

Conservation of Mass

$$\frac{\partial u}{\partial x} + \frac{\partial v}{\partial y} + \frac{\partial w}{\partial z} = 0 \quad (3.14)$$

Conservation of Horizontal Momentum

$$\frac{\partial u}{\partial t} + Ro \left[u \frac{\partial u}{\partial x} + v \frac{\partial u}{\partial y} + w \frac{\partial u}{\partial z} \right] - v = - \frac{1}{\rho} \frac{\partial p}{\partial x} + E_H \left[\frac{\partial^2 u}{\partial x^2} + \frac{\partial^2 u}{\partial y^2} \right] - \frac{\partial}{\partial z} \left[E_V \frac{\partial u}{\partial z} \right] \quad (3.15)$$

$$\frac{\partial v}{\partial t} + Ro \left[u \frac{\partial v}{\partial x} + v \frac{\partial v}{\partial y} + w \frac{\partial v}{\partial z} \right] + u = - \frac{1}{\rho} \frac{\partial p}{\partial y} + E_H \left[\frac{\partial^2 v}{\partial x^2} + \frac{\partial^2 v}{\partial y^2} \right] - \frac{\partial}{\partial z} \left[E_V \frac{\partial v}{\partial z} \right] \quad (3.16)$$

local acceleration convective acceleration Coriolis force pressure force horizontal eddy momentum transport vertical eddy momentum transport

Figure 3.2

Non-dimensional form of the governing equations

Conservation of Vertical Momentum (Hydrostatic Pressure)

$$\frac{\partial p}{\partial z} = - \frac{R_0}{F_r^2} \rho \quad (3.17)$$

Kinematic Boundary Condition

$$\frac{\partial \eta}{\partial t} + R_0 \left[u \frac{\partial \eta}{\partial x} + v \frac{\partial \eta}{\partial y} \right] = \frac{R_0^2}{F_r^2} w \quad \text{at } z = \eta \frac{F_r^2}{R_0} \quad (\text{surface}) \quad (3.18)$$

Surface and Bottom Boundary Conditions

$$\frac{\partial u}{\partial z} = \tau_X^s \quad \frac{\partial v}{\partial z} = \tau_Y^s \quad \text{at } z = \eta \frac{F_r^2}{R_0} \quad (\text{surface}) \quad (3.19)$$

$$\frac{\partial u}{\partial z} = \tau_Y^s \quad \frac{\partial v}{\partial z} = \tau_X^s \quad \text{at } z = -h \quad (\text{bottom}) \quad (3.20)$$

Figure 3.2
continued

3.2 Modeling Strategies

A large number of lake circulation models of many different types have been developed and applied to various lakes. In this section, we will draw upon our own search of the literature as well as published reviews by Cheng, Powell and Dillon (1976), Lindijer (1976,1979) and Simons (1979) to outline three major classes of models. The classes, as defined by Cheng, Powell and Dillon, are single layer models, multi-layer models and Ekman-type models.

3.2.1 Single Layer Models

Single layer models proceed from the assumption that the lake is vertically homogeneous (unstratified) to eliminate the consideration of vertical variations in currents and other parameters. The vertical variation is removed by integrating the continuity and momentum equations from the free surface to the lake bottom, reducing the three-dimensional problem to one of only two dimensions. The integration process transforms the problem variables from velocities to horizontal mass transports, defined as:

$$U = \int_h^{\eta} u dz \quad v = \int_h^{\eta} v dz \quad (3.21)$$

The integration also incorporates the surface and bottom boundary conditions into the resulting equations.

Single layer models, although simulating free surface motion well, are often found to be poor current predictors. Thus, their use is largely confined to storm surge studies. A number of single layer model applications are listed in Table 3.1.

3.2.2 Multi-layer Models

Multi-layer models extend the single layer methodology to stratified water bodies. Basically, the process applied to the entire water column in the single layer models is applied piecewise to a number of layers through the lake. A different density may exist in each layer, and the vertical eddy viscosity may vary from layer to layer as well. The equations of continuity and momentum are vertically integrated over the depth of each layer, incorporating the free surface boundary condition into the top layer equation, and the bottom condition into the equation for the lowest layer. Inter-layer conditions must also be specified, and become part of the layer equations as well. The final

result of this procedure is a series of equations which represent the motion within each layer individually. The layers are, of course, coupled via the inter-layer conditions.

Two approaches to the construction of the layers exist. In the Type I approach, the position of the layers is fixed in space and vertical transports occur between layers to maintain continuity. These transports also transfer momentum between the layers. In the Type II models, the layers are considered to be distinct, as if separated by thin membranes. No mass transport occurs between the layers; rather, the layers displace vertically to maintain continuity. The layers communicate via momentum transport due to interfacial stress.

Multi-layer models correct the deficiencies of the single layer models, and the Type I models especially predict both free surface elevation and currents well. The Type II approach is less common than the Type I, and is most appropriate to distinctly stratified lakes with a clearly developed thermocline. A selection of multi-layer models from the published literature is summarized in Table 3.2.

3.2.3 Ekman-type Models

The Ekman-type models simplify the equations of motion considerably more than the methods above. Based upon the assumption that the Rossby number is small, the horizontal momentum equations are linearized by dropping the convective acceleration terms. This important simplification permits the form of the vertical distribution of the horizontal velocities to be determined analytically. Once the form of the vertical structure is known, completion of the solution requires only that the variation in horizontal space be defined. This information is supplied by the solution of the vertically integrated conservation equations. The Ekman-type model solution specifies the three-dimensional variation of the horizontal currents only. The smaller vertical velocity component is not determined.

The Ekman-type solution, owing to the simplification of the equations, is the easiest method for computation. However, the assumptions made in simplifying the equations reduce the model's applicability and require that the model's suitability be evaluated for each application. The model remains useful for a wide range of lakes nevertheless, as attested by the examples shown in Table 3.3.

Table 3.1 Published single layer lake circulation models

<u>Lake</u>	<u>Reference</u>	$\frac{\text{Length}}{(\text{km})}$	$\frac{\text{Width}}{(\text{km})}$	$\frac{\text{Depth}}{(\text{m})}$	$\frac{A_H}{(\text{cm}^2/\text{s})}$	$\frac{A_V^*}{(\text{cm}^2/\text{s})}$	$\frac{\Delta x}{(\text{km})}$	$\frac{\Delta y}{(\text{km})}$	<u>Comments</u> **
Erie	Platzman (1963)	400	100	64	--	40	13.9	13.9	Unsteady
Erie	Cheng and Tung (1970)	400	100	64	--	30	20	10	Finite Element
Huron	Murty and Rao (1970)	400	150	230	--	f(W)	15.2	15.2	
Michigan	Murty and Rao (1970)	500	125	80	--	f(W)	12.7	12.7	
Erie	Murty and Rao (1970)	400	100	64	--	f(W)	10.2	5.1	
Superior	Murty and Rao (1970)	600	400	406	--	f(W)	13.9	13.9	
Ontario	Simons (1971)	285	70	220	10^6	f(W)	7 & 5	7 & 5	Unsteady
Ontario	Paskausky (1971)	285	70	220	--	22.5	2.5	2.5	Unsteady Vorticity Simulation

* f(z) indicates variation with depth, f(W) indicates variation with wind speed
 ** unless noted, models are steady and use a finite difference solution

Table 3.2 Published multi-layer lake circulation models

<u>Lake</u>	<u>Reference</u>	<u>Length</u> (km)	<u>Width</u> (km)	<u>Depth</u> (m)	A_H (cm ² /s)	A_V^* (cm ² /s)	Δx (km)	Δy (km)	<u>Layers</u>	<u>Comments</u> **
Ontario	Simons, 1972	285	70	220	106	f(W)	5	5	3	Unsteady
Constance	Hollan and Simons, 1978	60	15	250	?	50	1	1	5	Unsteady
Baikal	Paul et al, 1979	600	75	1600	107	10 to 1000 f(z)	7.8	15	8	Unsteady
Sea of Azov	Paul et al, 1979	360	220	13	3x10 ⁶	25	9.5	6.8	8	Unsteady
Michigan	Kizlauskas and Katz, 1973	500	125	80	--	50	10.8	10.8	2	Unsteady, Type II

* f(z) indicates variation with depth, f(W) indicates variation with wind speed
 ** unless noted, models are steady, Type I and use a finite difference solution

Table 3.3 Published Ekman-type circulation models

Lake	Reference	Length (km)	Width (km)	Depth (m)	$\frac{A_H}{(cm^2/s)}$	$\frac{A_V}{(cm^2/s)}$	$\frac{\Delta X}{(km)}$	$\frac{\Delta Y}{(km)}$	Comments **
Okeechobee	Su, Pohl and Shih, 1976	55	49	4.5	--	10	2.5	2.5	Finite Element
Ontario	Gallagher, Liggett and Chan, 1973	285	70	220	--	200	4	4	Finite Element
Superior	Lien and Hoopes, 1978	600	400	406	--	100	25.4	25.4	
Erie	Gedney and Lick, 1972	400	100	64	5×10^5	38	3.2	3.2	
Velen	Bengtsson, 1973	7	1	9	--	15	?	?	
Mendota	Nelson, 1979	10	7	22	--	15 f(z)	0.73	0.73	Unsteady
Geneva	Bauer and Graf (described by Sundermann, 1979)	70	15	310	--	460	1	1	
Ontario	Bonham-Carter and Thomas, 1973	285	70	220	--	?	2.5	2.5	

* f(z) indicates variation with depth, f(W) indicates variation with wind speed

** unless noted, models are steady and use a finite difference solution

4 MAJOR MODEL ASSUMPTIONS

The discussion in Section 3 indicates many possible simplifications and assumptions which the modeler may employ. In this section, the various assumptions will be examined and criteria to evaluate their applicability will be given. Many of these criteria are drawn from Lindijer (1979).

4.1 Vertical Variability

When the depth of the lake is much smaller than its length, one can invoke a family of simplifications which Lindijer calls the shallow water approximation. The approximation consists, in fact, of three approximations. The first is the commonly used hydrostatic approximation, Equation 3.4. This is valid in all but the deepest lakes, and is found in virtually every circulation model.

The second shallow water approximation is the assumption that vertical velocities are so much smaller than those in the horizontal that they may be neglected in the equations for horizontal momentum (Equations 3.2 and 3.3). This approximation yields a model which is three-dimensional in the sense that the variation of horizontal velocity is determined in all three coordinate directions, but not in the sense that the three velocity components are determined.

The third shallow water approximation is that the water body is vertically homogeneous, that is, that it does not exhibit any density stratification. Field studies have shown this to be a reasonable assumption for shallow lakes, where the influence of strong winds penetrates throughout the water column and produces complete vertical mixing (Entz, 1976; and Seki, et al, 1980). Although brief periods of weak stratification can occur during the summer, even moderate winds will remix very shallow lakes. Usually, stratification persists no longer than a day or two.

4.2 Convective Accelerations

Neglect of the non-linear convective terms leads to a considerable simplification of the momentum equations, and is the key assumption of the Ekman-type models. The magnitude of the Rossby number, the ratio of the inertial forces to the Coriolis force, determines whether or not this is a valid assumption. If the Rossby number is much less than one, the convective terms will have negligible impact upon the lake-wide circulation, and may be omitted.

The phrase "lake-wide circulation" was used in the last paragraph to purposely exclude local effects. Recently, there has been a good deal of attention in the literature to the importance of local inertial effects and the ability of numerical models to capture such effects (Abbott, 1976; Abbott and Rasmussen, 1977; and Lean and Weare, 1979). Unfortunately, these investigations have addressed channel, estuarine and coastal flows where velocities, and thus convective inertia, are much greater than in wind-induced lake circulation. Nevertheless, we can conclude from these studies that where there are large abrupt changes in the bathymetry or shoreline geometry numerical models which omit the convective terms will fail to capture induced secondary circulations correctly. The severity of these local errors depends upon the coarseness of the finite difference grid, the character of the geometry, and the strength of the currents. We expect that the errors will be minor for low velocity wind-induced flow.

4.3 Free Surface Effects

An assumption with major impact upon lake circulation models is the rigid lid approximation. As the name implies, the assumption is that the lake behaves as if it were covered with a slippery rigid lid. This lid prevents vertical motions at the free surface, but still allows horizontal motions and pressure variations. By preventing the kinematic effects of surface motion, the rigid lid filters out high frequency inertial and gravity waves without affecting steady state solutions and with only small distortion of low frequency movements. The consequence of eliminating the high speed gravity waves is to permit an order of magnitude increase in the time step of numerical solution methods, and greater numerical accuracy and stability (Bryan, 1969).

Operationally, the rigid lid approximation is to assume $w = 0$ in the kinematic boundary condition, Equation 3.5. Calculation of free surface displacements is still possible with this approximation by first solving the horizontal momentum equations for pressure, and then using the hydrostatic equation to determine the free surface displacement from the pressure (Cheng, Powell and Dillon, 1976).

The rigid lid approximation has very great computational advantages over the alternative free surface representation, but not without a cost in certain circumstances. Beford and Rai (1978) give the criterion that the square of the ratio of the seiche period to the inertial period must be much less than one to use the rigid lid approximation. This is expressed mathematically for a lake of length L as:

$$\frac{L^2 f^2}{(2\pi)^2 gH} \ll 1$$

Others give a similar criterion without the factor of $(2\pi)^2$.

Two papers from the research group headed by Lick at Case Western Reserve explore the rigid lid approximation in some detail (Haq and Lick, 1975; and Sheng, Lick, Gedney and Molls, 1978). Their comparisons of rigid lid and free surface models were made using actual events on Lake Erie, where the ratio criterion above is not met. Their findings indicate that the rigid lid model converges to a steady state many times faster than the free surface model, but that transient currents and seiches are incorrect in the rigid lid model results. The free surface model does preserve these effects, and thus predicts greater bottom shear stresses and sediment resuspension in their linked

circulation and sediment transport model.

One aspect of the approximation at the free surface is poorly presented in some papers and easily confused with the rigid lid approximation. This approximation, which we will call the small amplitude approximation, is that the free surface boundary conditions are applied at $z = 0$, rather than at the actual free surface, $z = \eta$. (Cheng, Powell and Dillon (1976) are particularly unclear in distinguishing this approximation from the rigid lid approximation.) The small amplitude approximation is commonly used in both free surface and rigid lid models. The validity of the approximation may be evaluated with the surface boundary parameter as a guide. This parameter, which is the ratio of the square of the Froude number to the Rossby number, arises when the kinematic and wind stress boundary conditions are made dimensionless. (See Figure 3.2.) If the parameter is small, it may be assumed reasonable to employ the small amplitude approximation and apply the boundary conditions at $z = 0$ rather than at $z = \eta$.

4.4 Horizontal Shear Effects

In most analytical solutions and in many of the Ekman-type models, the equations are simplified by neglect of the horizontal shear forces (term e in Equations 3.2 and 3.3). This approximation may be justified by the size of the horizontal Ekman number, the ratio of the frictional force to the Coriolis force. Where the horizontal Ekman number is small compared to one, the terms may be safely ignored.

A subtle aspect of this approximation must be considered along the shoreline, where frictional influences may be important locally. Lindijer (1979) gives an evaluation criterion for these effects based upon the bottom slope, s . The criterion states that the horizontal shear terms may be neglected for gradual slopes:

$$s \ll s_c = \frac{H}{L} \sqrt{\frac{E_v}{E_H}}$$

where, s_c is the critical bottom slope;
 H and L are the depth and length of the lake; and
 E_v and E_H are the vertical and horizontal Ekman numbers.

This condition can be interpreted as a requirement that vertical shear stresses (represented by $H\sqrt{E_v}$) remain much larger than those in the horizontal ($L\sqrt{E_H}$) despite the bottom slope.

5 MODEL PARAMETERS

In this section we examine a number of key parameters which significantly affect the predictions of circulation models. Unfortunately, the literature presents multiple alternatives for these parameters, but no clear consensus as to which are superior.

5.1 Vertical Eddy Viscosity

The momentum equations presented earlier employ the assumption that the turbulent flux of momentum due to the Reynolds stresses can be represented as the product of an eddy viscosity and the first spatial derivative of the velocity. The validity of this assumption is often questioned. (See, for example, Babajimopoulos and Bedford, 1980.) However, a working practical alternative does not now exist, and it is a rare circulation model that does not make use of the eddy viscosity assumption.

5.1.1 Published Formulae

Perhaps because the concept is without rigorous theoretical grounds, a bewildering variety of formulations for the eddy viscosity may be found in the literature. A selection of the available formulae for the vertical eddy viscosity are shown in Figure 5.1. The obvious diversity in the proposed forms reflect significant differences in the originators' views of the turbulent transport process.

Some convergence of the literature may nevertheless be found for particular aspects of the vertical eddy viscosity formulation. There is agreement that the eddy viscosity depends upon the intensity of the turbulence and the density instability of the water column, and that it varies throughout the lake. Lick (1976) lists the following turbulence generating processes: surface wind stress, vertical shear currents due to horizontal pressure differences, internal waves, bottom friction and bathymetry, and density stability. For shallow, homogeneous lakes the surface and bottom sources of turbulence are the most influential.

The value of the eddy viscosity at the lake bottom appears to be another point of common ground within the literature. As explained by Thomas (1975), the rigid bottom inhibits vertical eddy motions and thus the viscosity

Vertical eddy viscosity (A_v)

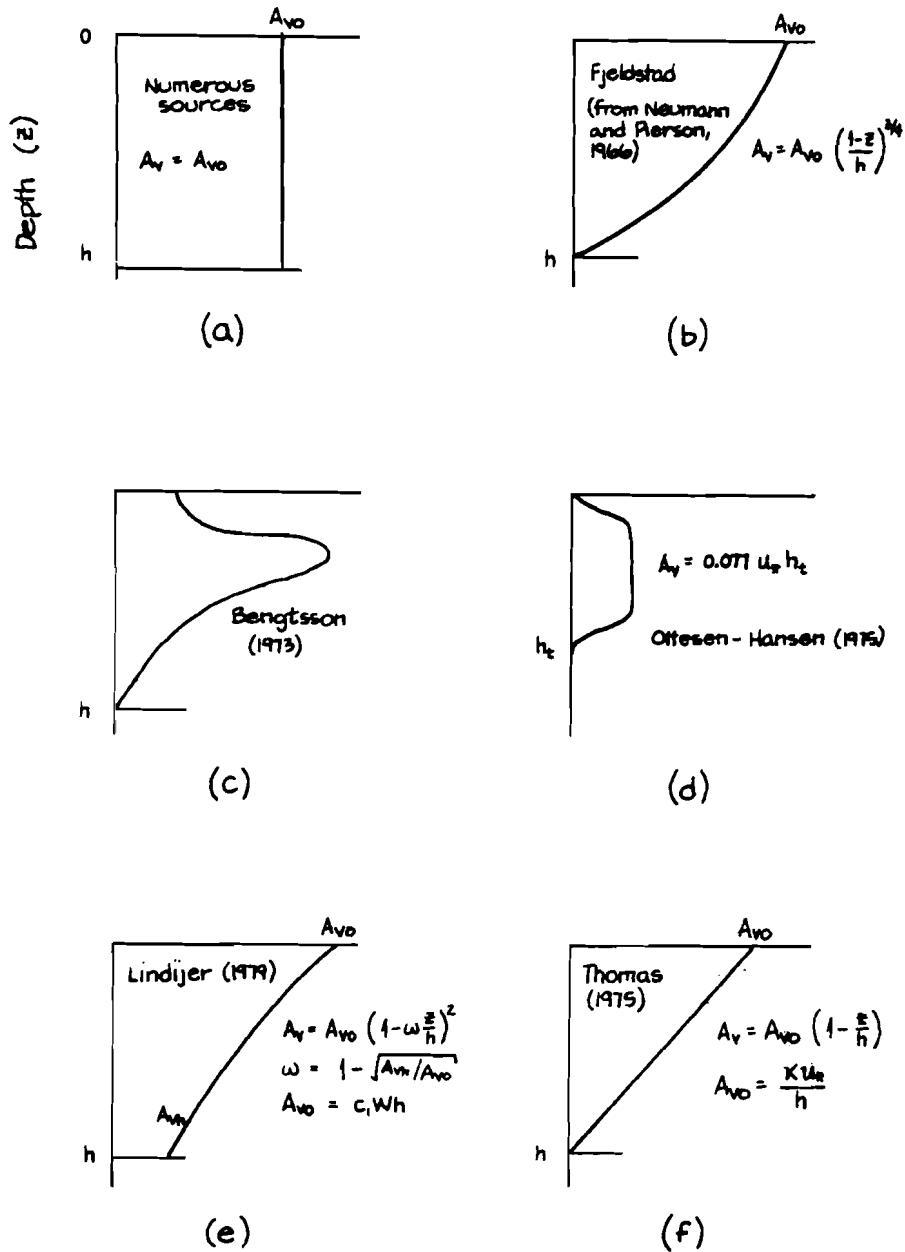


Figure 5.1

Representations of the vertical eddy viscosity

Vertical eddy viscosity (A_v)

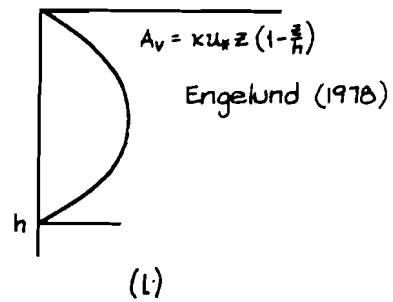
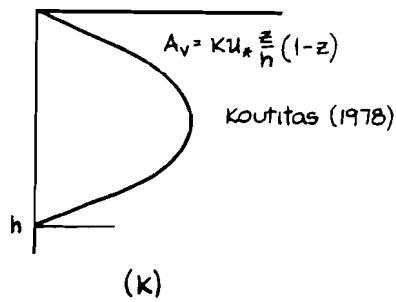
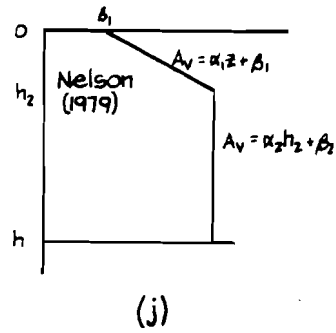
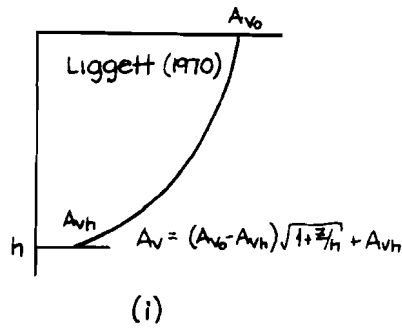
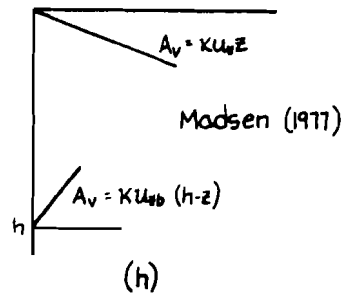
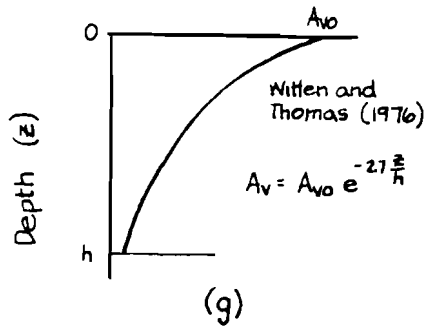


Figure 5.1 (continued)

Representations of the vertical eddy viscosity

closes to zero. With a few exceptions, the formulae of Figure 5.1 follow this behavior.

There is far less agreement on the proper formulation at the water surface. Many researchers view the wind stress as the driving source of turbulence and therefore feel that the vertical viscosity should be maximal at or near the surface (Lick, 1976; Lindijer, 1976; Thomas, 1975; and Bengtsson, 1973). Opposing this view is Madsen (1977), who argues that the eddy viscosity will behave similarly near any sheared boundary in the fashion described by Thomas. Accordingly, he proposes a linear increase from zero viscosity at both the surface and the bottom.

Most researchers do agree that the eddy viscosity will increase as the boundary shear increases, although this dependency is not well defined. The uncertainty about this dependency, as well as an increase in computational difficulty, leads most modelers to assume the eddy viscosity not to vary with boundary shear or wind speed. Where a variation is modeled, the procedure is to generally assume a linear proportionality to either the wind speed or the wind friction velocity as seen in Figures 5.1d, e, f, h, k and l.

The great diversity of opinion about the vertical eddy viscosity is troublesome for the modeler who seeks a more sophisticated representation than to simply assume constant viscosity. Hamblin and Salmon (1975) point out the importance of this parameter in the circulation model:

A number of experiments in which model predictions are compared with observed currents have indicated that the vertical diffusion of momentum is probably the most important internal parameter of the model.... Drastic variability in the vertical profile of current can result from the specification of the magnitude and variation of the vertical eddy viscosity.

5.1.2 Comparison with Observations

A basis for evaluation of the eddy viscosity formulations is found in the results of laboratory and field investigations. Laboratory flume studies, such as those reviewed by Shemdin (1973), invariably reveal logarithmic velocity profiles at both the water surface and the flume bottom. The near-surface logarithmic profile has been confirmed in the field by observations of wind-drift currents in lakes (Bye, 1975; and Bhowmik and Stall, 1978). Field and laboratory data (summarized in Stolzenbach et al, 1977) also indicate that the wind factor (the ratio of the surface drift current to the wind speed) varies over the

narrow range of approximately 1 to 6 percent, and that the drift current is deflected by no more than 15 degrees from the wind direction.

These observations should be replicated in the results of mathematical circulation models. The simplest of those models, the classic analytical solution by Ekman for an infinitely deep ocean and constant vertical eddy viscosity, predicts a wind factor of 3% but a surface deflection angle of 45 degrees. The development of more complex eddy viscosity formulations has largely been a reaction to his poor prediction of the deflection. Results using two of the more complex formulae are compared with those of the constant viscosity and with laboratory findings by Stolzenbach et al. (1977). They consider two cases: wind-driven flow in an infinite channel, and in a closed finite channel. They conclude that the constant eddy viscosity (Figure 5.1a) and the linear eddy viscosity (5.1f) produce unrealistic results, while the parabolic form (5.1k or l) yields a velocity profile similar to the laboratory findings. Madsen's formula (Figure 5.1h) also duplicates the log velocity profiles and predicts a deflection of roughly 10 degrees. Interestingly, the very dissimilar equation proposed by Fjeldstaad (discussed in Neumann and Pierson, 1966) was developed empirically by matching observations at a 22 meter deep location in the ocean, and thus agrees with at least one set of field data.

5.2 Wind Stress on the Water Surface

The specification of the surface boundary condition (Equation 3.5) requires the determination of the stress on the free surface due to the wind. This is generally given in the form:

$$\tau_s = C_z \rho_a W_z^2 \quad (5.1)$$

where, τ_s is the surface stress exerted in the same direction as the wind;
 C_z is the drag coefficient for a wind measured at height z ;
 ρ_a is the density of the air; and
 W_z is the wind speed measured at a height z above the water surface (usually 10 meters).

Many investigators have proposed formulae for the 10 meter drag coefficient, and these are summarized in Table 5.1. Wu's (1969) formulae, which are approximations of more complex theoretical formulae, are probably the most frequently used.

A recent, and as yet not fully developed finding concerns anomalously low drag coefficients over shallow water (Hicks, Drinkrow and Grauze, 1974; and Hsu, 1975). Hicks hypothesizes that this may be due to the absence of high frequency surface waves in shallow water, producing an aerodynamically smooth surface. He qualifies this hypothesis, however, by noting the possible influence of a biological film on the water surface, a factor which is probably also present in Hsu's study. Despite this possible interference, Hicks proposes a relation for shallow water based on an aerodynamically smooth surface:

$$C_z = \frac{\kappa}{\ln(Bu_*z/\nu)}$$

where, κ is von Karman's constant, 0.41;
 B is a constant, equal to 9;
 u_* is the wind friction velocity; and,
 ν is the kinematic viscosity of water.

The equation is plotted in Figure 5.2 along with Wu's formula. Hicks' formula is implicit since u_* is a function of C_z , and thus it must be solved iteratively. Hicks had

insufficient data to specify an exact range of applicability, but roughly estimated the formula to be appropriate for water shallower than 3 to 7 meters.

Table 5.1
Wind stress drag coefficients

<u>Reference</u>	<u>C₁₀, Drag Coefficient</u>	<u>Wind Speed Range</u>
Wu (1969)	$1.25 \times 10^{-3} W_{10}^{-1/5}$	$W_{10} < 1 \text{ m/s}$
	$0.5 \times 10^{-3} W_{10}^{1/2}$	$1 < W_{10} < 15 \text{ m/s}$
	2.6×10^{-3}	$W_{10} > 15 \text{ m/s}$
Wilson (1960)	1.66×10^{-3}	light winds
	2.37×10^{-3}	strong winds
Ottesen-Hansen (1975)	0.8×10^{-3}	$W_{10} < 7 \text{ m/s}$
	1.0×10^{-3}	$W_{10} > 7 \text{ m/s}$
Banks (1975)	$9.0 \times 10^{-3} W_{10}^{-1/2}$	"small" winds
	3.8×10^{-3}	"medium" winds
	$0.7 \times 10^{-4} W_{10}$	"large" winds
Ruggles (1970)	1.6×10^{-3}	$2 < W_{10} < 10 \text{ m/s}$

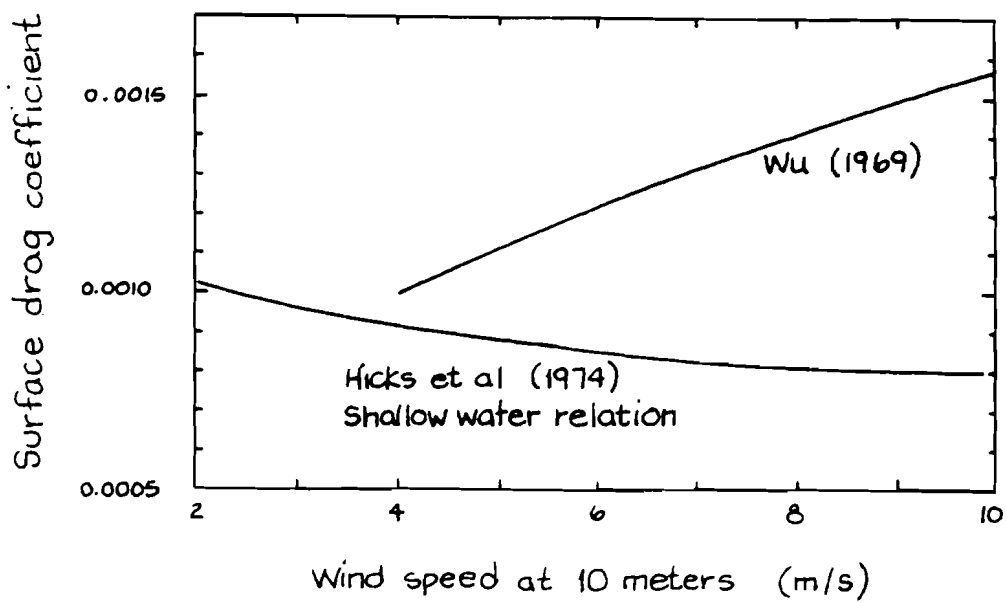


Figure 5.2

Surface drag coefficients as a function of wind speed
 (from Hicks, Drinkrow and Grauze, 1974)

5.3 Bottom Friction

There are two possible boundary conditions which may be specified at the lake bottom: the no-slip condition,

$$u = v = 0 \quad \text{at } z = H \quad (5.2)$$

or, a shear condition,

$$\rho A_v \frac{\partial u}{\partial z} = \tau_b^x \quad \rho A_v \frac{\partial v}{\partial z} = \tau_b^y \quad (5.3)$$

Lien and Hoopes (1978) state that the solution for mass transport in deep lakes is not influenced by the bottom condition. They define a deep lake as one having a depth, H , such that:

$$H > 4 \sqrt{\frac{2A_v}{f}} = \frac{4d}{\pi} \quad (5.4)$$

where the parameter,

$$d = \pi \sqrt{\frac{2A_v}{f}}$$

is known as the Ekman depth, or the depth of frictional influence.

The choice of bottom boundary conditions carries greater influence in shallow water. For example, Murray (1975) found that a no-slip boundary led to unrealistically low current predictions when compared to field observations. His findings may result partially from his use of a constant vertical eddy viscosity as well, however. In any event, the shear boundary condition is favored by most modelers.

Cheng, Powell and Dillon (1976) describe the possible forms for the shear boundary condition in terms of the general relation,

$$\tau_b^x = BU \quad \tau_b^y = BV \quad (5.5)$$

where, U and V are the mass transports in the x and y horizontal directions; and, B may take on a number of forms.

They define three possible forms for B, which will be described in turn.

Linear friction laws define $B = k/h$ where k is a constant. We may broaden their definition somewhat to include all linear relations of the form:

$$\tau_b^x = c_b u_b \quad \tau_b^y = c_b v_b \quad (5.6)$$

where c_b is a constant; and, u_b and v_b are the velocities at or near the bottom.

Linear relations of the form of Equation 5.6 are used by Nelson (1979) and Lien and Hoopes (1978). These linear forms are sometimes called slip conditions, since they permit a slip velocity at the bottom. In the limit that k or c_b approaches infinity, the linear forms converge to a no-slip condition. The linear laws lead to a weak dependence of friction on the depth or current strength.

In quasi-linear friction laws, B takes the form,

$$B = k/h^2 .$$

These forms remain linear with respect to the mass transport, keeping the computation simple, but include higher order depth dependence. They show strong influence due to depth, but not currents.

The most rigorous friction laws are based on the Chezy or Manning relations of open channel hydraulics. For these non-linear, or quadratic, friction laws, B takes the form:

$$B = \frac{k \sqrt{U^2 + V^2}}{h^2}$$

which includes strong dependency on both current and depth. Leenderste (1970) employs this form in his model, using the Chezy coefficient, C:

$$\tau_b^x = \frac{\rho g U}{C} \sqrt{U^2 + V^2} \quad \tau_b^y = \frac{\rho g V}{C} \sqrt{U^2 + V^2} \quad (5.7)$$

The quadratic is considered the most accurate friction law, but carries a substantial computational burden due to the non-linear dependence on current. The additional computation is needed since the current must be determined by an iterative solution, rather than the direct solution possible with linear and quasi-linear friction laws.

Lick (1976) also reviews the common friction laws, though using a slightly different general form than Cheng, Powell and Dillon. He recommends that the quasi-linear law be used for shallow water, defining

$$k = \rho A_v \frac{du}{dz}$$

For deep water, he suggests the linear form.



6 LAKE BALATON: MODELING BACKGROUND

6.1 General Characteristics of Lake Balaton

This section will be purposefully brief, giving only a summary of the important characteristics of Lake Balaton, since thorough and complete information on the lake is available elsewhere in van Straten, Jolankai and Herodek (1979) and van Straten and Somlyody (1980). We choose instead to concentrate our efforts on a detailed examination of circulation and hydrodynamics in the section which follows.

Lake Balaton, the largest lake in central Europe, is located in western Hungary. The lake is long and narrow (75 km by 8 km) with a surface area of roughly 600 square kilometers. It is a lake which is extremely shallow, particularly in relation to its large horizontal extent. The average depth of the lake is only 3.14 meters, and it is everywhere less than 5 meters deep except in one very small area. In this one deep section, where the Peninsula of Tihany nearly divides the lake, the width is less than 2 km and the depth reaches 11.7 meters. A map of the lake showing depth contours is included as Figure 6.1.

Lake Balaton and the surrounding countryside are a major tourist attraction for both Hungarian and foreign visitors. Pleasant weather and good water quality make the lake a particularly popular summer resort. Unfortunately, increasing population and development are apparently taking their toll on the lake, a fact demonstrated by the deterioration of the lake water quality over many years of measurements. This deterioration has been particularly rapid during the last decade, and indicates an accelerating eutrophication of the lake.

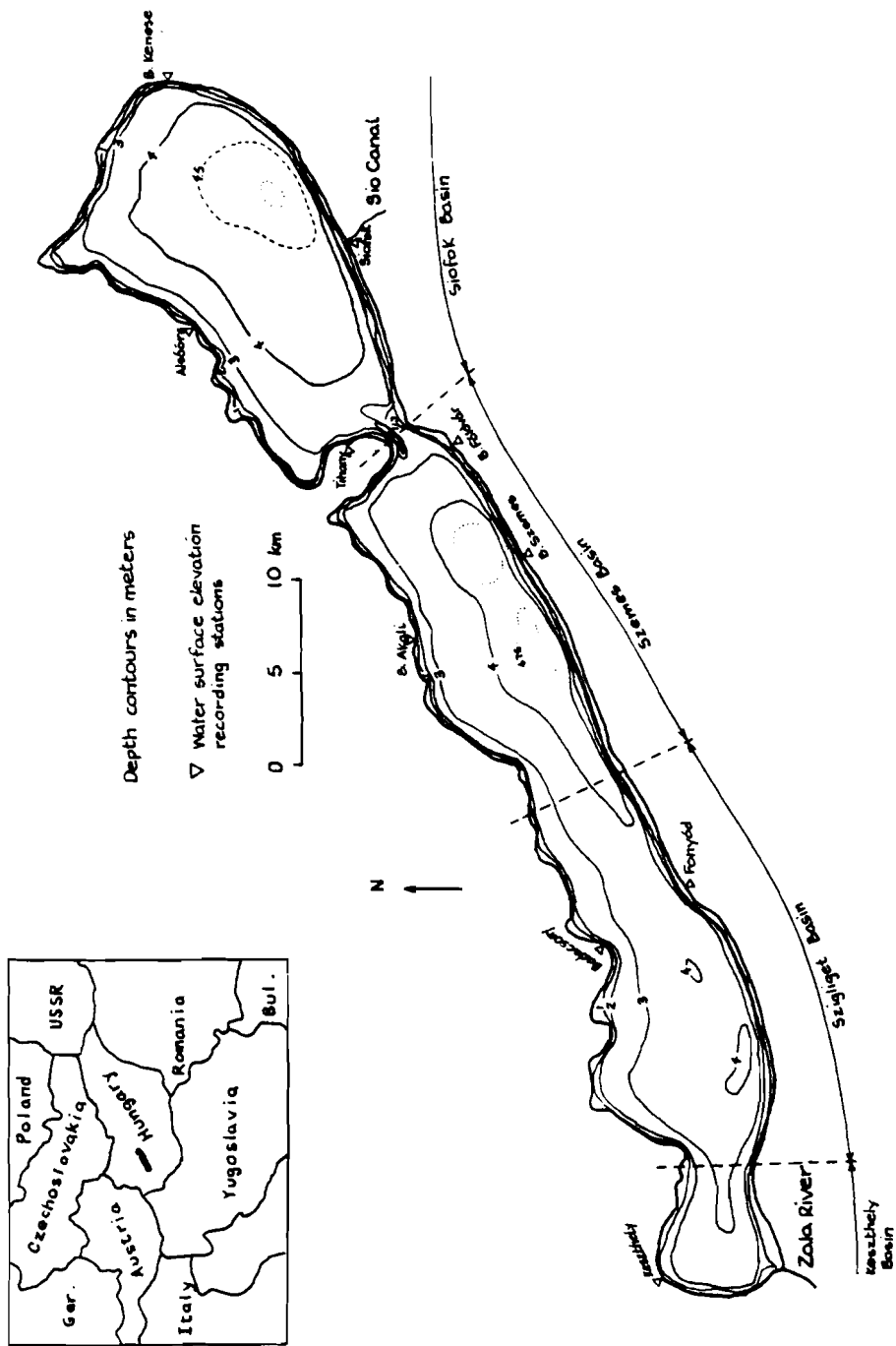


Figure 6.1
Map of Lake Balaton

6.2 Circulation in Lake Balaton

Although the existing data base is far from complete, sufficient information exists to construct an approximate description of Lake Balaton's circulation. The circulation is a composite produced by hydrologic flow through the lake, wind-induced currents, seiching, and other lesser influences. The major unknown aspects of water motion in the lake are the character of spatial variations in the current over both horizontal and vertical space, and the response of the circulation to changes in wind forces over short time periods.

6.2.1 Hydrologic Flow

We define hydrologic flow as that produced by the inflow of water to the lake from streams, runoff and rainfall, and the outflow from the lake by evaporation and stream discharge. In Balaton, such flow is dominated by the mean flow established by the stream and river inflows concentrated at the southwestern end of the lake, and the sole outlet at the Sio Canal at the lake's opposite end. The largest inflow is that from the Zala River, which drains roughly half of the watershed contributing to the lake.

The mean annual flow quantities due to the various hydrologic components are 18 m³/s due to streamflow and runoff, 12 m³/s from precipitation, 17 m³/s removed by evaporation, and the discharge of 13 m³/s at the Sio Canal. The total lake volume is 1860 million cubic meters, so that the mean hydraulic residence time is roughly two years. The longitudinal transport velocities associated with these hydrologic flows are small, on the order of 0.05 cm/sec.

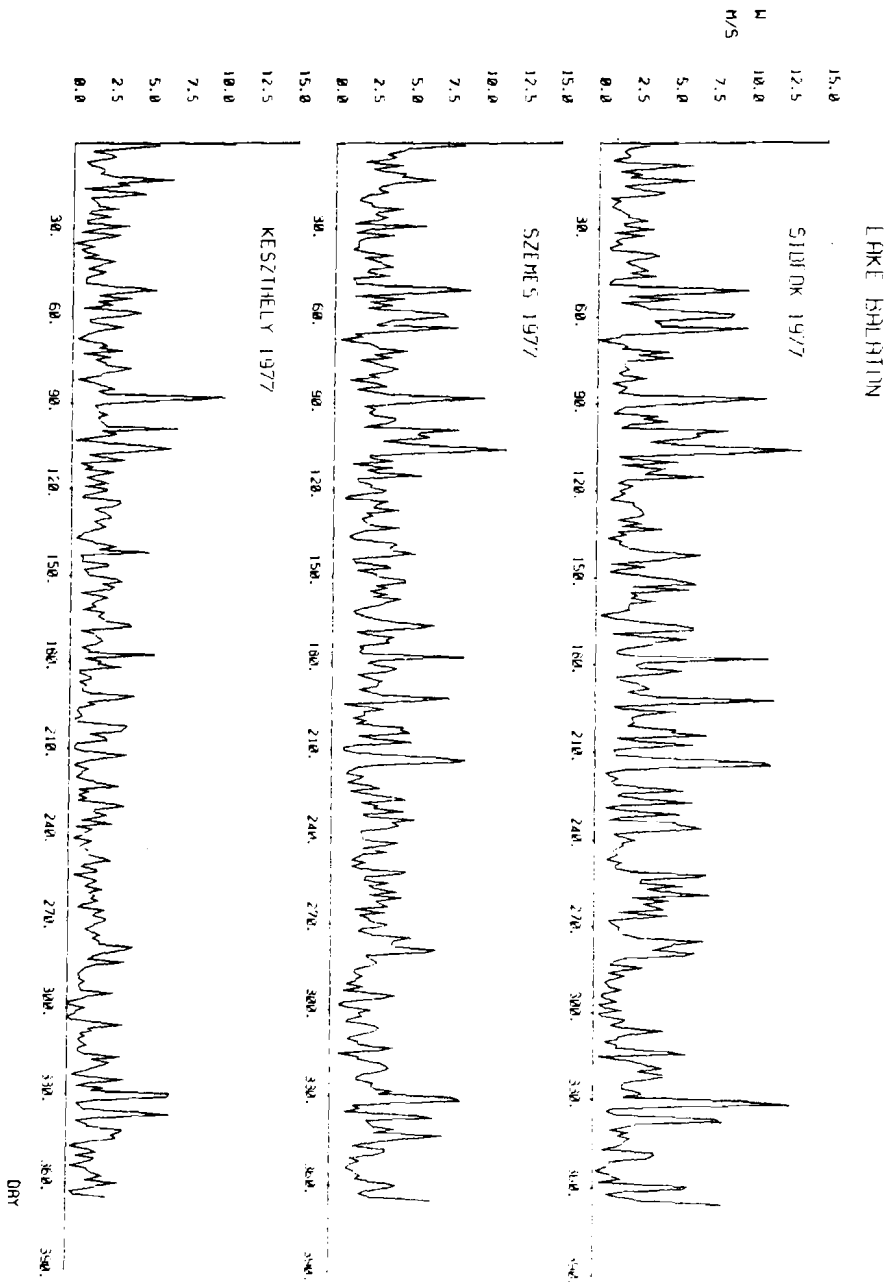
6.2.2 Wind-Driven Flows

The influence of the wind overwhelms the slow hydrologic flow in establishing the pattern of flow in Lake Balaton. The shallowness of the lake permits a circulation response to even mild winds, producing currents at least an order of magnitude greater than those due to the hydrologic flow.

Surrounding hills, and the geography of the lake itself, exert a major influence upon the circulation caused by the wind. The hills produce local sheltering effects by blocking the wind, leading to a spatially non-uniform wind field. Keszthely Bay, for example, typically experiences lighter winds than most of the lake (Figure 6.2). The circulation is further modified by the constraints imposed by the lake boundaries. Although comprehensive field observations of the lake circulation have not been made, a very rough picture of the circulation is found in the work

Comparison of observed daily average wind speeds at Kesztheley, Siófok and Balatonszemes, 1977

Figure 5.2



of Gyorko (cited in Somlyódy, 1979). Gyorko used a physical hydraulic model of the western part of the lake to model circulation and sediment transport under artificial steady winds. Owing to a severe vertical scale distortion in the model (a factor of 20), the results must be considered qualitative. They do show, nevertheless, a complex system of flow gyres greatly influenced by the lake geometry (Figure 6.3).

The vertical structure of wind-induced currents in the lake were the subject of recent field measurements conducted as a part of this study. The theory of wind-driven circulation predicts, for steady conditions, a profile such as that shown in Figure 6.4, where currents at the surface align with the wind, but an opposing return current is found along the bottom (Plate, 1970 or Liu and Perez, 1971). Although derived for steady winds and idealized geometry, a generally similar velocity profile could be reasonably anticipated in a lake.

In our field studies, we sought a qualitative description of the actual vertical velocity profile in Balaton, to be contrasted with the profiles given by theory and our model results. We employed a simple electromagnetic current meter (Marsh-McBirney Model 201) capable of measuring speeds between 2 and 300 cm/sec in a single direction to an accuracy of $\pm 2\%$. The meter is equipped with a velocity probe which is connected by 12 meters of cable to an electronics case with a visually read meter. Observations were made by lowering the probe, attached to a measured metal pipe, to various elevations in the water and rotating the pipe until the direction of maximum velocity was found. A complete description of the field studies, including tables and figures of the observed currents, is included as Appendix A of this report. In brief, the observations adhered to the theoretically predicted profile only occasionally. More typical was a highly transient velocity structure, with increasing variability as the measurement depth increased. Apparently, the currents experience the conflicting influences of the lake-wide seiche motion and the local wind-driven motion as well as the inherently transient process of turbulent momentum transport. One exception to this picture of transience and variability was in the Strait of Tihany where our observations of strong, unidirectional currents in the upper five meters corroborate Muszkalay's (1973) observations discussed in the following section.

6.2.3 Seiches

A seiche is the pendulum-like motion of the lake water surface after the cessation of a force which has displaced the surface from its equilibrium, level position. The most

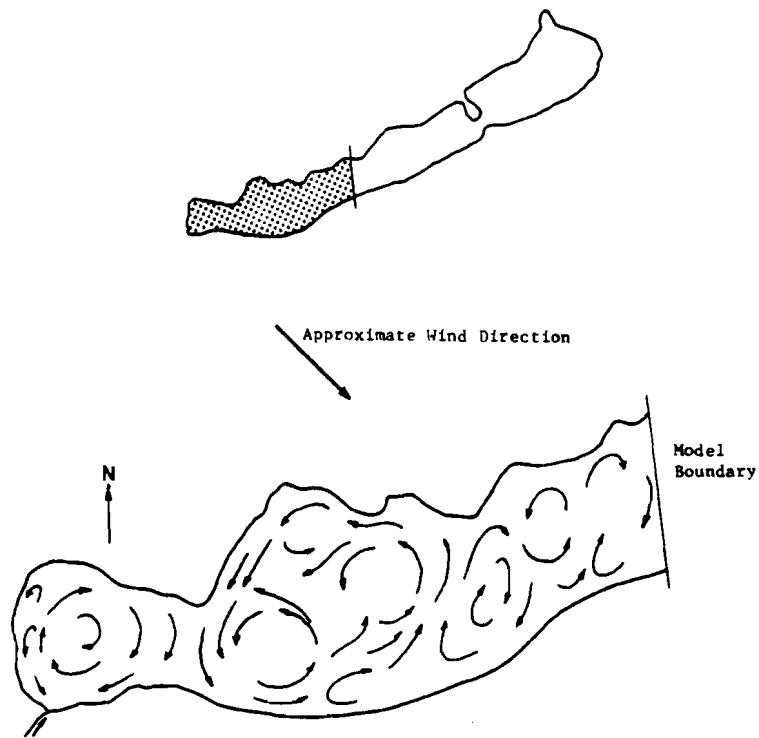


Figure 6.3

Circulation from physical hydraulic model
(from van Straten et al, 1979)

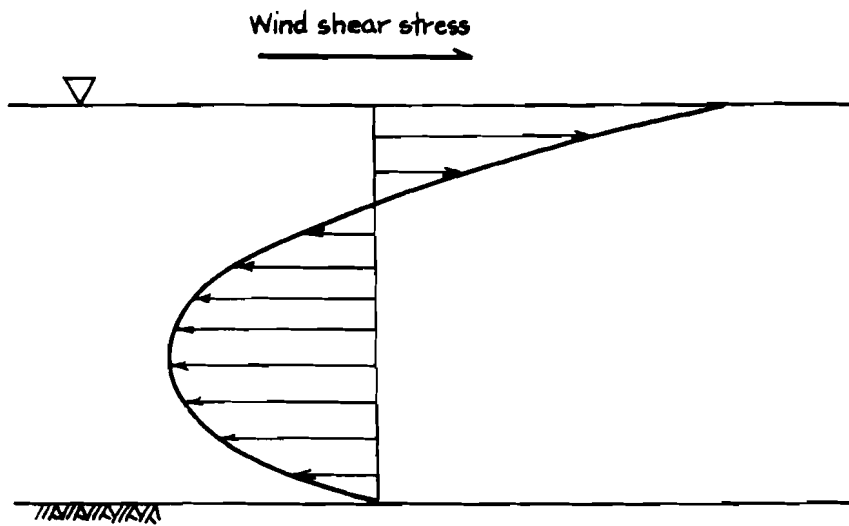


Figure 6.4

Theoretical wind-induced velocity profile
(after Liu and Perez, 1971)

common forcing agent causing seiches is the shear force of a sustained wind. Such a wind will cause a set-up, the superelevation of water level on the upwind shore above the level, undisturbed position. When the wind stops blowing, the superelevated waters will flow downward, initiating the periodic seiche motion. Seiches may be especially significant in shallow lakes, since the magnitude of set-up increases as mean water depth decreases (Sibul, 1955).

The seiche is a well observed phenomenon in Lake Balaton, with different seiche periods arising according to the direction and location within the lake. Hutchinson (1975) reports a longitudinal seiche period of between 10 and 11.5 hours, while the transverse seiche is but 40 minutes. Other seiche periods have been distinguished for the portions of the lake to the east and west of Tihany Strait (1 hour and 2.5 hours respectively).

The most detailed studies of Lake Balaton's seiche are those of Muszkalay (1973). Muszkalay collected nearly a full decade of water surface elevation observations at up to ten stations around the lake. Simultaneous measurements of wind speed at one or two stations and occasionally of water current in the Strait of Tihany complete his data base. The measurements show the lake to be in seemingly constant motion. A strong wind, of only a few hours duration, can lead to observable seiches and a typical month-long record from Muszkalay clearly shows frequent events with both longitudinal and transverse modes evident (Figure 6.5).

With his observations as a basis, Muszkalay (1966) determined empirical formulae relating the wind strength, duration and direction to the resulting denivellation. His formula for longitudinal slope due to winds directed within 22.5 degrees of the lake's long axis is:

$$J = 0.038 T^{0.25} (W_L - 2.8)$$

where, J is the slope of the water surface (cm/km);
 T is the wind duration (hours); and,
 W_L is the longitudinal wind component (m/s).

In this relation, J is determined from the difference in the extreme stages at Kesthely and Balatonkenese. It is a fictitious quantity in the sense that these stages may not, in fact, occur at precisely the same time; however, the time

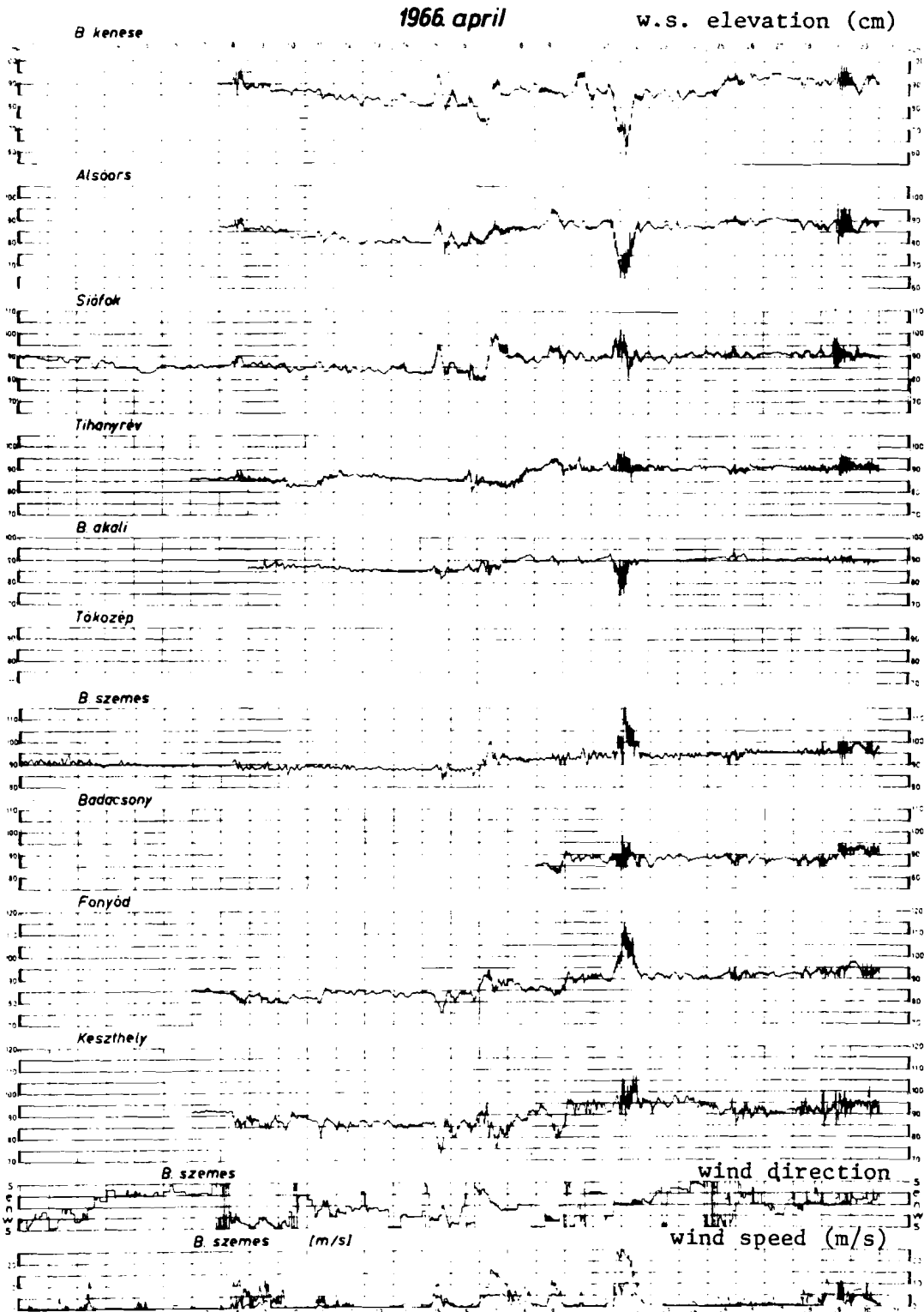


Figure 6.5

Typical water surface elevation records showing seiche motions (from Muszkalay, 1973)

lag is not large. The maximum observed longitudinal denivellation (that is, the net difference from one end of the lake to the other) is roughly one meter. In the transverse, which is the more common direction for strong winds, a denivellation of 0.4 meter has been observed.

The creation of a set-up, and subsequent seiche oscillation, is accompanied by the transport of considerable quantities of water. This is particularly obvious where the Lake narrows at Tihany. Muszkalay took advantage of this geometry and deployed four current meters in the Tihany Strait, placing the meters along a single vertical mooring line. Unfortunately, only intermittent records of these measurements are available, and then as the plot of a single velocity history at one meter below the water surface. Muszkalay reports that his measurements were virtually always unidirectional throughout the water depth; thus, the 1 meter observation is probably a good indicator of velocity for the entire water column. The maximum velocity observed by Muszkalay was 1.4 meters/sec (reported in Somlyody, 1979). Figure 6.6 shows a typical set of measurements relating wind, water surface motion, and velocity at Tihany. The event of Figure 6.6 is caused by a wind transverse to the lake, the predominant direction for storm winds and the type of event comprising most of Muszkalay's published examples.

A significant factor in the behavior of seiches is the force of friction, an influence magnified by the shallowness of Lake Balaton. The effects of friction are to lengthen the observed oscillation period to greater than that predicted by frictionless theory, and to quickly attenuate the seiche amplitude (Hutchinson, 1975). Frictionless theory predicts the period, T, to be:

$$T = 2L/\sqrt{gH}$$

where, L is the lake length;
g is the acceleration of gravity; and
H is the mean lake depth.

This computes to 7.3 hours in Balaton, well below the observed period of 10 to 11.5 hours. According to Hutchinson, such a marked decrease in the period is a phenomenon unique to shallow lakes, with Balaton and Lake Okeechobee in Florida the only observed examples.

The seiche motions caused by transient winds on Lake Balaton are very complex and tend to obscure the underlying basic behavior. Some of this complexity may be eliminated

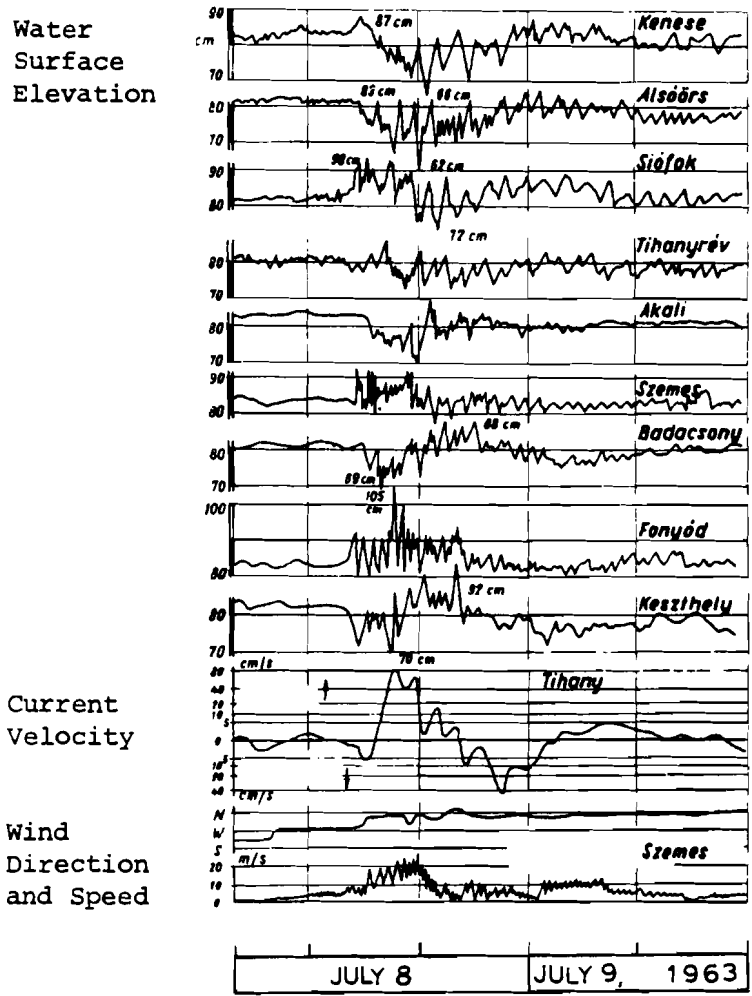


Figure 6.6

Example of Muszkalay's (1973) seiche observations.

by invoking simple models of the lake which can be solved analytically. The simplest such model is to consider the lake as two connected oscillating basins, each with a level water surface, and presuming that all frictional energy losses are concentrated at the Strait of Tihany. With this model, we can address two fundamental aspects of the lake's seiche behavior: the free response and the forced response. Seiches are primarily free oscillation responses, the actions occurring in the absence of forces: that is, after the wind has stopped. If the equations of the two-body system are solved for the free oscillation problem we find that two major system responses occur depending upon the geometrical and frictional characteristics of the lake. With the first response type, that of a heavily damped system, any initial displacement of the system from equilibrium simply decays exponentially, without any subsequent oscillatory motion. The second response is the lightly damped system, in which the system exhibits a sinusoidal oscillation, but with an exponentially decreasing magnitude.

The forced response of the lake concerns behavior under imposed wind forces of various frequencies. The two-body model yielded credible results for Kenney (1980) in an analysis of the forced response of Lake Winnipeg, Canada. Winnipeg is surprisingly similar to Balaton in its geometry: it is relatively shallow (12 m), long and narrow (440 by 55 km), and consists of two distinct basins separated by narrows. As in Balaton, the narrows are the location of the greatest depth in the lake (roughly 37 m) and experience strong currents (up to 90 cm/s) due to seiche motion. Kenney employed the two-body oscillator as a conceptual model to explain the lake's frequency response behavior, which he had determined statistically by analysing time series of water surface elevation about the lake. Although his methods proved useful, and demonstrated the validity of the two-body system as a simple lake model, Kenney failed to relate the model parameters to the physical characteristics of the lake; he relied instead upon his considerable statistical information. Thus, it is not possible to extend his findings to Balaton without a similar statistical analysis.

A more physically-based study of seiching is Platzman's (1963) mathematical model of Lake Erie. Platzman solved the simplified one-dimensional equations of motion to relate the seiche response to the lake characteristics. The characteristics are represented by the Proudman number, which is related to the ratio of the viscous decay time to the seiche period, and is defined as:

$$P_r = \frac{A^2 v}{k^2 g H^5}$$

where, k is the wave number, equal to π/L for the uninodal seiche.

Platzman found from his simplified analysis that the seiche motion will be heavily damped if the Proudman number exceeds a critical value of 0.53. Only below this critical value will oscillatory motion be found. In Chapter 8, we will show this relation to hold for our computer simulations of Lake Balaton.

Platzman also investigated the nature of the decay in seiche amplitude and found it to be constant in time for his linear system. In contrast, attenuation of the seiche in Lake Balaton depends upon the seiche magnitude. Figure 6.5, for example, shows large initial damping of the seiche of April 22, 1966, although residual motions persist through the 23rd and 24th despite very light winds. The different rates in attenuation of high and low amplitude waves is contrary to Platzman's linear theory, and suggests that non-linear frictional forces are important in Balaton.

7 A MODEL OF WIND-DRIVEN CIRCULATION IN SHALLOW LAKES

7.1 Brief Description of the Model

The model which has been employed in this study was developed by Cooper and Pearce (1977) for application to coastal oceanic waters, and later modified by Nelson (1979) for studies of lake circulation. It has been additionally modified in this study for application to shallow lakes. The model solves the simplified equations of motion to determine the three-dimensional structure of the horizontal currents in the lake, as well as the variation in elevation over its surface. A Galerkin technique is used to represent the horizontal velocity as a continuous function in the vertical. With the Galerkin scheme, the velocity is given as a summation series of the form:

$$u(z) = u_0(z) + \sum_{j=1}^n c_j \cos \frac{a_j z}{h} \quad (7.1)$$

where, u_0 is a defined base function dependent upon the surface shear stress, water depth, and eddy viscosity;
 c_j are expansion coefficients; and
 a_j are prescribed constants which depend upon the boundary conditions and eddy viscosity.

Using this method, solution for the horizontal velocities becomes the problem of solving for the expansion coefficients, c_j , as a function of the horizontal coordinates, x and y . The technique permits the eddy viscosity to be a variable function of the depth.

The Galerkin model is fully transient, determining the horizontal current velocities and the water surface elevation as functions of time due to unsteady wind forces. In terms of its formulation, the model is of the Ekman-type, in that it employs the linearized equations of motion (without the convective terms) and uses analytical expressions for the vertical velocity distribution. The Ekman solution method is enhanced, however, by the ability of the Galerkin technique to form a weighted average of multiple vertical velocity distributions. The resulting equations are solved by finite difference techniques.

7.2 Galerkin Model Formulation

7.2.1 Governing Equations

The equations of motion upon which the Galerkin model is based employ the shallow-water approximation and omit both the convective acceleration terms and the horizontal shear terms. The simplified equations are thus:

$$\frac{\partial u}{\partial t} = -g \frac{\partial \eta}{\partial x} + fv + \frac{\partial}{\partial z} (A_v \frac{\partial u}{\partial z}) \quad (7.2)$$

$$\frac{\partial v}{\partial t} = -g \frac{\partial \eta}{\partial y} - fu + \frac{\partial}{\partial z} (A_v \frac{\partial v}{\partial z}) \quad (7.3)$$

where the notation is the same as in Chapter 3. The vertically integrated form of the mass conservation equation is employed:

$$\frac{\partial U}{\partial x} + \frac{\partial V}{\partial y} = \frac{\partial \eta}{\partial t} \quad (7.4)$$

where the mass transports, U and V , are defined by Equation 3.21.

The equations of motion are subject to shear boundary conditions at the surface and lake bottom. The surface boundary condition relates the wind surface stress to the gradients of horizontal velocity:

$$\tau_s^x = -\rho A_v \frac{\partial u}{\partial z} \quad \tau_s^y = -\rho A_v \frac{\partial v}{\partial z} \quad \text{at } z = 0 \quad (7.5)$$

Here, the small amplitude approximation is used to apply the surface condition at $z=0$ rather than at $z=\eta$. The wind-induced surface stress is calculated using Equation 5.1 with either the Wu (1969) or Hicks et al (1974) definitions of the drag coefficient.

At the bottom boundary, the model employs a linearized shear stress condition:

$$\tau_b^x = -\rho A_v \frac{\partial u}{\partial z} = \rho c_b u \quad \text{at } z = h \quad (7.6)$$

$$\tau_b^y = -\rho A_v \frac{\partial v}{\partial z} = \rho c_b v \quad \text{at } z = h$$

or,

$$\frac{\partial u}{\partial z} = -\frac{c_b u}{A_v} \quad \frac{\partial v}{\partial z} = -\frac{c_b v}{A_v} \quad \text{at } z = h \quad (7.7)$$

where c_b is a frictional coefficient.

The model permits the vertical eddy viscosity to vary with depth as shown in Figure 7.1. The formula for A_v in the k th linear segment is:

$$A_v = \alpha_k z + \beta_k \quad h_k < z < h_{k+1} \quad (7.8)$$

where, α_k is the slope of the k th linear segment; and β_k is its intercept with the free surface.

7.2.2 Galerkin Formulation

The Galerkin technique begins by approximating the dependent variables, u and v , by the expressions:

$$\hat{u} = u_o + \sum_{j=1}^n c_j \Omega_j \quad (7.9a)$$

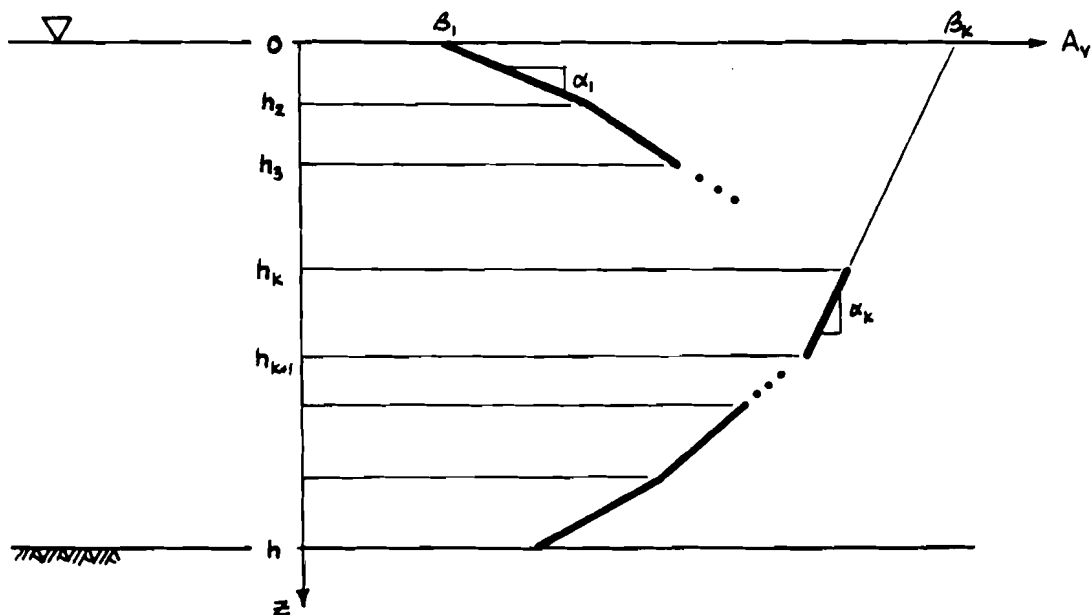


Figure 7.1

Piecewise linear form of the vertical eddy viscosity

$$\hat{v} = v_0 + \sum_{j=1}^n d_j \Omega_j \quad (7.9b)$$

where \hat{u} and \hat{v} represent approximations to u and v . The functions u_0 , v_0 and Ω_j are prescribed functions of z , selected so as to satisfy the boundary conditions at the free surface and bottom. The base functions, u_0 and v_0 , which include dependencies upon the vertical eddy viscosity, surface shear stress and water depth, are fully described in Appendix B. The c_j and d_j are expansion coefficients which must be determined in this application as functions of x and y .

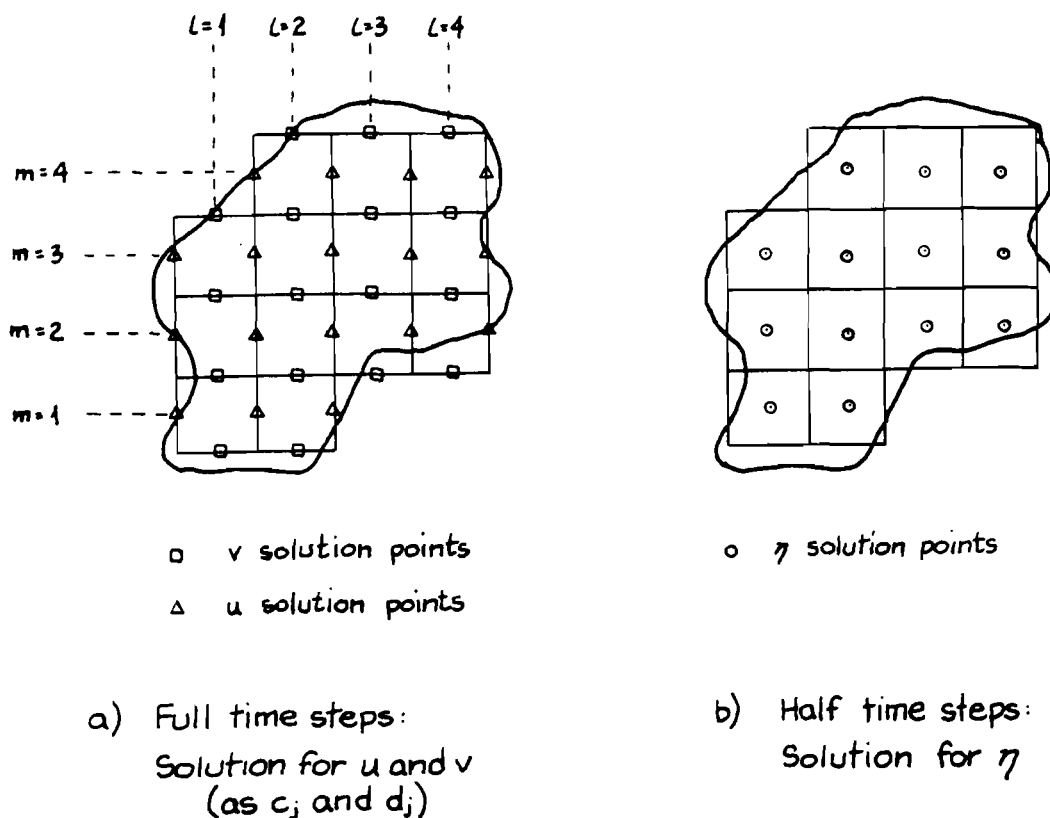


Figure 7.2

Finite difference solution procedure

A mixed finite difference method advances the solution in time: the momentum equation is solved explicitly over horizontal space, but is treated implicitly within each finite difference grid to find the variation of velocities in the vertical. Solution of the continuity equation alternates with that of the momentum equation, with explicit solution for the water surface displacements at the grid centers. This implies the use of a so-called "staggered grid", since velocities are found on the grid sides rather than centers. (See Figure 7.2.) The net result of the solution process is the time history of horizontal velocity and water surface elevation throughout the lake.

More complete details of the model formulation and its derivation are included as Appendix B of this report.

7.3 Modeling Considerations

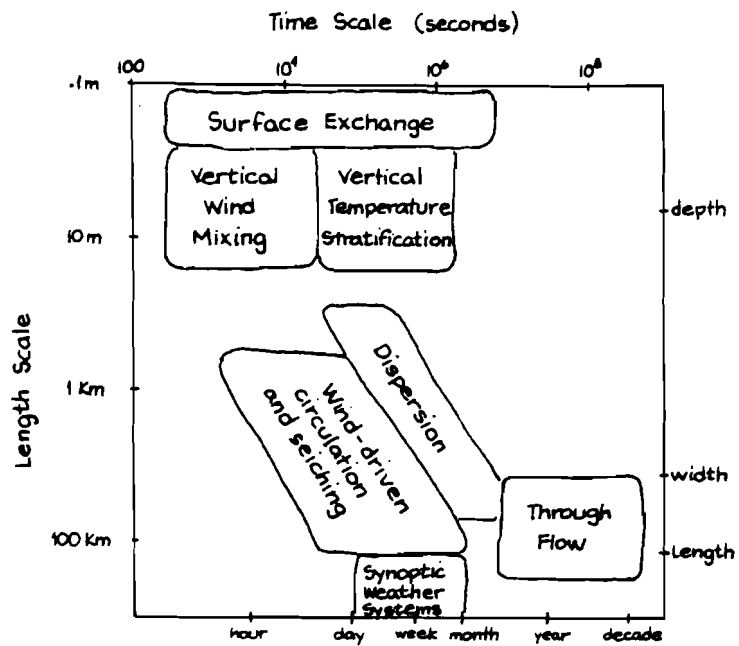
A preliminary analysis of the requirements for a circulation model can simplify its application and better its possibilities for success. In this section, therefore, we will examine our model in two contexts: as a coupled component of a water quality model, and as a model of lake hydrodynamics alone. The first examination will identify those phenomena which the model must consider if it is to be consistent with the biochemical processes which are our eventual modeling objective. The second examination will consider the suitability of the circulation model formulation to the geometry and hydrodynamics occurring in the lake.

7.3.1 Coupled Circulation and Water Quality Models

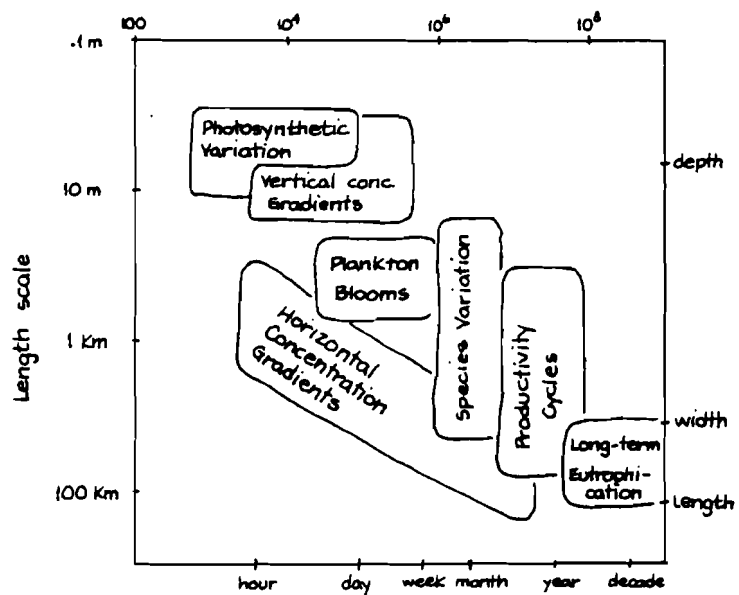
Although we restrict our attention in this report to modeling the circulation of shallow lakes, our eventual research goal is the development of a comprehensive eutrophication model which couples both hydrodynamic and biochemical components. Hence, we cannot consider the circulation model only in terms of its ability to model the lake's hydrodynamics, but must consider how it fits within the broad framework as well. At this point in the research, the form of the biochemical model and the method of coupling remain undetermined, preventing detailed examination of model compatibility. Nevertheless, the circulation model can be evaluated for consistency with the processes transpiring in the lake - a necessary condition for the success of any model, either hydrodynamic or biochemical.

Very roughly, the biochemical model represents the transport and transformation of important substances, particularly nutrients, within the lake. It is based upon the equations of mass conservation for a set of chemical and biological state variables, for example, dissolved oxygen or the various forms of phosphorus. Most of the effort in such models is expended in representing the transformations between the state variables.

Hydrodynamic processes in the lake interact with the biochemical processes by transporting and mixing the state variables. Only by coupling hydrodynamic and biochemical model components can the crucial description of advective and diffusive transports be provided. The success of such a coupled model depends, however, upon the consistency of the components with each other and with the processes within the lake. A good indication of this consistency is supplied by an examination of the length and time scales important in the lake's behavior.



a) Physical Processes



b) Biogeochemical Processes

Figure 7.3

Approximate length and time scales in Lake Balaton
 (Based upon Harleman and Shanahan, 1980 and Brown, 1978)

The magnitudes of the length and time scales of the major physical and biochemical processes in Lake Balaton are depicted in Figure 7.3. Though approximate, the time and length scale diagrams serve to illustrate some important considerations for modeling. For example, we can see that wind-driven circulation corresponds with horizontal concentration gradients at a length scale on the order of a kilometer and a time scale of one or a few days. Vertical processes occur over somewhat shorter time scales with a length scale on the order of the lake depth, a few meters. Long-term eutrophication proceeds slowly at lake-wide length scales in rough correspondence with the hydrologic through-flows. These correspondences of physical and biological scales illustrate clearly those processes which we can expect to interact strongly, and those which we can assume to be essentially independent. For example, hydrologic through-flows will not affect the vertical variation of nutrient and organism concentrations, which respond instead to the wind-induced vertical mixing and the creation and destruction of temperature stratification.

We can add substance to these qualitative comparisons with at least one quantitative example from Lake Balaton: an evaluation of the relative importance of hydrologic through-flow and seiche currents. For estimates of the hydrologic through-flow, we draw upon van Straten, Jolankai and Herodek (1979). Through water balance calculations, they compute inter-basin flows for the four lake basins shown in Figure 6.1. Translating their results into volume transports over various time periods produces the quantities given in Table 7.1. For comparison, the volume of water transported by a typical amplitude seiche can be estimated. Assuming a difference in water surface elevation of one half meter between the ends of the lake and a linear water surface profile, the amount of water transported across the seiche nodal line is on the order of 75 million cubic meters in a time period of about 6 hours. This volume is roughly twice that transported in a month by the hydrologic flows, and two orders of magnitude greater than the monthly flows scaled down to six hours. Yet, over a year, the seiche motion produces no net flow into or out of the lake, while the hydrologic flows replace roughly 50% of the total lake volume. Our conclusion is clear: over the short time scale, the seiche dominates; over long time periods, the hydrologic flow governs.

This analysis of length and time scales illustrates some important concepts which the modeler must consider. First, the water quality model must account not only for the particular biochemical processes of interest, but also the corresponding physical processes as well. And, to represent these processes and their interaction successfully, the model must operate at the correct length and time scales.

Table 7.1

Volume transports between the Balaton sub-basins
(from van Straten, Jolankai and Herodek, 1979)

	Keszthely to Szigliget	Szigliget to Szemes	Szemes to Siofok
Annual	297	439	444
Summer Half-Year	133	197	200
Winter Half-Year	164	242	244
Monthly Average	25	37	37
Maximum Monthly	42	58	53
Minimum Monthly	16	25	28

All quantities are in million cubic meters.

This latter point has been demonstrated in an extensive modeling study of Lake Ontario conducted by the Canadian Centre for Inland Waters (Simons and Lam, 1980). Simons and Lam coupled hydrodynamic and biochemical models to develop a three-dimensional model of Lake Ontario's transient water quality. The lake was simulated over a number of years using a time step on the order of a day and a spatial grid of roughly 5 kilometers. Significantly, the authors conclude that the model, though able to predict seasonal and shorter term trends, is unable to model trends over a few years with high accuracy. (This is not a serious fault, in our opinion, for the evaluation and comparison of alternative lake water quality control schemes, for which seasonal simulations are sufficient indicators.)

Our water quality model of Lake Balaton is intended to represent spatial variation within the lake and dynamics over periods of a few days to as long as seasons. These scales clearly fall below the realm dominated by hydrologic flows only, and we must thus consider the motion due to seiche and wind-driven circulation as well.

7.3.2 Circulation Model Applicability

The Ekman-type circulation model, as explained in Chapter 3, offers both advantages and disadvantages. By far its greatest advantage is its simplicity and consequent low simulation expense. This is made possible, however, by a number of assumptions and approximations which may limit the use of the model. Therefore, before we can use such a model with confidence, we must first examine its assumptions in light of the criteria given in Chapter 4 and the physical characteristics of the application lake.

The Galerkin model proposed for our study of Lake Balaton makes use of the shallow water approximation, neglect of convective accelerations, and neglect of horizontal frictional forces. In addition, the rigid lid approximation, though not currently employed in the model, is possible and would allow significantly longer simulation time steps. These approximations will be examined in turn below. The basis for the examination are the physical parameters gathered from various sources in Table 7.2. In this table, the value of the horizontal eddy viscosity has been assumed based on similar data published for other lakes. Although the value used is reasonable for Lake Balaton, it was not, in fact, determined by actual measurements. Also included in Table 7.2 are the various dimensional numbers (force ratios) computed from the physical parameters.

The shallow water assumptions are permitted if the lake depth is sufficiently small. In Balaton, the ratio of depth to length is on the order of 10^{-4} . Additionally, the Ekman friction depth, which indicates roughly the depth to which wind surface stress will be influential, is at least 14 meters. This is sufficiently greater than the average lake depth that the lake may be classified as "very shallow" under criteria given by Lindijer (1979). Finally, field measurements reveal that the lake's vertical stratification is weak and intermittent (Entz, 1976). These data safely assure the propriety of using the shallow water assumptions.

Neglect of convective acceleration is permissible if the Rossby number, the ratio of inertial to Coriolis forces, is small. As seen in Table 7.2, this ratio lies within the range of 0.02 to 0.2, sufficiently small to permit neglect of the convective terms and allow the Ekman model to be used. Even smaller is the horizontal Ekman number, easily allowing the neglect of viscous effects in the horizontal plane.

The condition to impose a rigid lid condition is that the square of the seiche period be much less than the square of the inertial period. This criterion is easily satisfied in

Table 7.2
Physical parameters for Lake Balaton

Length	$L = 75 \text{ km}$
Width	$W = 8 \text{ km}$
Depth	$H = 3.2 \text{ m}$
Velocity (due to seiche)	$U = 0.20 \text{ m/s}$
Coriolis parameter	$f = 10^{-4} \text{ rad/s}$
Horizontal eddy viscosity (assumed value)	$A_H = 10^6 \text{ cm}^2/\text{s}$
Vertical eddy viscosity	$A_V = 5 \text{ to } 100 \text{ cm}^2/\text{s}$
Froude number	$Fr = U/\sqrt{gH} = 0.025$
Rosby Number	$Ro = U/fL = 0.02, \text{ or}$ $Ro = U/fW = 0.2$
Surface boundary parameter	$Fr^2/Ro = 0.035 \text{ or } 0.0035$
Horizontal Ekman number	$E_H = A_H/fL^2 = 0.0002, \text{ or}$ $E_H = A_H/fW^2 = 0.015$
Vertical Ekman number	$E_V = A_V/fH^2 = 0.5 \text{ to } 10$
Ekman friction depth	$D = \pi\sqrt{2A_V/f} = 10 \text{ to } 44 \text{ m}$
Critical bottom slope	$s_c = H\sqrt{E_V}/L\sqrt{E_H}$ $= 0.002 \text{ to } 0.01$
Longitudinal seiche period (computed) (observed)	$T_1 = 2L/\sqrt{gH} = 7.5 \text{ hr}$ $T_1 = 10 \text{ to } 11.5 \text{ hr}$
Transverse seiche period (computed) (observed)	$T_t = 2W/\sqrt{gH} = 48 \text{ min}$ $T_t = 40 \text{ min}$
Inertial period	$T = 2\pi/f = 18 \text{ hr}$
Proudman number	$Pr = A_V^2/(\pi/L)^2 gH$ $= 0.04 \text{ to } 17$

Lake Balaton for transverse seiches, but only marginally for longitudinal. Since the rigid lid approximation may greatly distort predicted transient motions, it would be unwise to employ it given its small safety margin for Lake Balaton. It is safe, however, to employ the small amplitude approximation and apply boundary conditions at undisplaced free surface location.

Unfortunately, the data of Table 7.2 do not give a complete picture of the lake's behavior since important local effects are ignored. Along the shoreline, and at Tihany Peninsula, local influences can be expected to produce significant divergence from the general behavior outlined above. At Tihany, for example, convective accelerations may be important and possibly frictional influences as well (large Rossby and horizontal Ekman numbers, respectively). In this local region, therefore, the Ekman-type model may not be able to reproduce the lake circulation with great accuracy. As long as this error is confined to a small region, however, the Ekman model remains useful for the lake-wide circulation in Balaton.

Local effects must also be considered in the form of frictional influences along the shoreline (see Section 4.4). It is reasonable to neglect horizontal frictional forces in the shoreline regions if the bottom slope, s , is less steep than the critical slope, s_c . From Table 7.2, the critical slope is at most 0.01, corresponding to a very steep slope. Thus, this criterion is satisfied in all but a few locations, most obviously the deep channel at Tihany.

7.3.3 Conclusions

To summarize our findings concerning the choice of a hydrodynamic model for Lake Balaton, we found in Section 7.3.1 that congruence of the physical and biological models of the lake required a hydrodynamic model which considered processes at the scales of a few hours and a few kilometers. At this level, wind-induced motion and seiching were far more important than hydrologic through-flows, thus requiring a circulation model of the hydrodynamics. An Ekman model, such as the proposed Galerkin model, was identified as an economic and practical model alternative.

In Section 7.3.2 we have examined the suitability of such a model for Lake Balaton. Mathematical criteria were used to evaluate the propriety of the shallow water assumptions, of assuming that convective accelerations and horizontal shear forces are negligible, and of using the rigid lid and small amplitude approximations. Of these, we found that all

but the rigid lid approximation was justified for Balaton. The rigid lid, which is not used in the Galerkin model, would distort the transient response to an unacceptable degree. A qualification to these findings is the likelihood that locally irregular bathymetry, such as at Tihany Strait, would violate the acceptability criteria and lead to some errors in small regions. These errors are not expected to compromise the lake-wide predictions needed in the water quality modeling schemes. We thus conclude that the Galerkin model is suitable for application to Lake Balaton.



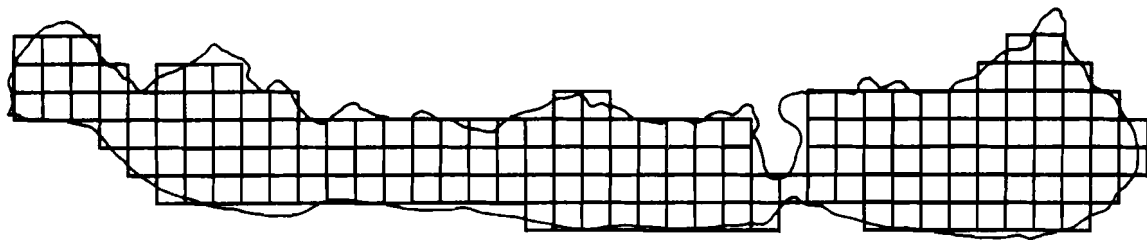
8 MODEL APPLICATION TO LAKE BALATON

Application of the Galerkin model to Lake Balaton proceeded in two phases. Lacking a consensus from the literature on the value and form for the important parameters, the first phase consisted of a series of model sensitivity studies. Through trial and error, reasonable values for the parameters were sought, simultaneously determining the sensitivity of the results to the various parameters. After this step was completed, and a reasonable set of input parameters was available, the second phase, verification, was possible: testing the model results against actual historical events.

8.1 Model Input Data

Execution of the circulation program requires the specification of such inputs as the model parameters, the lake geometry, a wind history, and various execution and output controls. Of the program inputs, the eddy viscosity and bottom friction parameters constitute the major unknowns, to be determined by calibration. These parameters, as well as the wind histories employed, will be described in the sections to follow.

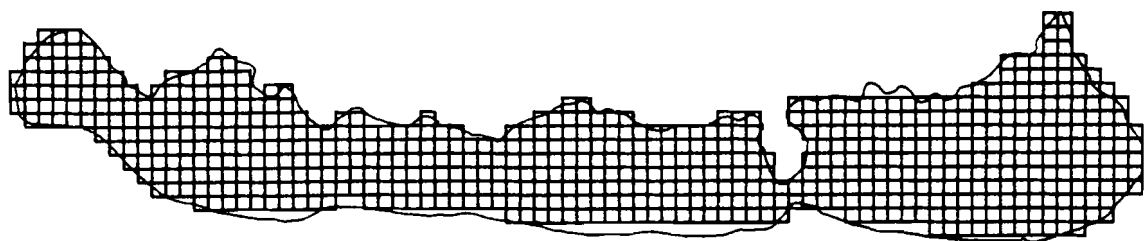
The geometry and bathymetry of Figure 6.1 is the basis of the input geometry data. Using a detailed version of Figure 6.1, two finite difference grids have been constructed. The first, denoted as the coarse grid, used a grid size of 1900 meters and is shown in Figure 8.1. This grid size was felt to be the largest grid able to reasonably approximate the geometry of Tihany Strait. An alternative grid, the fine grid, employed a grid spacing of 950 meters, one half that of the coarse grid. The fine grid is shown in Figure 8.2.



GRID SPACING = 1900 METERS

Figure 8.1

Coarse finite difference grid for Lake Balaton



GRID SPACING = 950 METERS

Figure 8.2

Fine finite difference grid for Lake Balaton

8.2 Calibration and Parameter Sensitivity Studies

8.2.1 General Description

In an effort to calibrate the wind circulation model, a large number of simple seiche events were simulated. These simulations sought to exercise the model under uncomplicated conditions which would reveal the basic behavior of the model and system. The alternative calibration standards, actual historical events, include many complex and extraneous factors which obscure the basic behavior and make calibration difficult. However, the historical record, and published studies of actual seiche events, did supply a data base upon which calibration could be based.

The basic seiche simulations consider the following situation. A steady wind of 10 m/s blows along the long axis of the lake, directed from the western end (Keszthely) to the eastern end (Balatonkenese). The lake is initially still and level, but responds to the wind with a set-up at Balatonkenese and set-down at Keszthely. The wind blows steadily during the first three hours of the simulation; then decreases linearly from 10 m/s at 3 hours time to 0 m/s at 4 hours. The ensuing seiche motion was simulated until the 24 hour time point using the coarse grid defined in Section 8.1 and the Wu wind shear formulae from Section 5.2.

The simulations determined the effects of the magnitude of the linear bottom friction coefficient, c_b , and the form and magnitude of the linear eddy viscosity function, A_v . Before the simulations were started, we made rough estimates for these parameters. The various forms for the eddy viscosity have been shown in Figure 5.1, but with little indication of magnitude. The magnitudes used by other investigators, given in Tables 3.1 to 3.3, vary from 10 to 1000 cm^2/s - a wide range due in part to the wide variety of lakes considered. We can narrow this range by employing a number of empirical relations from the literature with Balaton's characteristics. The estimates of the eddy viscosity, shown in Table 8.1, fall between 1 and somewhat over 100 cm^2/s .

Even more uncertain than the eddy viscosity is the magnitude of the linear bottom friction coefficient required for the Galerkin model. Nelson (1979), in her application to Lake Mendota, used a value of 0.015 cm/s . However, Mendota is considerably deeper than Balaton, and thus less sensitive to this parameter. A more useful guide is Dronkers (1964), who proposes a method to estimate the linear friction coefficient for tidal flows. He bases his results upon the requirement that the linear friction condition produce the same energy loss as the quadratic

Table 8.1

Estimates of vertical eddy viscosity in Lake Balaton

<u>Reference</u>	<u>Method</u>	<u>Estimate</u>
Platzman (1963)	Formula based on seiche decay rate	1.2 cm ² /sec
Ranks (1975)	Function of wind shear and lake depth	11.7
Lindijer (1976)	Rule of thumb (A _v = H/1000)	32
Defant (cited in Hutchinson, 1975)	Theory based on lengthening of seiche period	45
Lick (1976)	Function of wind shear	125
Thomas (1975)	Function of wind shear	128

condition. His formula is:

$$c_b = \frac{8}{3\pi} \frac{g u_{\max}}{C^2 H}$$

where, C is the Chezy friction coefficient; and, u_{max} is the maximum tidal velocity.

The similarity of seiche motion to tidal flow suggests that this formula would be useful for our purposes. Applying it to Balaton, we can roughly estimate c_b to fall in the range 0.0001 to 0.05.

Results from the simulations are shown in Figures 8.4 to 8.9 which follow this section. The Figures include histories of the water surface elevation at Keszthely and selected vertical velocity profiles in Tihany Strait. The profiles at Tihany are for two hours in the simulation (under wind conditions) and six hours (without wind).

In evaluating the results, the model predictions were closely examined for certain responses. For example, it is known from Muszkalay's (1973) field data that the longitudinal seiche persists for at least two or three cycles. Thus, model results depicting an overdamped system,

that is with no oscillation, can be immediately rejected. Similarly, we can look for the presence of small short period oscillations superimposed upon the primary oscillation. These small oscillations, due to transverse and other secondary seiches, are quite obvious in Muszkalay's field observations and should be reproduced by the model. Another criterion with which to examine the model predictions is the period of the longitudinal seiche. As stated in Section 6.2.3, friction lengthens the seiche period to 10 or 11 hours. A third examination point was the predicted set-up after three hours of wind. From Muszkalay's (1966) empirical formula, the three hour set-up at Keszthely should be on the order of 10 to 15 cm. A fourth judging criterion was the form of the velocity profile at Tihany. Again from Muszkalay (1973), we know that the velocity profile is unidirectional, at least during seiche events. And, though less objective, the general shape of the velocity profile serves as a good indicator of the trustworthiness of the results. Abrupt direction reversals and excessively steep gradients, for example, would not be reasonable results. Along the same lines, a well known rule of thumb for ocean currents states that the surface velocity should equal about 3% of the wind speed. Predicted surface velocities far greater than this are therefore probably in error except where other influences can explain the higher velocities - for example, the seiche current in Tihany Strait. These various criteria, though approximate, served as a consistent and reasonable test of the model's ability to reproduce the system behavior and permitted the selection of a set of parameters judged to credibly represent the system.

One factor not considered in the simulations bears mention. Flow boundary conditions are not a present capability of the model, and hence, inflows and outflows could not be included. This should have small effect on the general circulation, but will obviously compromise the results near the Zala River inflow and the Sio Canal outflow.

8.2.2 Study Results

The sensitivity studies considered many eddy viscosity forms and parameter values - too many to reproduce all results here. What will be presented instead is a selection of the results from three major categories. First is the depth-constant eddy viscosity, the simplest and most common form in use. Second is what we have termed the bi-linear eddy viscosity, a function which is constant from the water surface to some depth in the water column, from where it decreases linearly to zero at the bottom. The third category includes a sampling of eddy viscosity forms in which proposals from the literature are approximated by the

model's piecewise linear viscosity function. Figure 8.3 illustrates the forms tested.

Simulations with a constant eddy viscosity evaluated the ability to match observed behavior as well as the sensitivity of the results to the viscosity and bottom friction coefficients. Figures 8.4 and 8.5 show the simulation results. None of the parameter combinations produced the desired behavior. Response typical of a lightly damped system was achieved only in simulations which also showed unreasonable set-up and surface velocities. The results indicate extreme sensitivity to the eddy viscosity and moderate sensitivity to the bottom friction factor.

The bi-linear eddy viscosity led to the behavior most like that found in Lake Balaton. Oscillatory behavior consistent with observation was produced over a range of parameter values, although marked sensitivity to the eddy viscosity was again found. The results were tested for sensitivity to the magnitude of the eddy viscosity and bottom friction coefficient, as well as to the location of the inflection point in the eddy viscosity function. This last parameter is denoted by h_1 in Figure 8.3.

The results of the bi-linear viscosity simulations are given in Figures 8.6 through 8.8. Sensitivity to the magnitude of the eddy viscosity (Figure 8.6) is great. A value of $A_{v0} = 20 \text{ cm}^2/\text{sec}$ produced an initial surface displacement near that desired, along with a continuing seiche oscillation. The vertical velocity profile is unidirectional during seiche motion (6 hours), but shows a small bottom reversal under wind conditions (2 hours). Further testing of this parameter combination showed little sensitivity to bottom friction (Figure 8.7) and mild sensitivity to the location of the viscosity function inflection point (Figure 8.8).

A variety of other, more complex, eddy viscosity forms were also looked at. Inspection of the results in Figure 8.9 shows that most gave poor results in one respect or another. The most nearly reasonable results were produced by the near-surface maximum form. The results with that function are flawed, however, by the anomalous increase in the seiche amplitude on the second peak. The many formulas in which the eddy viscosity closes to zero at both the surface and bottom are roughly represented by the tri-linear form in Figure 8.3d. These equations lead to unreasonable velocity gradients near the water surface. The parabolic approximation, Figure 8.3e, leads to an overly damped system response, as does Nelson's bi-linear form (Figure 8.3f). Nelson's viscosity formula also produces an excessive surface velocity.

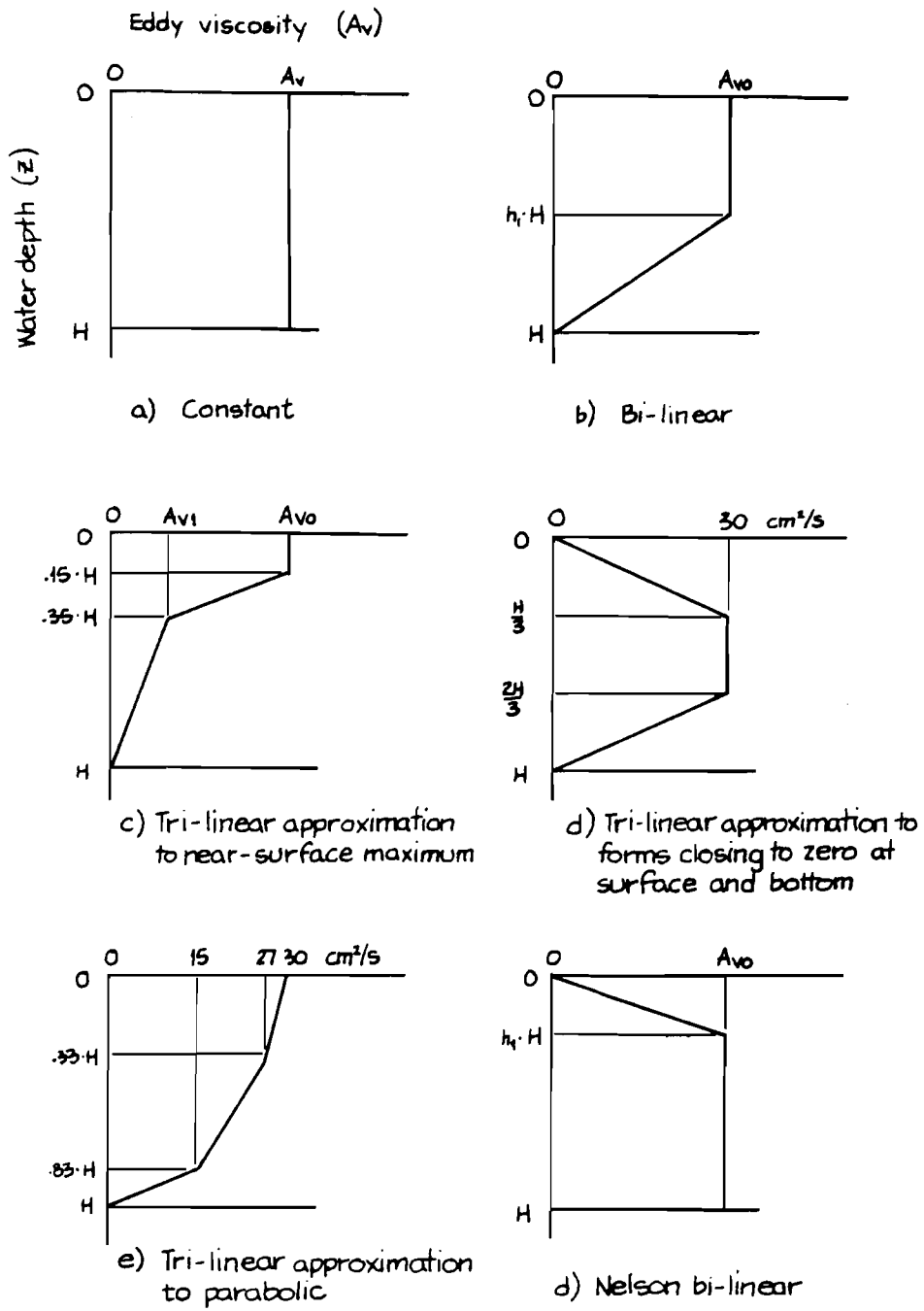


Figure 8.3

Eddy viscosity functions used in the simulations

The results of the sensitivity studies have been summarized in Figure 8.10 and Table 8.2. The depth-averaged eddy viscosity (or corresponding Proudman number) was selected as the most important parameter to characterize the simulations. To capture the various calibration criteria, we have used the initial water surface set-down at Keszthely, the ratio of the magnitude of the third to second peak in the water surface displacement history, and the two-hour water surface velocity at Tihany. Seiche period was not included since its variation proved small; we believe that the period is determined far more by the lake geometry than the parameters varied in these simulations. Figure 8.10 does reveal significant variations in the other parameters, however. In general, initial set-down and surface velocity decrease as the average eddy viscosity increases. Within this general trend, significant variations are observed, however. For example, the initial set-down shows a systematic variation between the constant viscosity form (the curve labeled Figure 8.4) and the bi-linear forms (labeled 8.6 and 8.8). Similarly, divergence from the general trend is obvious in points S, T and V in the surface current speeds (Figure 8.10b). The seiche damping ratio, represented in Figure 8.10c, behaves as predicted by Platzman (1963), with virtually no oscillation occurring above the critical Proudman number threshold.

Figure 8.10 can lead us to the parameter set which yields the closest approximation to Balaton's behavior. Comparison of the results in Figure 8.10 with the evaluation criteria defined above reveals only a few simulations performed satisfactorily in all respects: runs J, M, N and possibly O. J, M and N correspond to the following parameter set, which we consider to be the calibrated parameters: a bi-linear eddy viscosity form with a surface value of $20 \text{ cm}^2/\text{sec}$ and an inflection point located at mid-depth, together with a bottom friction factor in the range 0.015 to $0.00015 \text{ cm}/\text{sec}$.

8.2.3 Conclusions

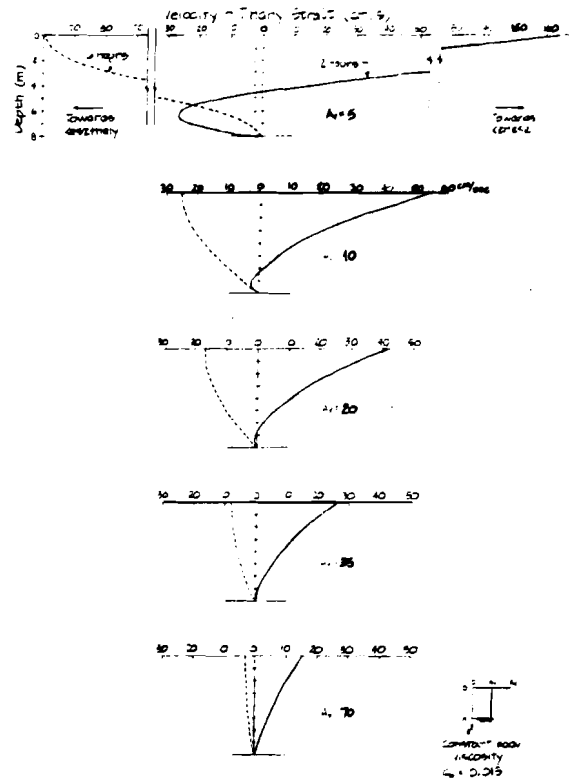
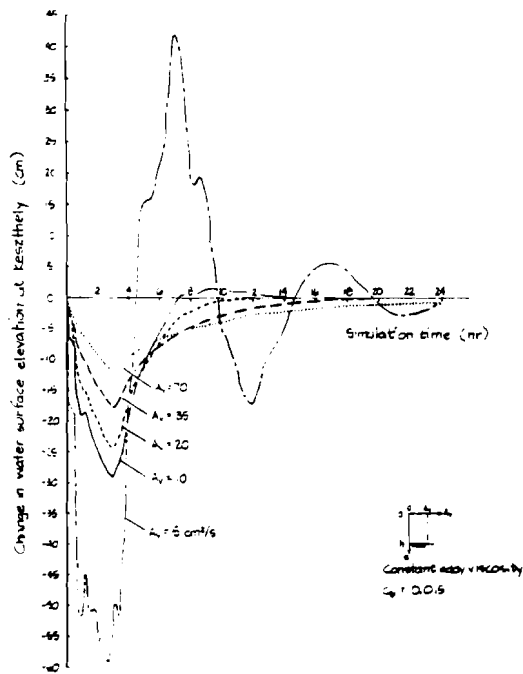
Two salient features emerge from the sensitivity studies. First, with the proper choice of input parameters, the model is able to simulate a response similar to that found in the actual lake. Secondly, the model is highly sensitive to the input parameters, producing greatly exaggerated or underpredicted behavior as a consequence of poorly chosen inputs. One other important conclusion has been reached. The commonly used constant eddy viscosity does not yield good results in a shallow lake, at least not with the model formulation employed here.

Despite the parameter sensitivity noted above, the series of runs performed has led us to an eddy viscosity form which

produces an approximately correct response for Lake Balaton: a bi-linear function, as in Figure 8.3b, with $h_1 = 0.5$, $A_v = 20 \text{ cm}^2/\text{sec}$ and $c_b = 0.0015$. At this stage, therefore, we consider the model to have been calibrated.

It is useful at this point to return to the analysis of Section 7.3.2 in which we evaluated the model assumptions in light of the physical characteristics of Lake Balaton, given in Table 7.2. In Table 7.2 the eddy viscosity parameter could not be defined precisely, and a likely parameter range was given. Using our calibration results we can now define the depth average eddy viscosity, $A_v = 15 \text{ cm}^2/\text{sec}$. Other values in Table 7.2 affected by this change are the vertical Ekman number, E_v , now equal to 1.5; the Ekman friction depth, $D = 17 \text{ m}$; the critical bottom slope, $s_c = 0.004$; and, the Proudman number, $Pr = 0.4$. These changes do not alter the conclusions of Section 7.3.2, that the model assumptions are valid for Lake Balaton.

In the next section, we will investigate the model behavior and sensitivity somewhat further, before proceeding to the model verification with actual historical events.

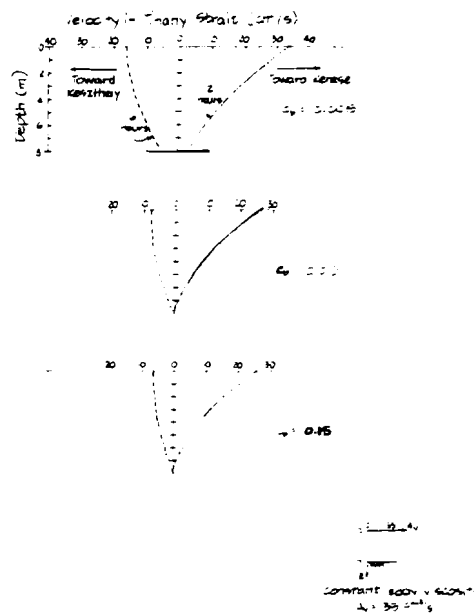
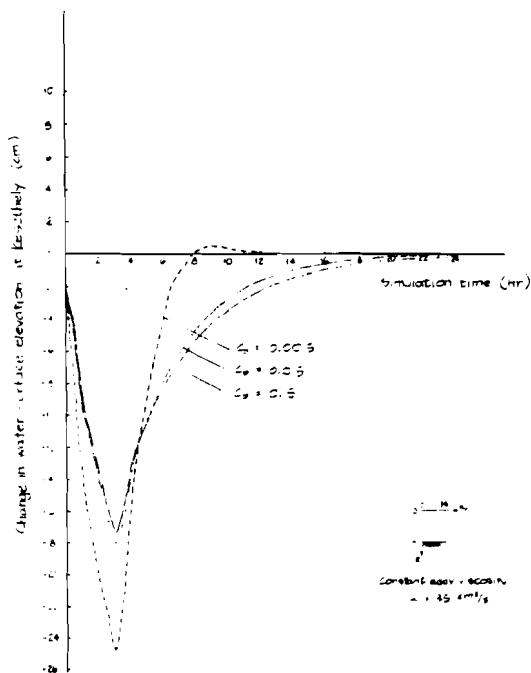


a) Water surface elevation at Keszthely

b) Current in Tihany Strait

Figure 8.4

Sensitivity of seiche to constant eddy viscosity

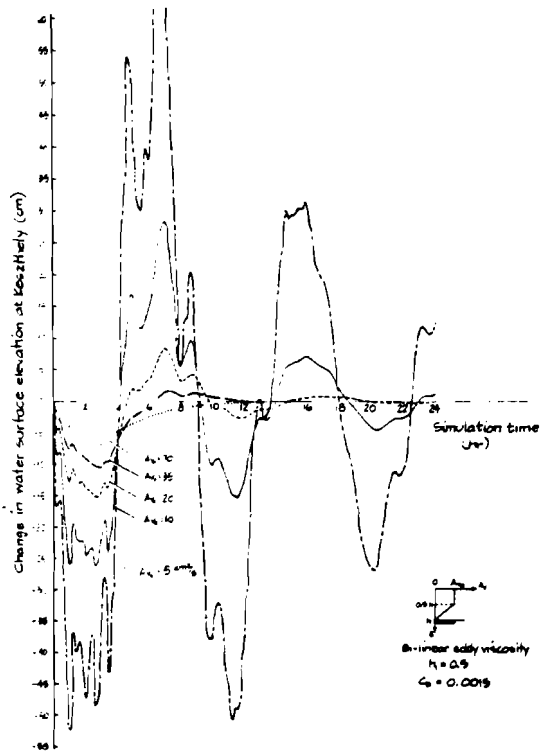


a) Water surface elevation at Keszthely

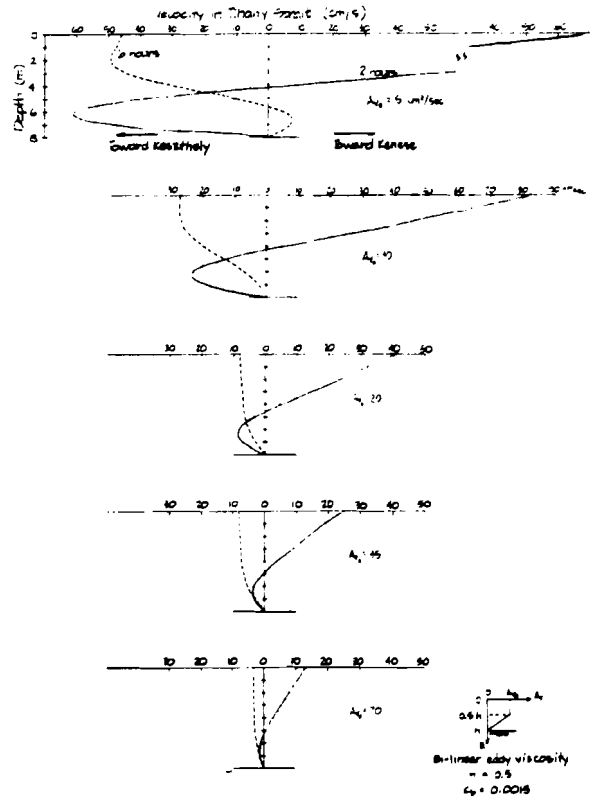
b) Current in Tihany Strait

Figure 8.5

Sensitivity of seiche to bottom friction coefficient with constant eddy viscosity



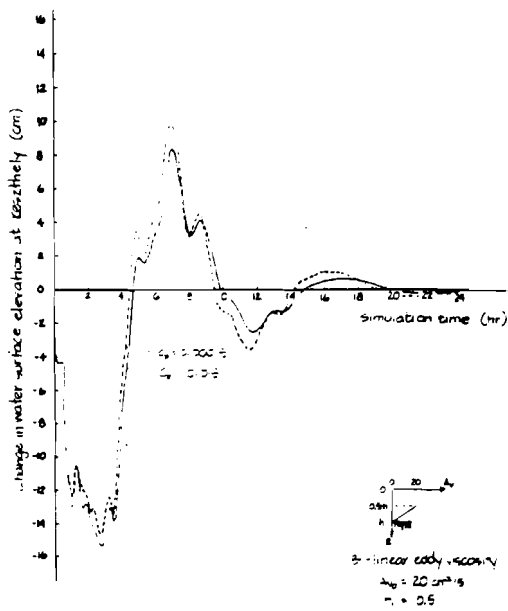
a) Water surface elevation at Keszthely



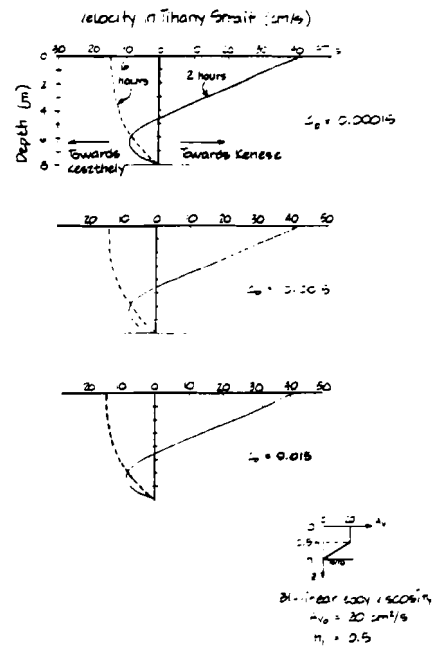
b) Current in Tihany Strait

Figure 8.6

Sensitivity of seiche to bi-linear eddy viscosity



a) Water surface elevation at Keszthely



b) Current in Tihany Strait

Figure 8.7

Sensitivity of seiche to bottom friction coefficient with bi-linear eddy viscosity

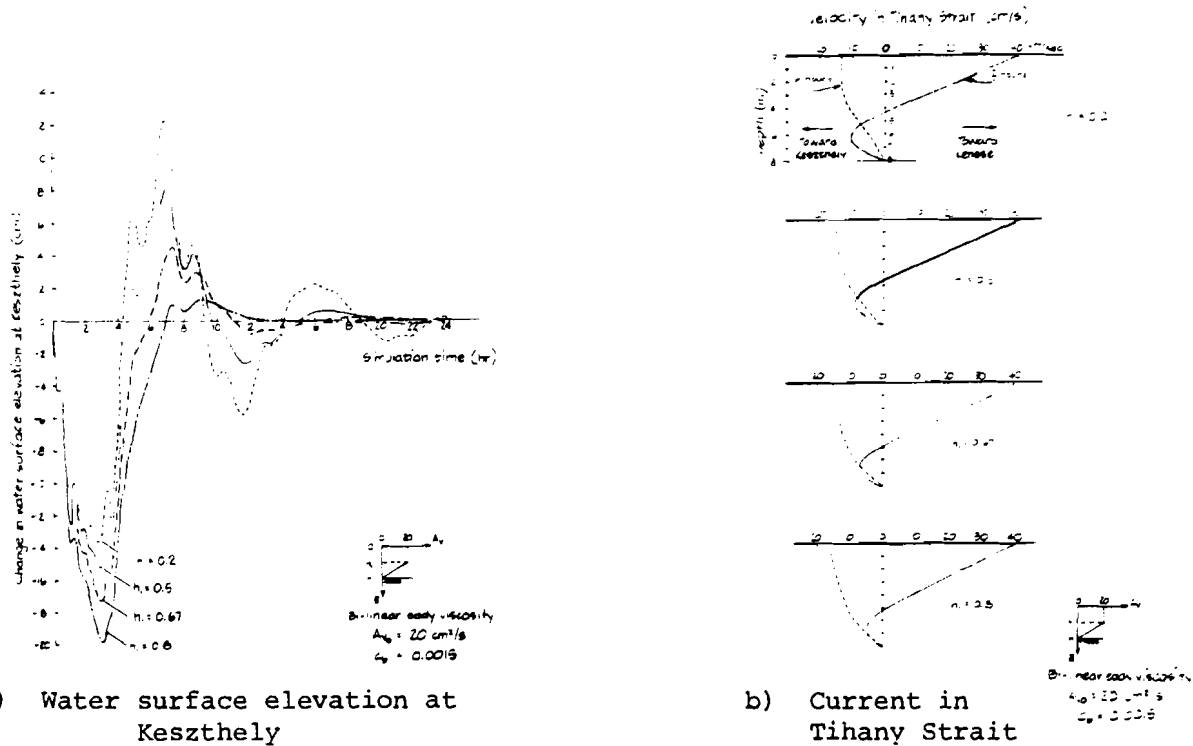


Figure 8.8

Sensitivity of seiche to bi-linear eddy viscosity inflection point

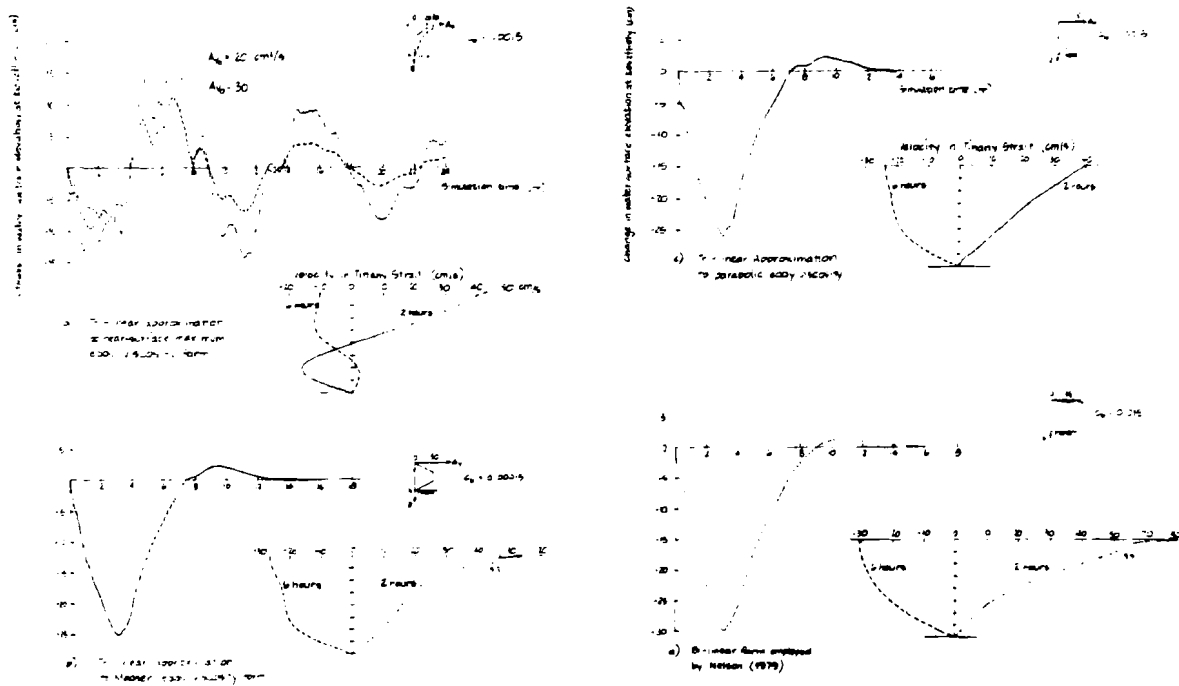


Figure 8.9

Sensitivity of seiche to various eddy viscosity forms

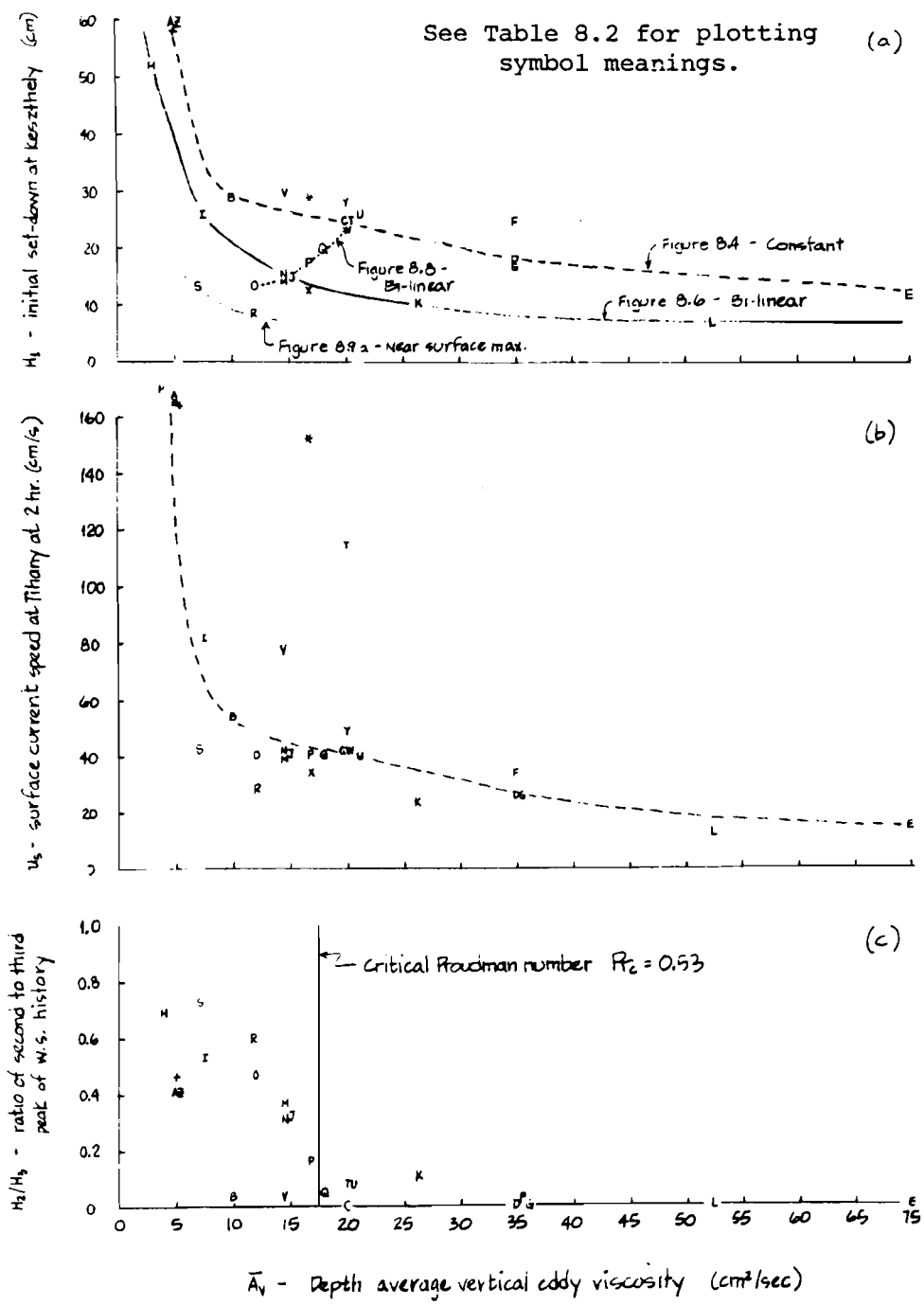


Table 8.2

Summary of sensitivity run results

Figure	Viscosity Form	Parameters	\overline{A}_V	Pr	H_1	H_2/H_3	u_s	Plot Symbol
8.2	Constant	$c_b=0.0015, A_V=5$	5	0.04	59.5	0.41	168	A
		$c_b=0.0015, A_V=10$	10	0.17	29.3	0.04	54	B
		$c_b=0.0015, A_V=20$	20	0.69	24.8	0	42	C
		$c_b=0.0015, A_V=35$	35	2.1	18.0	0	26	D
		$c_b=0.0015, A_V=70$	70	8.5	12.3	0	15	E
8.3	Constant	$A_V=35, c_b=0.0015$	35	2.1	24.8	0.03	34	F
		$A_V=35, c_b=0.15$	35	2.1	17.3	0	26	G
8.4	Bi-linear	$c_b=0.0015, h_1=0.5, A_{V_0}=5$	3.8	0.03	52.5	0.69	170	H
		$c_b=0.0015, h_1=0.5, A_{V_0}=10$	7.5	0.10	26.1	0.53	82	I
		$c_b=0.0015, h_1=0.5, A_{V_0}=20$	15	0.39	15.2	0.32	41	J
		$c_b=0.0015, h_1=0.5, A_{V_0}=35$	26.3	1.2	10.5	0.11	24	K
		$c_b=0.0015, h_1=0.5, A_{V_0}=70$	52.5	4.8	6.9	0	13	L
8.5	Bi-linear	$A_{V_0}=20, h_1=0.5, c_b=0.00015$	15	0.39	14.7	0.37	41	M
		$A_{V_0}=20, h_1=0.5, c_b=0.015$	15	0.39	15.3	0.31	41	N
8.5	Bi-linear	$A_{V_0}=20, c_b=0.0015, h_1=0.2$	12	0.25	13.6	0.47	41	O
		$A_{V_0}=20, c_b=0.0015, h_1=0.67$	16.7	0.48	17.3	0.16	41	P
		$A_{V_0}=20, c_b=0.0015, h_1=0.8$	18	0.56	20.0	0.05	41	Q
8.7a	Near-surface Maximum	$c_b=0.0015, A_{V_0}=20$	11.8	0.24	8.6	0.60	28	R
		$c_b=0.0015, A_{V_0}=30$	7.1	0.09	13.1	0.73	43	S
8.7b	Madsen	$c_b=0.00015, A_V=30$	20	0.69	25.2	0.08	115	T
8.7c	Parabolic	$c_b=0.0015, A_{V_0}=30$	21.1	0.77	26.0	0.08	40	U
8.7d	Nelson	$c_b=0.0015, A_{VH}=15, h_1=0.04$	14.7	0.37	29.8	0.04	79	V
not shown	Bi-linear	$A_{V_0}=20, c_b=0.0015, h_1=0.99$	20	0.69	24.3	-	41	W
		$A_{V_0}=24, c_b=0.0015, h_1=0.4$	16.8	0.49	12.7	-	34	X
		$A_V=20, c_b=0.0015$ $A_V=5, c_b=0.15$ $A_V=5, c_b=0.0015$	20 5 5	0.69 0.04 0.04	28.6 60.1 57.7	- 0.41 0.46	49 166 165	Y Z +
not shown	Nelson	$A_{VH}=20, h_1=0.33, c_b=0.0015$	16.7	0.48	29.1	-	153	*

8.3 Grid and Wind Field Sensitivity

Determination of a set of calibration parameters hardly eliminates all uncertainties and major sources of error from the model. In particular, two aspects of the model sensitivity require further study: the effect of the finite difference grid spacing and the influence of the wind boundary condition upon the simulations. These effects were examined through two types of simulations: the seiche simulations described in the previous section, and steady state circulation runs.

The seiche events are, of course, transient runs. Though they are designed to simplify many aspects of the lake's behavior, their transient nature confuses the lake circulation patterns. To clarify the circulation response, we also ran the program with a constant wind input until the lake reached a steady state. Vector plots of currents at various depths within the lake could then be drawn for direct comparisons of the circulation. Though these circulation patterns do suggest how the wind field and grid affect the model results, they are in one sense completely unrealistic. The lake itself is never in a steady state since the wind forcing function changes far more rapidly than the time for the lake circulation to become steady. The lake can reach a steady state only after the seiche motion has completely dissipated, a few days at least.

The steady state simulations were performed as follows. A steady wind of 15 m/s blowing from the northwest was modeled. The simulation was performed as a transient one, and run as long as necessary for variations in the surface elevation to become negligible. Having reached steady state, vector plots of the horizontal velocity at the water surface and depths of 1.5 and 3 meters were produced as output.

8.3.1 Wind Effects

A variety of wind shear formulae developed by various researchers has been presented in Section 5.2. For the most part, the formulae differ only slightly, with the important exception of Hicks' (1974) relation for shallow water. Lake Balaton lies within the range over which Hicks suggests the formula is applicable, so it is of interest to examine its effect upon the model results.

The importance of the wind shear formula was evaluated in a seiche simulation using the calibrated parameters. Two equations for the wind shear were contrasted, the formulae by Wu (1969) and the relation proposed by Hicks et al (1974) for shallow water. The Wu equations have been used in all of the simulations reported above in Figures 8.4 through

8.10. The Hicks formula, which is contrasted with Wu's in Figure 5.2, predicts a much lower drag coefficient and, therefore, lower shear force. A comparison of the seiche motion resulting from the two formulae is given as Figure 8.11. The character of the predictions remains the same, it is simply the magnitude of the response which changes. Since Hicks' equation is a tentative proposal pending further data, we will continue to use Wu's equation in the simulations to follow. In doing so, we assume that similar model behavior could be achieved with the Hicks formula using a slightly different set of calibration parameters.

Both the strength and direction of the wind can be expected to vary over the lake, a fact discussed in Section 6.2. Such variations are poorly represented by the wind measurement data available for historical events: often, only a single wind record is available. To appraise the possible effects of uncertainties in the wind field, a number of simulations were performed.

The effect of wind direction was examined in a series of seiche simulations in which a wind of 10 m/s was directed from eight points around the compass. The results, given in Figure 8.12 as the water surface elevation history at Keszthely, show a complete spectrum in relative strength of transverse and longitudinal seiching. Although the results do not consider direct variations in different parts of the lake, the importance of the wind direction is clearly indicated.

Although direction variations across the lake were not possible, the model was programmed to allow a variation in wind strength. This feature permits the user to specify a scaling factor for each grid in the lake model to be applied to the wind speed at that grid. Based on some rough information on the variation of wind over the lake, the wind field shown in Figure 8.13 was developed. This variation is entirely hypothetical, though it would not be an unreasonable pattern for a wind coming from the north or northwest.

The effect of wind field variation was determined through both seiche and steady state simulations. Figure 8.14a shows the resulting water surface elevation history at Keszthely due to three wind fields. The wind field of Figure 8.13 produces a response (dashed line) far weaker than that of the uniform field (solid line). This is entirely to be expected, though, since the varying wind field has an average speed less than that of the constant field. If the varying field is renormalized to have the same average speed as the uniform wind, the dotted line response is produced. Though similar to the constant wind response, some differences exist, particularly in the peak elevations produced.

Results from the steady state simulations contrast the uniform wind field circulation, in Figure 8.15, with that produced by the variable wind field normalized to the same average strength as the uniform, Figure 8.16. Vector plots of the horizontal current velocities at the water surface and at depths of 1.5 and 3 meters illustrate the simulation results. The currents are generally similar, although there are some local differences. Particularly striking are the greater velocities evident in the variable wind field results. This is shown clearly by Figures 8.18a and b, in which vertical velocity profiles are plotted for the mid-point of the Szemes basin. These differences between the circulation patterns illustrate the importance of accurate wind field specification to the program results.

The steady state circulation predictions make a striking contrast to the circulation found in the physical model studies of Lake Balaton made by Gyorke (Figure 6.3). The pattern predicted by the computer model is much alike the theoretical steady state flow profile: the surface current follows the wind, giving rise to a bottom return flow. This surface circulation is far simpler than that found by Gyorke, who indicates a very complex system of gyres. This may be explained in part by the great scale distortion in Gyorke's model.

If we consider the depth averaged currents predicted by the computer model, rather than the surface currents, a different picture emerges, however. For example, Figure 8.17 shows the depth averaged circulation due to the variable wind field: the same simulation as depicted in Figure 8.16. Unlike the circulations at any given layer, the depth averaged circulation, and thus the net transport, show numerous horizontal gyres. Although the general character of these predictions is much more similar to Gyorke's results, significant differences in the predicted patterns remain.

8.3.2 Grid Size Effects

The finite difference model of Lake Balaton shown in Figure 8.1 is rather rough, especially in its representation of shoreline features and transverse sections. The possibility of great error in such a coarse grid was raised in studies by Fisher (1980) who found very different circulation patterns in a hypothetical lake when modeled with coarse and fine grids. To evaluate this effect in the Balaton model, we constructed the second, fine grid shown in Figure 8.2 for a series of sensitivity runs to contrast with the coarse grid results.

Both seiche and steady state simulations were completed. The results of the seiche simulations, shown as the water surface elevation at Keszthely, are compared in Figure 8.19. Although the main features of the response are the same, there are clear differences. Most important is the more rapid attenuation of the seiche with time when using the fine grid. The attenuation behavior, a transient phenomenon, does not affect the steady state circulation shown in Figure 8.20. Comparison with the coarse grid circulation in Figure 8.15 shows no differences of note due to the fine grid. This is very clear in Figures 8.18a and c, which show the velocity profiles at the Szemes basin midpoint. Although the longitudinal velocities differ slightly, the transverse components are identical.

We conclude that a decrease in the grid size, though not insignificant, will not cause major changes in the predicted response of the lake. Further, the main difference produced is in the seiche attenuation behavior, a response which can be controlled by the chosen calibration parameters. Thus, the possibility for great error due to insufficient grid detail appears to be small. Further, whatever minor increases in accuracy could be achieved with the fine grid are far outweighed by a ten-fold increase in computation expense (see Section 9.1), and we therefore proceed with the historical simulations using only the coarse grid.

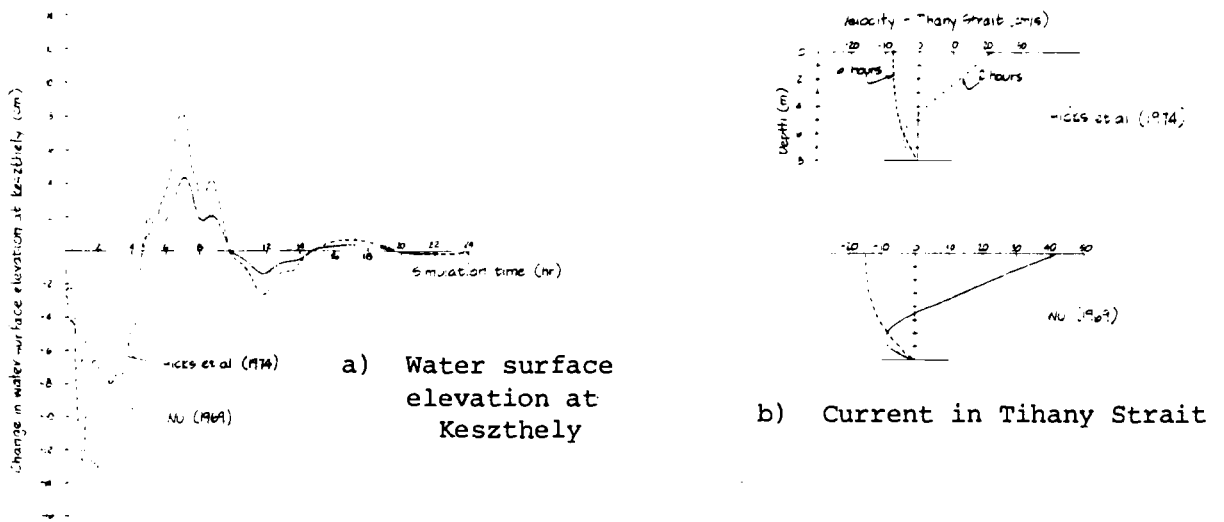


Figure 8.11

Effect of wind shear formula on seiche simulation

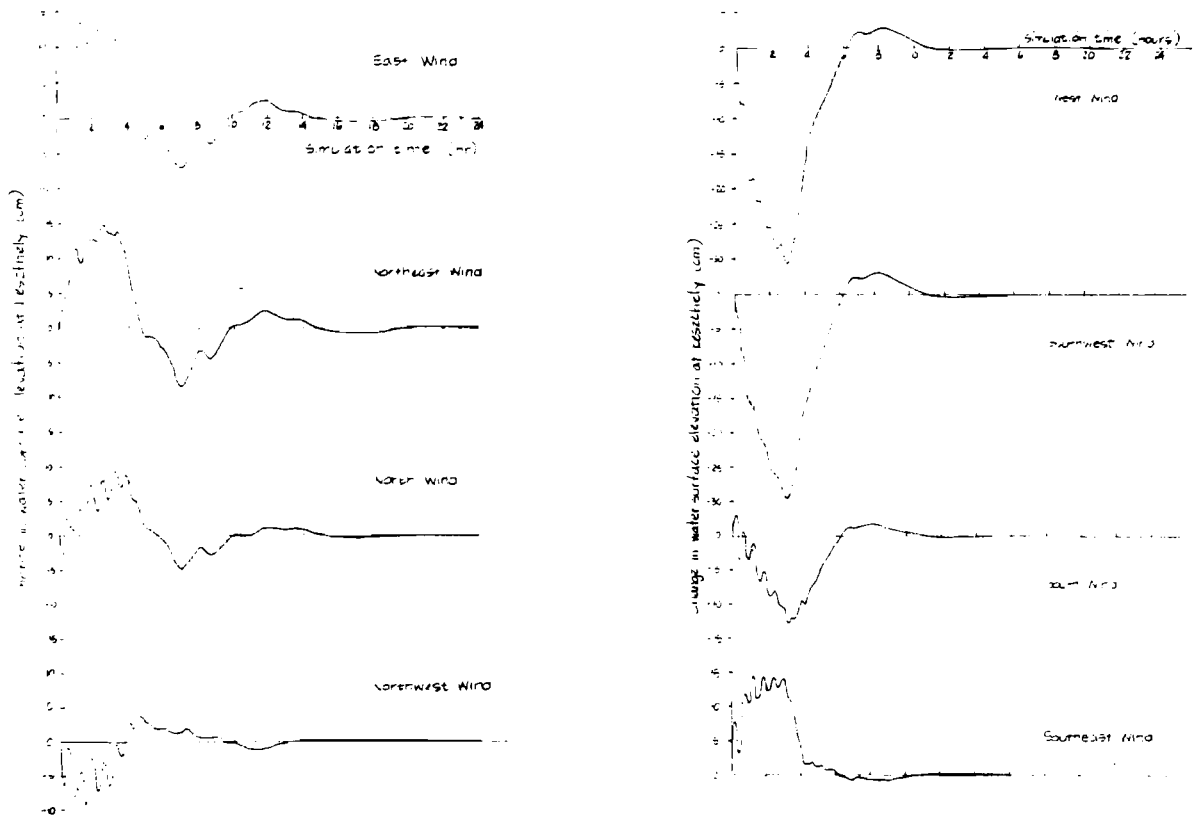


Figure 8.12

Effect of wind direction on seiche simulation

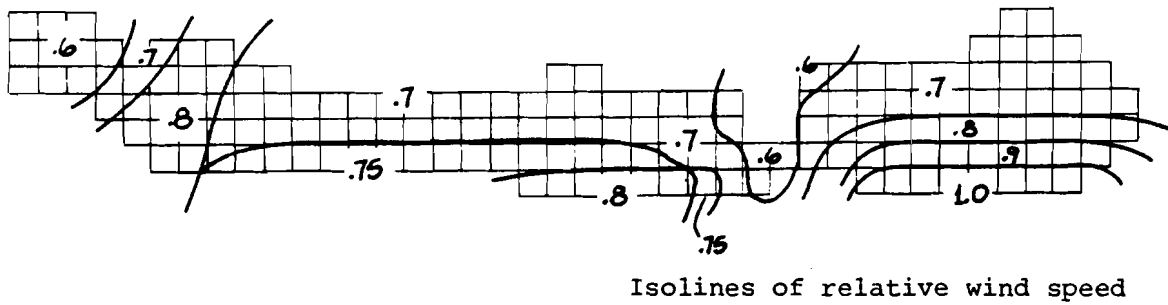


Figure 8.13
Hypothetical spatially varying wind field

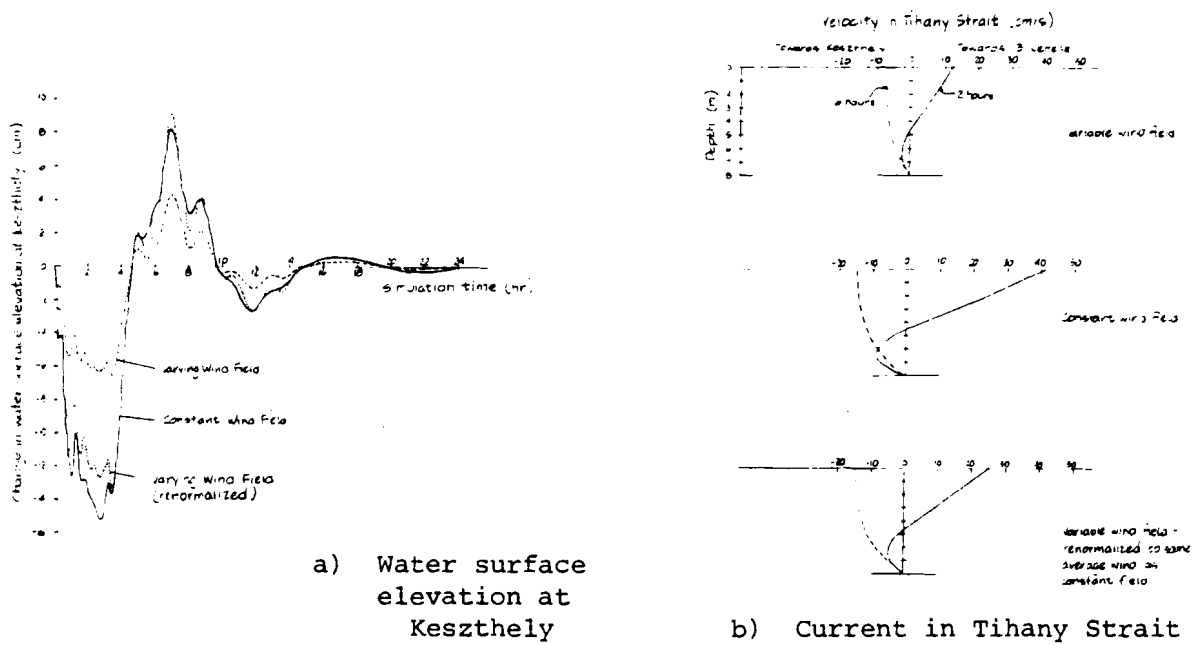
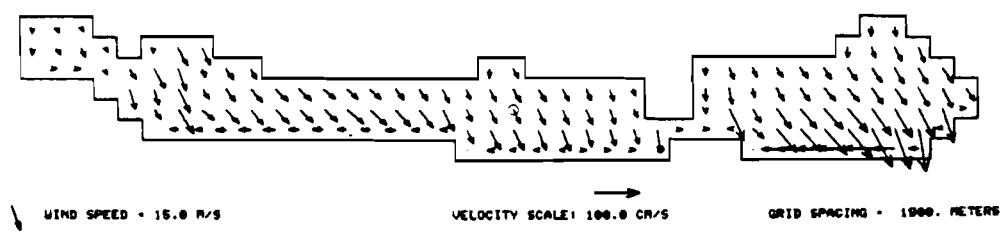
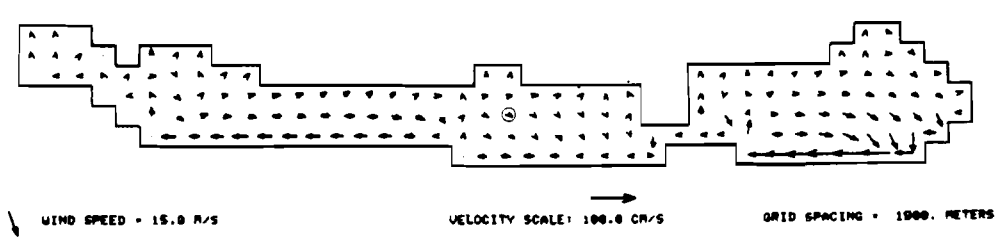


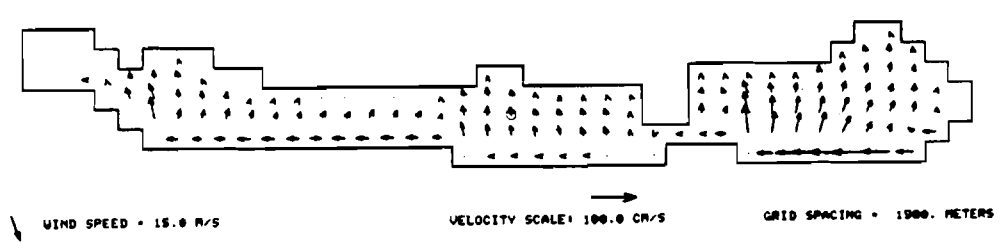
Figure 8.14
Effect of wind field variation on seiche simulation



a) Surface

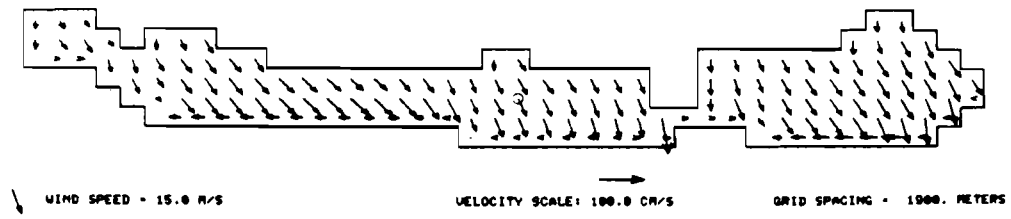


b) 1.5 meter depth

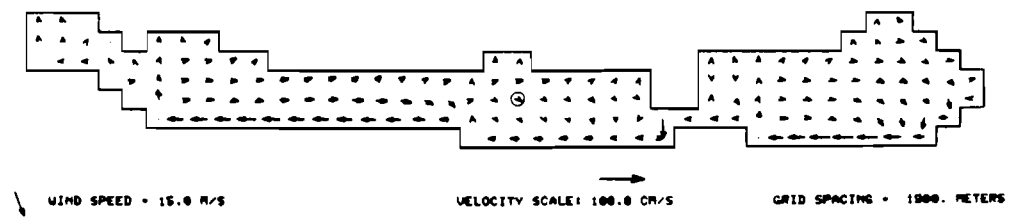


c) 3 meter depth

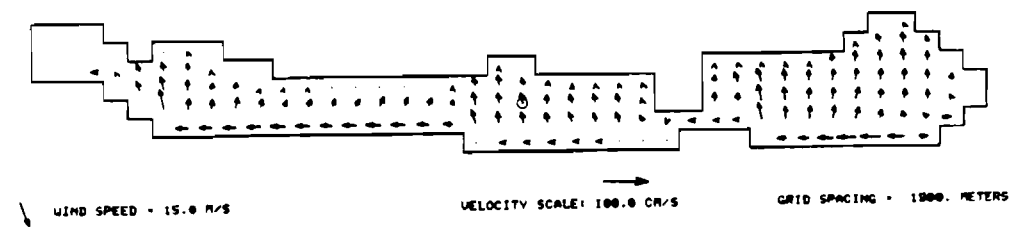
Figure 8.15
Steady state horizontal circulation
under uniform wind field



a) Surface



b) 1.5 meter depth



c) 3 meter depth

Figure 8.16

Steady state horizontal circulation
under spatially varying wind field

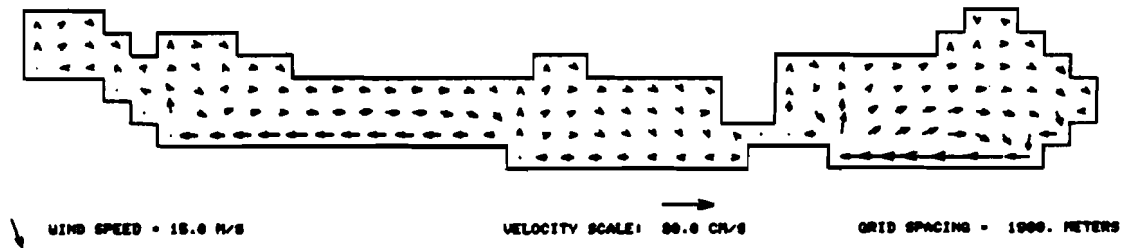


Figure 8.17

Steady state depth average circulation
under spatially varying wind field

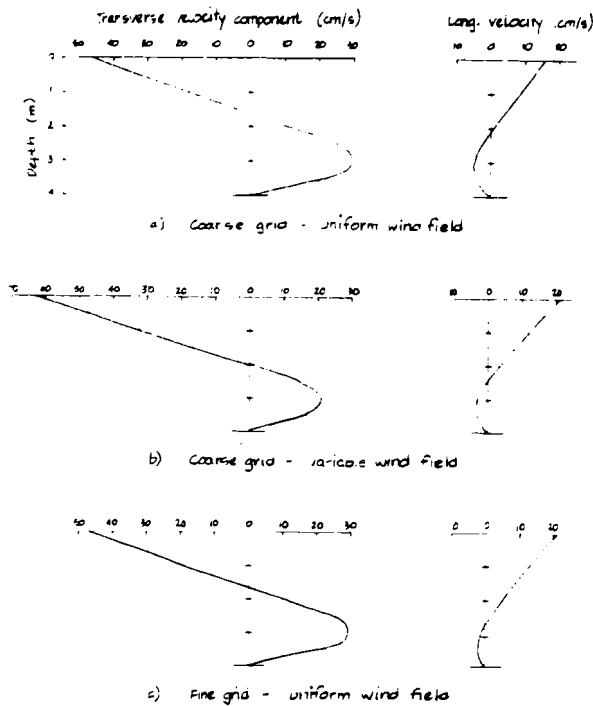


Figure 8.18

Steady state vertical
velocity profiles
at Szemes basin mid-point

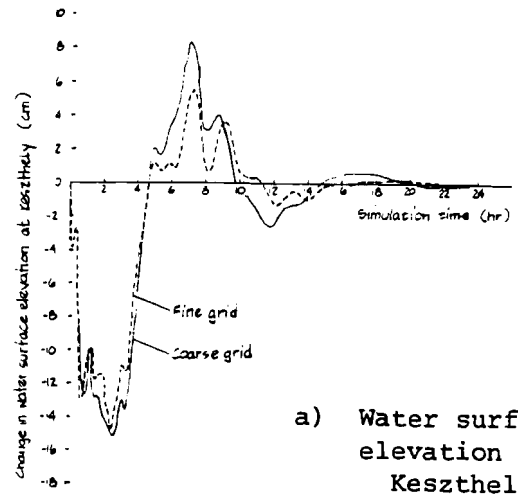
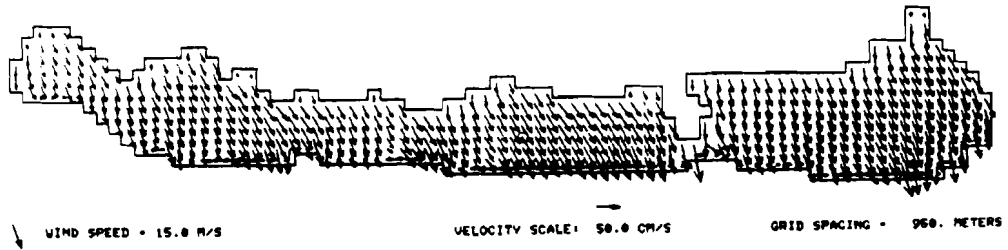
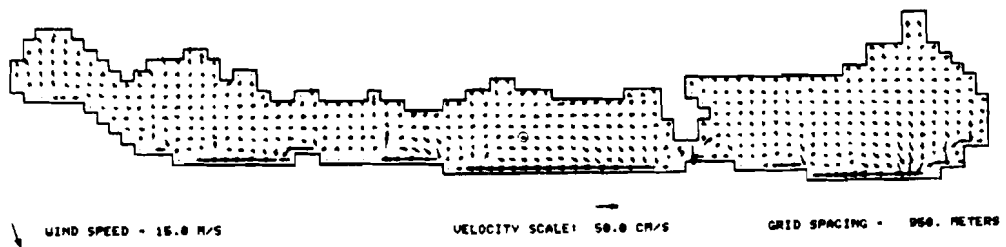


Figure 8.19

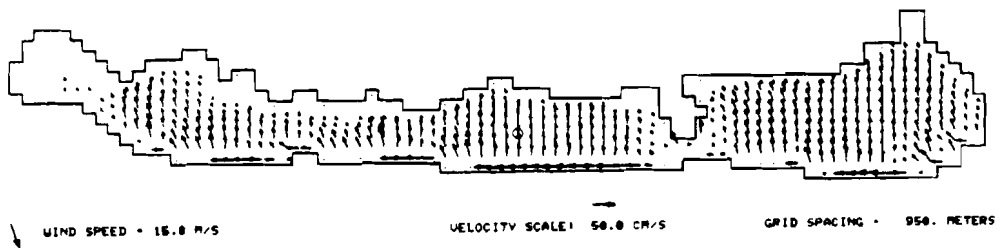
Effect of grid size
on seiche simulation



a) Surface



b) 1.5 meter depth



c) 3 meter depth

Figure 8.20

Steady state horizontal circulation with fine grid
under uniform wind field

8.4 Simulation of Historical Events

The Galerkin circulation model was verified by simulating actual historical events on Lake Balaton. These simulations used observed winds as input, and their predictions of water surface elevation were compared with the actual records. In addition, current predictions made at Tihany were compared with measurements if available.

Three events were selected for the verification runs: July 4 and 5, 1961, July 8 and 9, 1963 and October 5, 1963. Event selection was based on data availability and certain desirable characteristics. These events produced relatively strong and distinct seiches following a period of calm. The preceding calm period decreased the length of the simulation start-up period needed to establish initial conditions. The events also attempt to include a range of wind directions, although the range is fairly limited since most strong winds cross the lake from the north.

Most of the input wind data for the simulations were obtained from the plotted records of Muszkalay (1973). The format of Muszkalay's long term record (as in Figure 6.6) proved too condensed for conversion to the hourly values required for the computer program, but his detailed plots of selected events could be used (for example, Figure 6.7). The long term record supplied needed background information to identify reasonably isolated events. In addition to Muszkalay's records, some hourly wind records from Keszthely were available for the events of July 4 and 5, 1961 and July 8 and 9, 1963. The water surface elevation records and Tihany current measurements which supplied the comparison data were taken from Muszkalay.

The simulations were all performed using the coarse finite difference grid of Figure 8.1, the calibration parameters given in Section 8.1.3, and Wu's (1969) wind shear formula. The simulations used spatially varying wind fields based upon the distribution of Figure 8.13, but normalized to account for the location of the input wind record. (That is, the factors in Figure 8.13 were rescaled so that the factor value at the location of the wind recording station became equal to 1.0.)

8.4.1 Event of July 4 and 5, 1961

The recorded data for the event of July 4 and 5, 1961 is shown in Figure 8.21. A strong longitudinal seiche characterized this event, producing a net water surface elevation difference of 27 cm between Keszthely and Balatonkenese. Figure 8.22 contrasts the results from the computer program with the recorded stage records at these two locations. Though details of the motion are not

captured (particularly in the first 20 hours of simulation), the overall agreement is excellent. Muszkalay's data for this event did not include the current at Tihany, hence that comparison is not included here.

8.4.2 Event of July 8 and 9, 1963

The event of July 8 and 9, 1963 produced a longitudinal seiche with comparable displacement to the July 1961 event, but with much stronger simultaneous transverse seiching. Two wind records were used to simulate this event. A series of hourly wind data was developed from Muszkalay's record for Balatonszemes, and this was supplemented by the later receipt of hourly data for Keszthely. The two wind records are shown in Figure 8.23. Records of the water surface elevation at Keszthely and Balatonkenese were constructed from Muszkalay's data and are given in Figure 8.23c. In addition, Muszkalay's record of the velocity at Tihany was also employed, but required a major correction: the indicated directions of flow are apparently reversed in his drawing (reproduced in this report as Figure 6.6). The corrected, reconstructed record is included as Figure 8.23d.

Results from the computer simulations are compared with the historical records in Figure 8.24. Drastically different predictions resulted from the two input wind records: the Keszthely record producing a reasonable prediction, while the Balatonszemes record led to very poor results. Prediction of the stage at Keszthely, shown in Figure 8.24a, was not very good even using the Keszthely wind data. However, the Keszthely wind data produced an excellent prediction of the stage at Balatonkenese, with the exception of the large peak at 1600 hours (Figure 8.24b). The predictions using the Balatonszemes wind data show too great a response to the wind and excessive oscillation.

The model prediction of the velocity at the one meter depth in Tihany Strait is contrasted with Muszkalay's record in Figure 8.24c. The predictions based on the Keszthely wind data are in fair agreement with the observations, with the exception that peak flows are underpredicted. Less frequent program output was obtained from the Balatonszemes-based predictions, but these are sufficient to demonstrate the poor agreement with the data.

8.4.3 Event of October 5, 1963

The event of October 5, 1963 differs considerably from our two prior examples. Whereas those events began with longitudinally directed winds before shifting to a transverse direction, the storm of October 5 brought only transverse winds. Muszkalay (1973) includes this event as

an example of the transverse seiche and presents water surface elevation records for Balatonszemes and Balatonakali, on the southern and northern shores at roughly mid-lake. He does not supply records for Keszthely nor Balatonkenese to show the longitudinal seiche; however, velocity measurements in Tihany Strait are given. The sole source of wind data is Muszkalay's record for Balatonszemes. The wind, water surface elevation and current data are shown in Figure 8.25.

Comparison of the simulation results with the observations is included in Figure 8.26. These figures show very poor agreement between the predictions and the observations in virtually all aspects. Two major problems can be identified: poor prediction of longitudinal motion, and excessive oscillation in the transverse. The first problem is undoubtedly due to errors in the wind data, particularly direction. When the wind is directed from the NNW, as it was on October 5, it crosses the lake almost exactly transverse to the lake's long axis. In this situation, small changes in the wind direction lead to great changes in the magnitude of the longitudinal wind component, including frequent reversals in longitudinal direction. Under such conditions, local modifications of the wind field and errors in the wind data critically influence the prediction results. This extreme sensitivity makes accurate prediction of longitudinal motion under transverse winds a virtual impossibility unless accurate wind data from many locations around the lake are available.

The cause of the second problem, excessive oscillation, is more difficult to assign. However, a likely explanation is suggested if the results of the July 1961 and July 1963 simulations are examined closely. Were excessive oscillation an inherent model error, these simulations too should suffer from the problem. Instead, the simulations using input data derived from the Keszthely wind record have transverse oscillations comparable to those actually observed. In the July 1963 simulation employing the Balatonszemes wind data, however, the oscillation is again too large. Though this is most evident at mid-lake stations (not pictured), the tendency is apparent in Figure 8.24. While this evidence is far from conclusive, it is nevertheless suggestive. It may be that the Balatonszemes wind data is simply not representative of winds over the remainder of the lake, and thus leads to poor predictions. (This, of course, may also be the fault of the adjustment factor applied due to the assumed spatial variation.) Unfortunately, the generality of this explanation cannot be established until more data is available and more historical events are simulated. The inherent uncertainty and error in the wind measurement is another likely explanation.

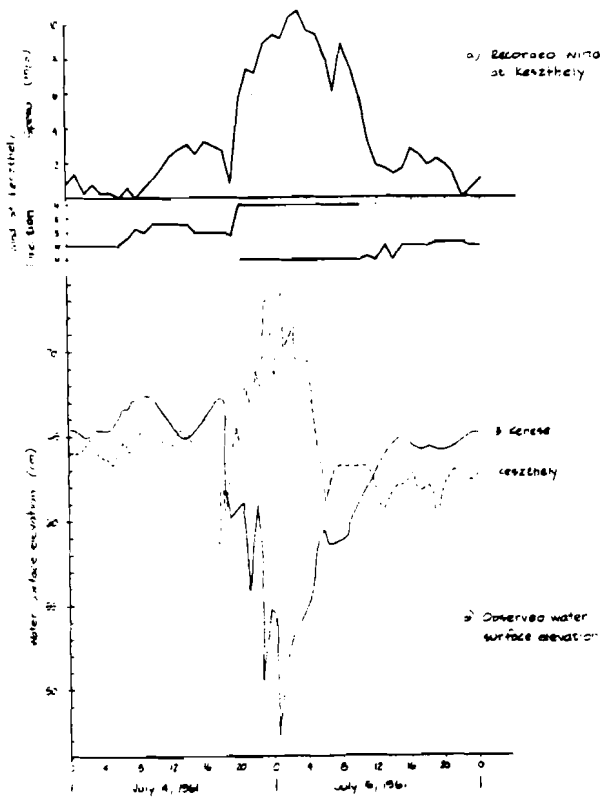


Figure 8.21

Observation data for event
of July 4 and 5, 1961

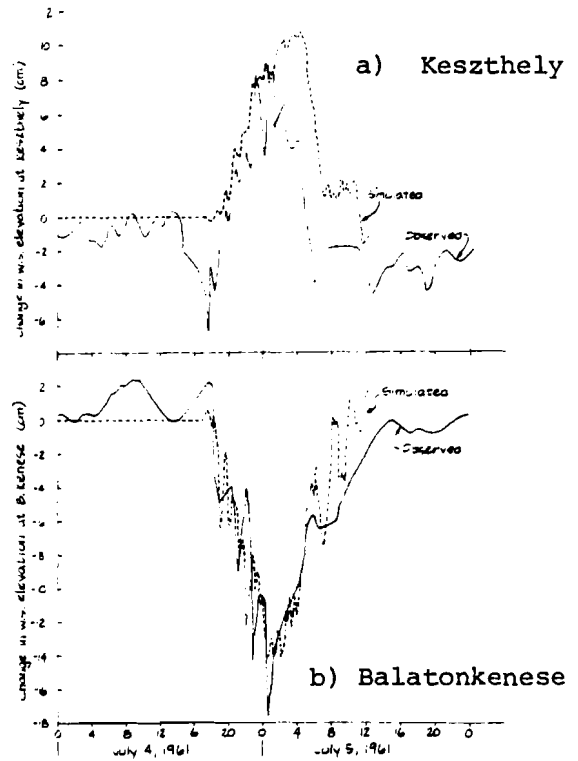


Figure 8.22

Comparison of simulation
results and observations
for event of
July 4 and 5, 1961

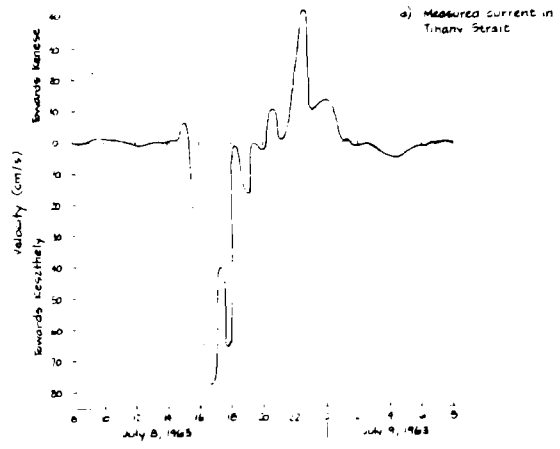
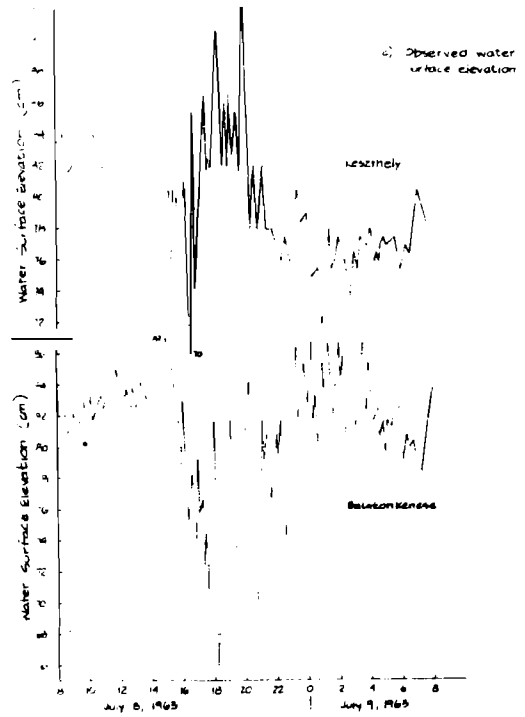
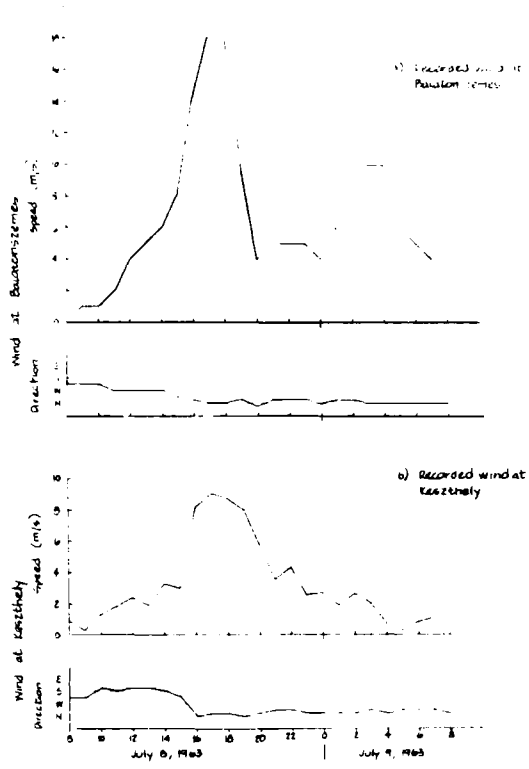
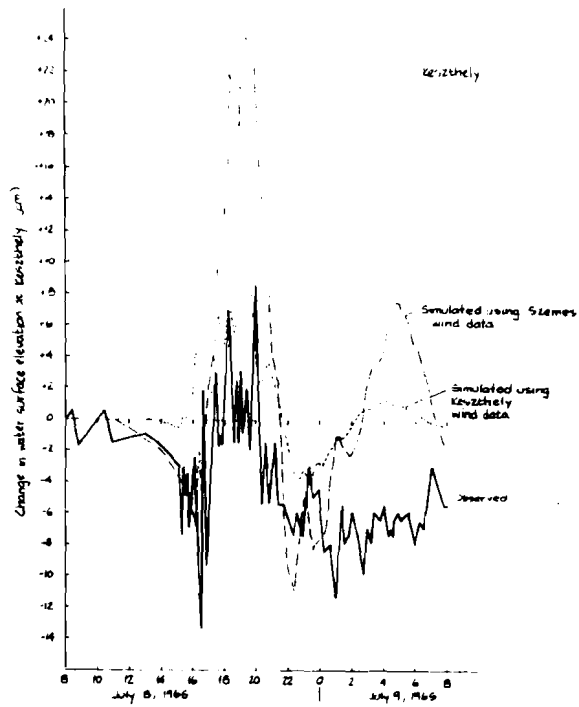
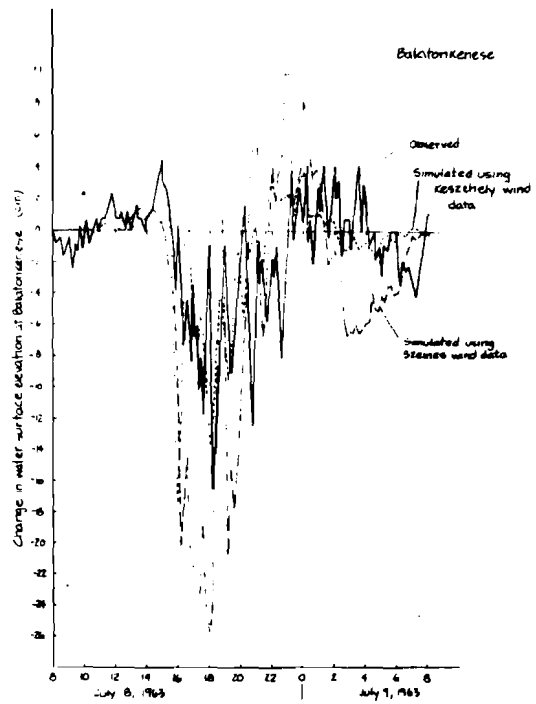


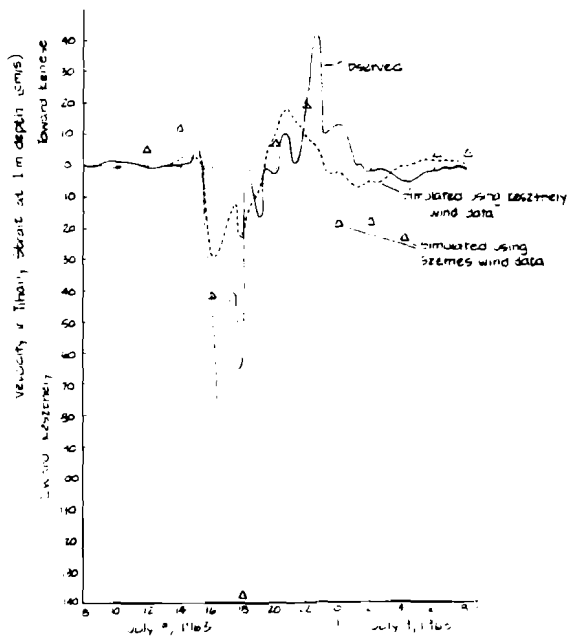
Figure 8.23
 Observation data for event
 of July 8 and 9, 1963



a) Water surface elevation at Keszthely



b) Water surface elevation at Balatonkenese



c) Current in Tihany Strait

Figure 8.24
Comparison of simulation
results and observations
for event of
July 8 and 9, 1963

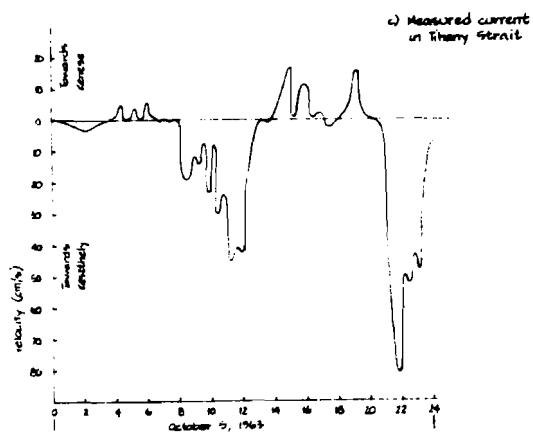
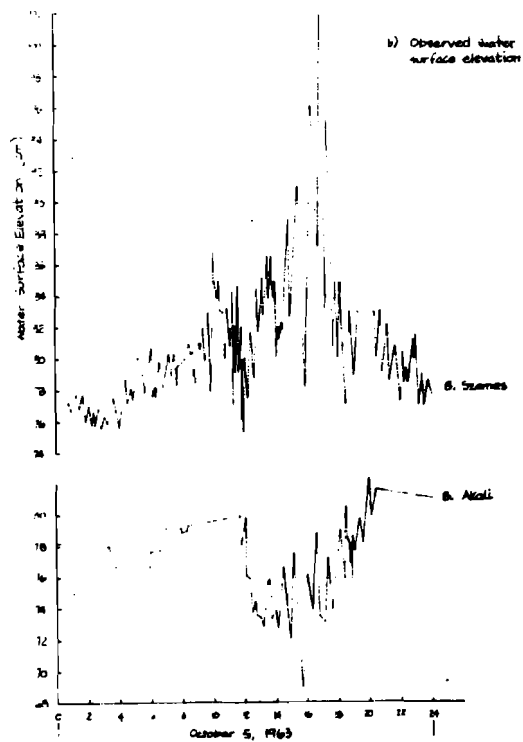
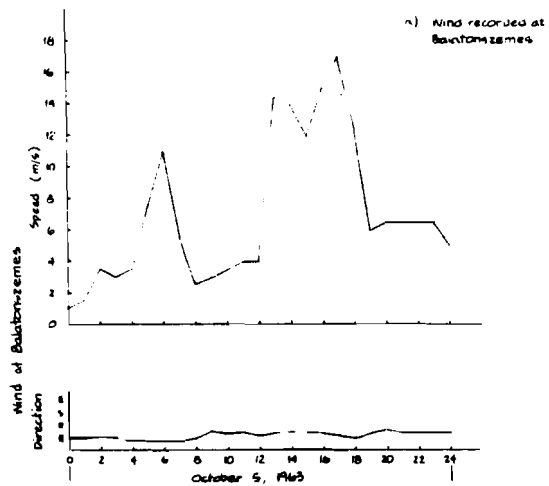
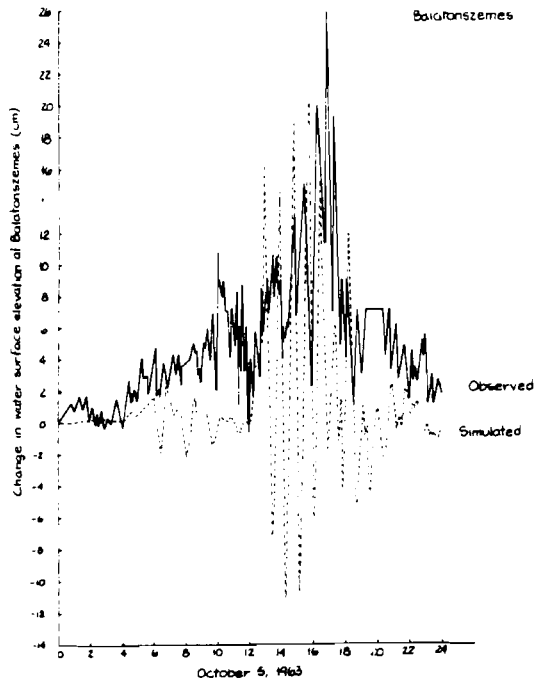
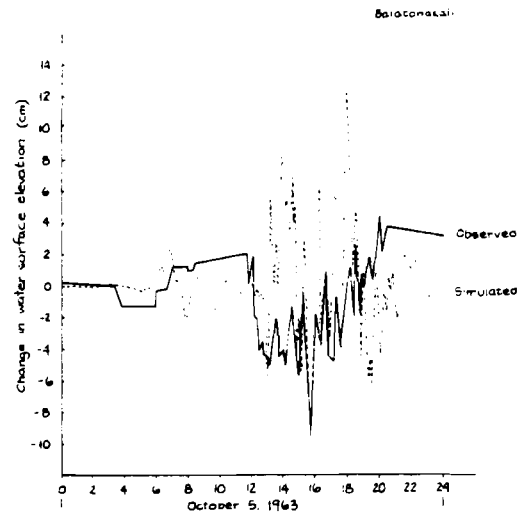


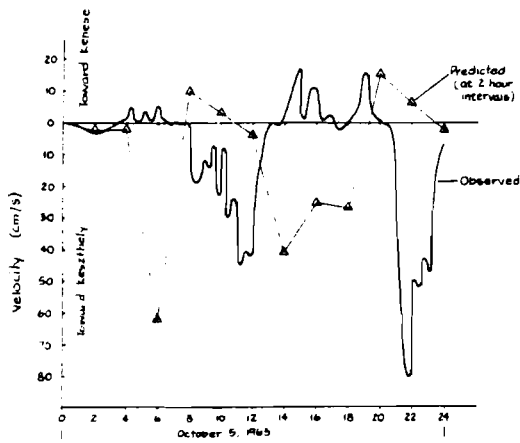
Figure 8.25
Observation data for event
of October 5, 1963



a) Water surface elevation at Balatonszemes



b) Water surface elevation at Balatonakali



c) Current in Tihany Strait

Figure 8.26
Comparison of simulation results and observations for event of October 5, 1963

8.5 Analysis and Conclusions

8.5.1 Conclusions

This chapter has described the process of calibrating, testing sensitivity and verifying the Galerkin model for application to Lake Balaton. Results from the calibration and sensitivity testing illustrate that the model, though it is sensitive to certain parameters, can be calibrated to produce seiche amplitude, period and attenuation similar to that observed in Balaton. Reproduction of the lake's behavior depends primarily on the choice of the form and magnitude of the vertical eddy viscosity function. Model results are relatively independent of the bottom friction factor and finite difference grid spacing over the range investigated. However, the speed and direction of the wind significantly affect the predicted water motion and water surface elevation.

Verification of the model against actual historical events proved successful, though not without exception. Two events characterized by a strong longitudinal seiche, in July 1961 and July 1963, were adequately predicted using input data based upon wind records from Keszthely. Repetition of the July 1963 simulation with wind data based on the Balatonszemes record led to incorrect results, however.

A strong transverse seiche dominated the motion of a third historical event, in October 1963. This event was not well represented by the model simulation due, we suspect, to inadequacies in the input wind data. Events such as this, where the wind is almost exactly transverse to the lake, promise to be difficult for any circulation model. Under these circumstances, small errors in the wind data can produce large errors in the predicted motion. This problem can most likely be reduced by more accurate and complete specification of the wind over the entire lake.

From the general success of the calibration and verification studies, we conclude that the model can be a useful and reasonably accurate tool for the study of Lake Balaton's water quality. How it can be integrated into the study of water quality is discussed in Chapter 9. Before turning to that discussion, however, it is useful to illustrate by example the type of information which the model can supply. This is the topic of the following subsection, an analysis of the simulation results for the July 1963 event.

8.5.2 Analysis of an Event Simulation

Having been successfully calibrated and verified, the circulation model becomes a tool which we can use to study and predict the motion within the lake. Of particular interest for the Lake Balaton study are those motions which will significantly affect the water quality within the lake. In this section we will examine selected results from our simulation of the July 8 and 9, 1963 event to illustrate the spatial and temporal character of motion within the lake.

As a framework for our analysis, we subdivide the lake into four basins as shown in Figure 8.27. This four basin configuration has been used previously in models of Balaton's water quality by Leonov (1980), van Straten (1980) and Csaki and Kutas (1980). In those models, each basin is as a separate fully mixed "box" in which the phosphorus transformations over time are simulated. The boxes interact only through the exchange and transport of mass between the boxes - an unknown factor which must be specified as input to the phosphorus models. In the past, monthly average hydrologic flow rates have been used as the mass transport rates. In this section, we will re-evaluate those transports using the circulation model.

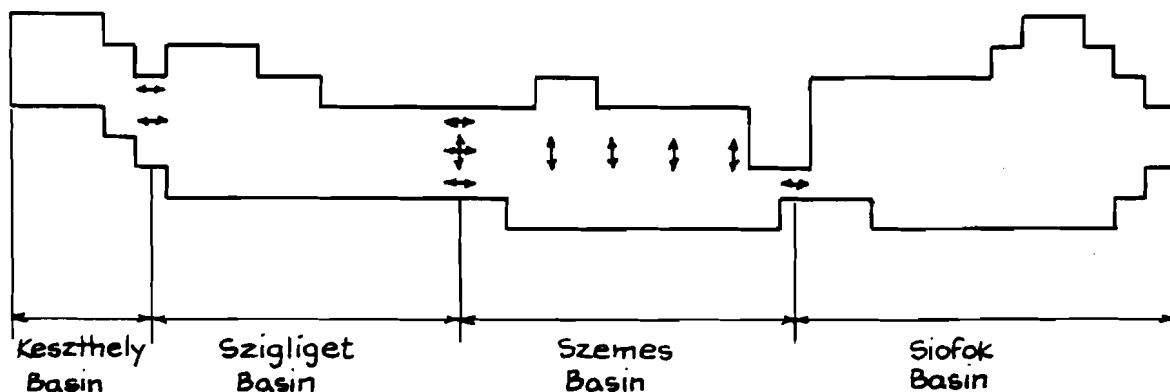


Figure 8.27

Correspondence of the Lake Balaton basins with the circulation model finite difference grid

The total, net transport between the basins is shown in Figure 8.28 as the time histories of flux rates (volume of water per unit time) predicted by the model. The fluxes shown are for the three inter-basin sections indicated by columns of horizontal arrows in Figure 8.27. We note two important characteristics of these fluxes. They are highly transient; for example, at the Szigliget to Szemes section the net transport reverses direction seven times in eight hours. The fluxes are also very large, exceeding the hydrologic through-flows by several orders of magnitude. When expressed in the same units as used in Figure 8.28 ($1000 \text{ m}^3/\text{s}$), the monthly average flows from Table 7.1 are 0.009, 0.014, and 0.014 for the inter-basin sections in order from Keszthely to Siofok. The results clearly indicate transports of far greater magnitude and transience than employed in the water quality models to date.

The transports shown in Figure 8.28, being net transports, ignore all variations in the current across the lake section. Such variations, if significant, would be important if water quality parameters varied across the section as well. They could also act to cause mixing along the lake. The magnitude of such current variations are shown in Figures 8.29 through 8.31. Figures 8.29 and 8.30 show the lateral profiles of velocity at the water surface (unshaded profile) and one meter above the lake bottom (shaded profile) at the sections between the Keszthely and Szigliget basins, and the Szigliget and Szemes basins. The section between the Szemes and Siofok basins, located at Tihany Strait, is represented more simply in the model: as a single grid square rather than the two or three lateral grids at the other sections. This permits the different presentation format used in Figure 8.31 for this section, showing the complete vertical velocity profile.

Figures 8.29 through 8.31 reveal generally unidirectional flow throughout a section. Large velocity variations in the vertical are not uncommon, however, and counter-currents at the lake surface and bottom are observed occasionally. However, it is clear that flow variations in time are considerably greater than those in the vertical and lateral directions.

Mass transport need not occur solely in the longitudinal direction, of course, lateral motions can influence water quality as well. The character of lateral transport within the Szemes basin is examined in Figure 8.32, a drawing similar to those in Figures 8.29 and 8.30, but showing the transport across an east-west, rather than a north-south, section. The section is located by the row of vertical arrows in Figure 8.27. Again, both surface and bottom currents are shown.

The model results pictured in Figure 8.32 indicate considerably greater spatial variation than in the inter-basin sections. Strong flow reversals occur both vertically and horizontally, showing that significant mixing occurs within the basin. To estimate the volume mixed by these flows, we can use Figure 8.32 to roughly compute the time integrals of the surface and bottom velocities. These integrals are the approximate distances parcels of water near the surface and bottom would be transported in the 9 hours in Figure 8.32. At both depths, the distance is over 1 kilometer, or roughly one-fifth of the basin width. This indicates a volume exchange of roughly the same fraction: one-fifth of the volume in a cross-section of unit width will exchange between the surface and bottom waters. Modeling the basin as fully-mixed laterally, as done in the existing water quality models, thus appears to be a reasonable approximation - at least if periodic wind events occur.

This brief look at the results from the simulation model has given us some new insights into the transport of water quality constituents in the lake. We have seen that lateral motion is strong and will cause considerable mixing across the lake's width. The strength of this mixing is sufficient to justify neglect of lateral variations in water quality constituents. In the longitudinal direction, the dominant transport mechanism is the back and forth motion caused by the longitudinal seiche. This motion is intermittent, since a strong wind is required to set the seiche in motion. Such events are fairly common on the lake, however, and when they occur the seiche current velocities exceed those of the hydrologic flow by about two orders of magnitude. Over time, we believe that the seiche-related motion dominates the longitudinal transport of nutrients and other water quality constituents along the lake. The hydrologic flow is a very minor factor in this transport, in our opinion.

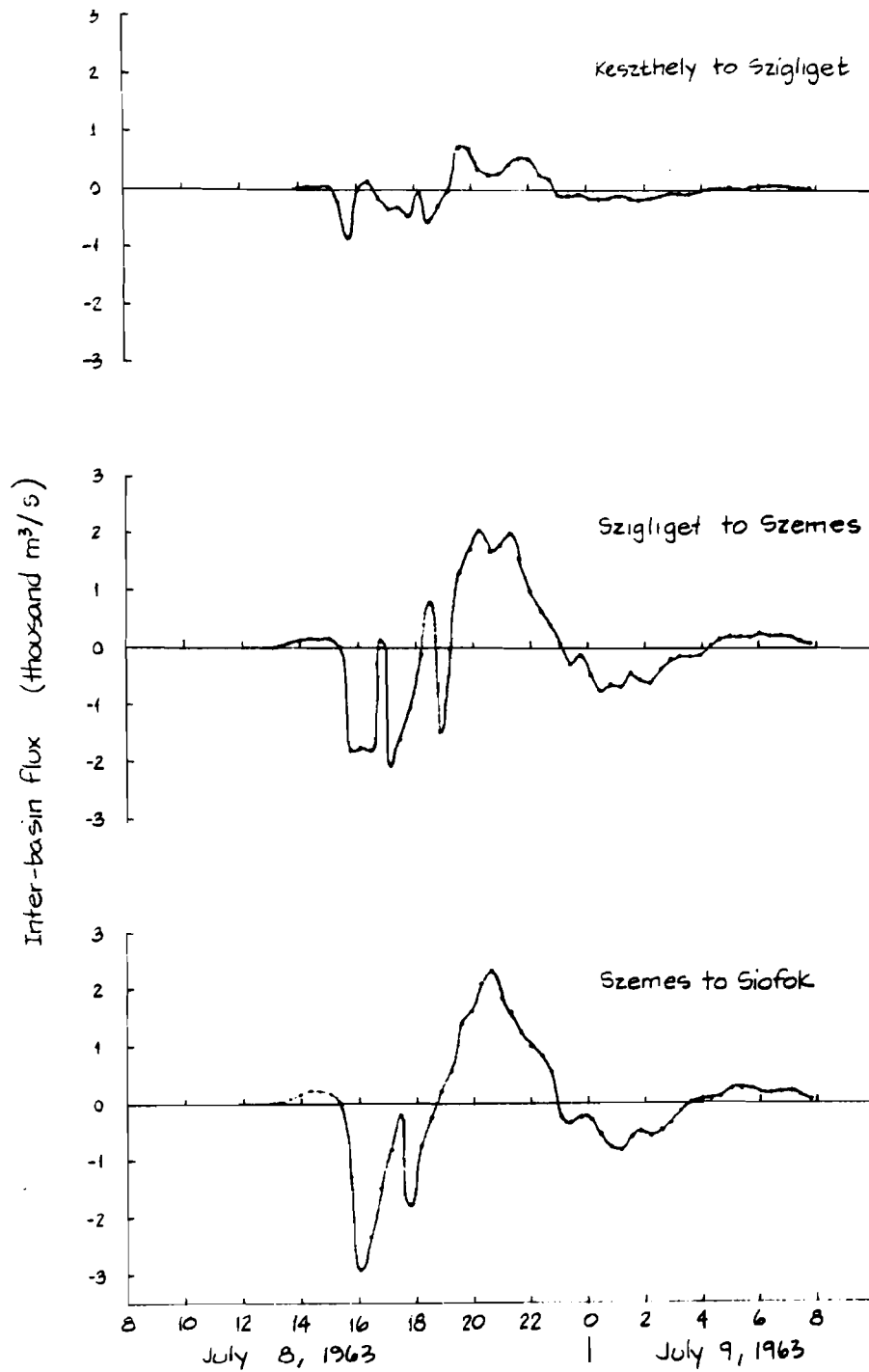


Figure 8.28

Net transport fluxes between the Lake Balaton basins
Simulation of July 8, 1963

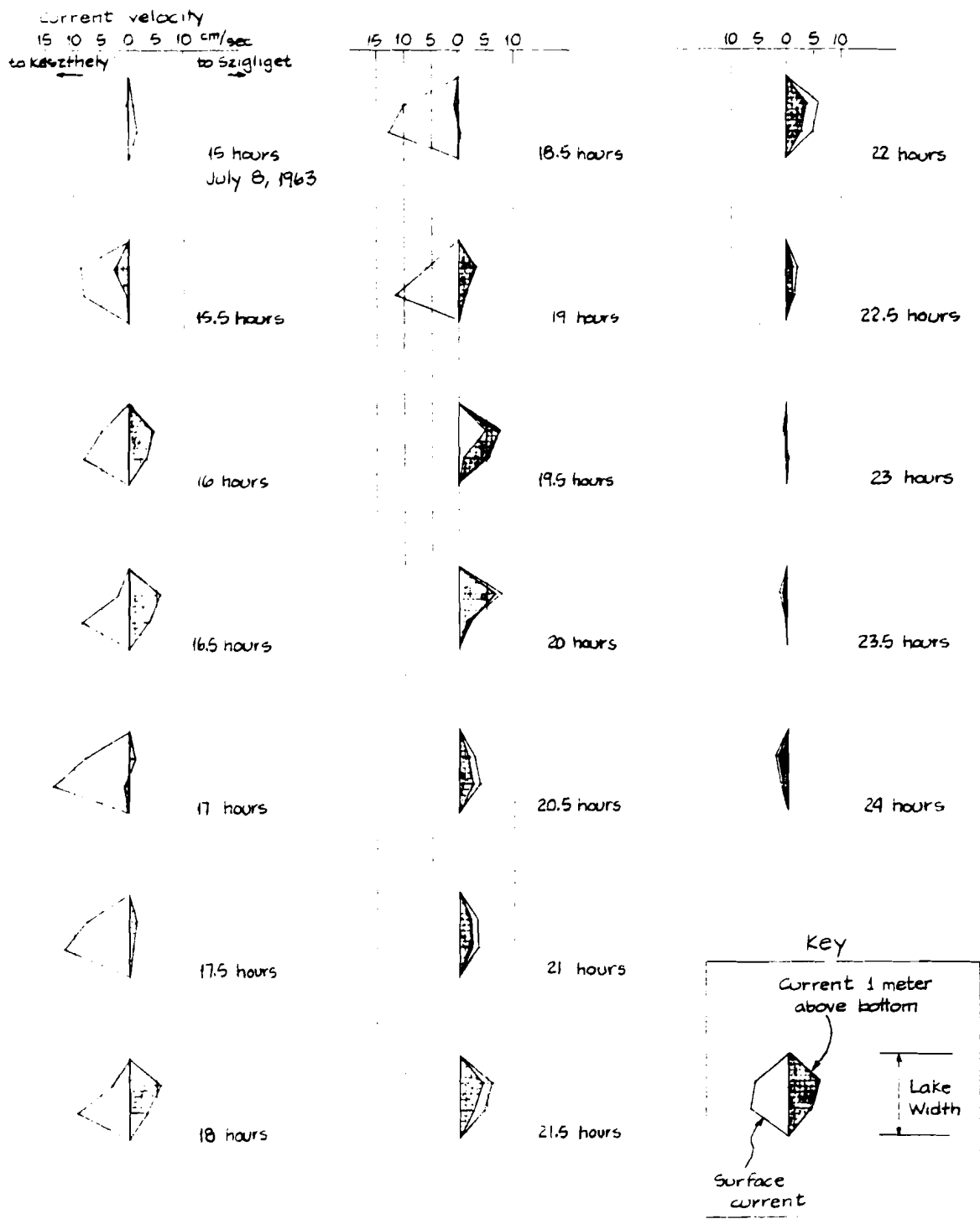


Figure 8.29

Lateral variation and vertical structure of longitudinal velocity from the Keszthely to Szigliget basin
Simulation of July 8, 1963

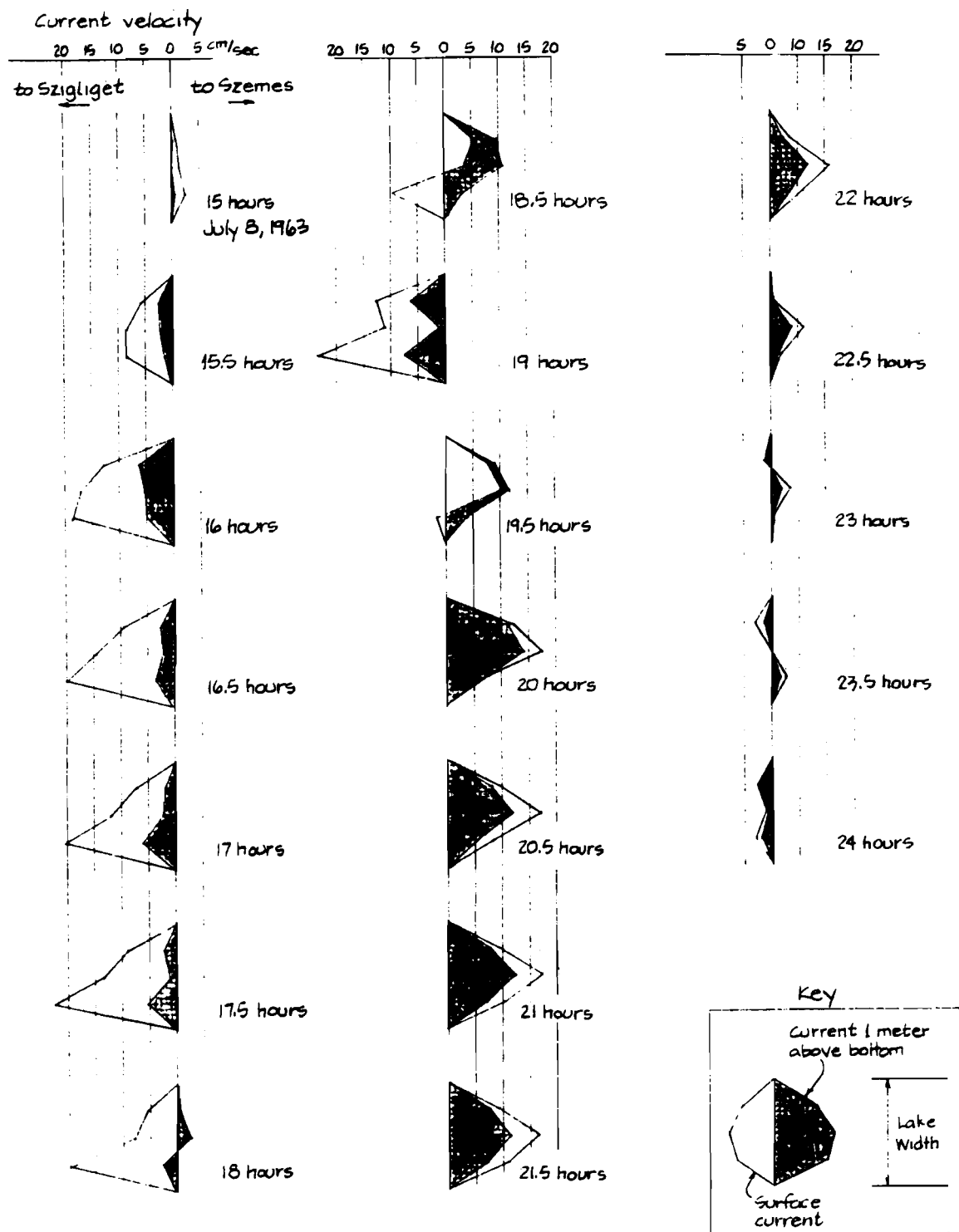


Figure 8.30

Lateral variation and vertical structure of longitudinal velocity from the Szigliget to Szemes basin
Simulation of July 8, 1963

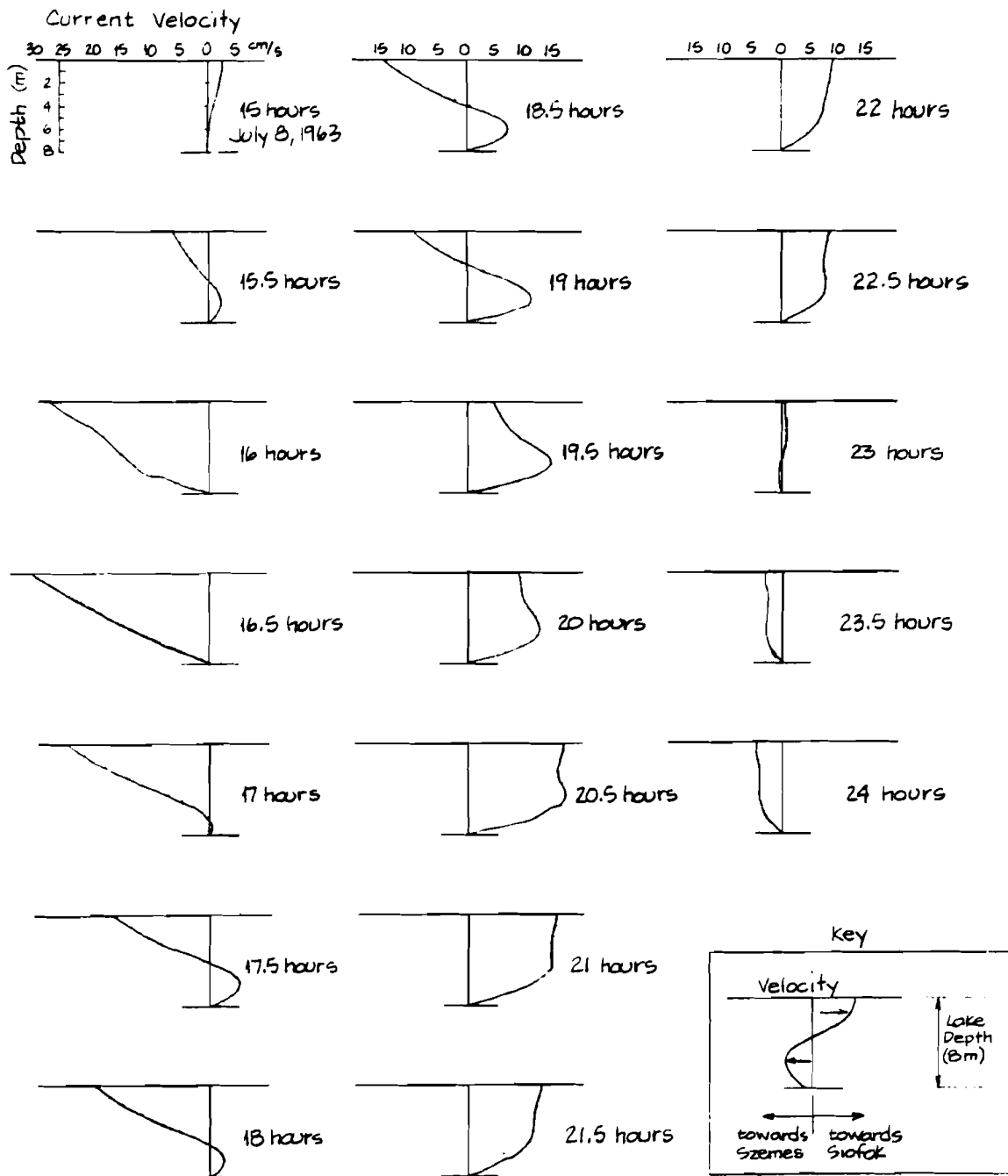


Figure 8.31

Vertical profile of longitudinal velocity
from the Szemes to Siofok basin
Simulation of July 8, 1963

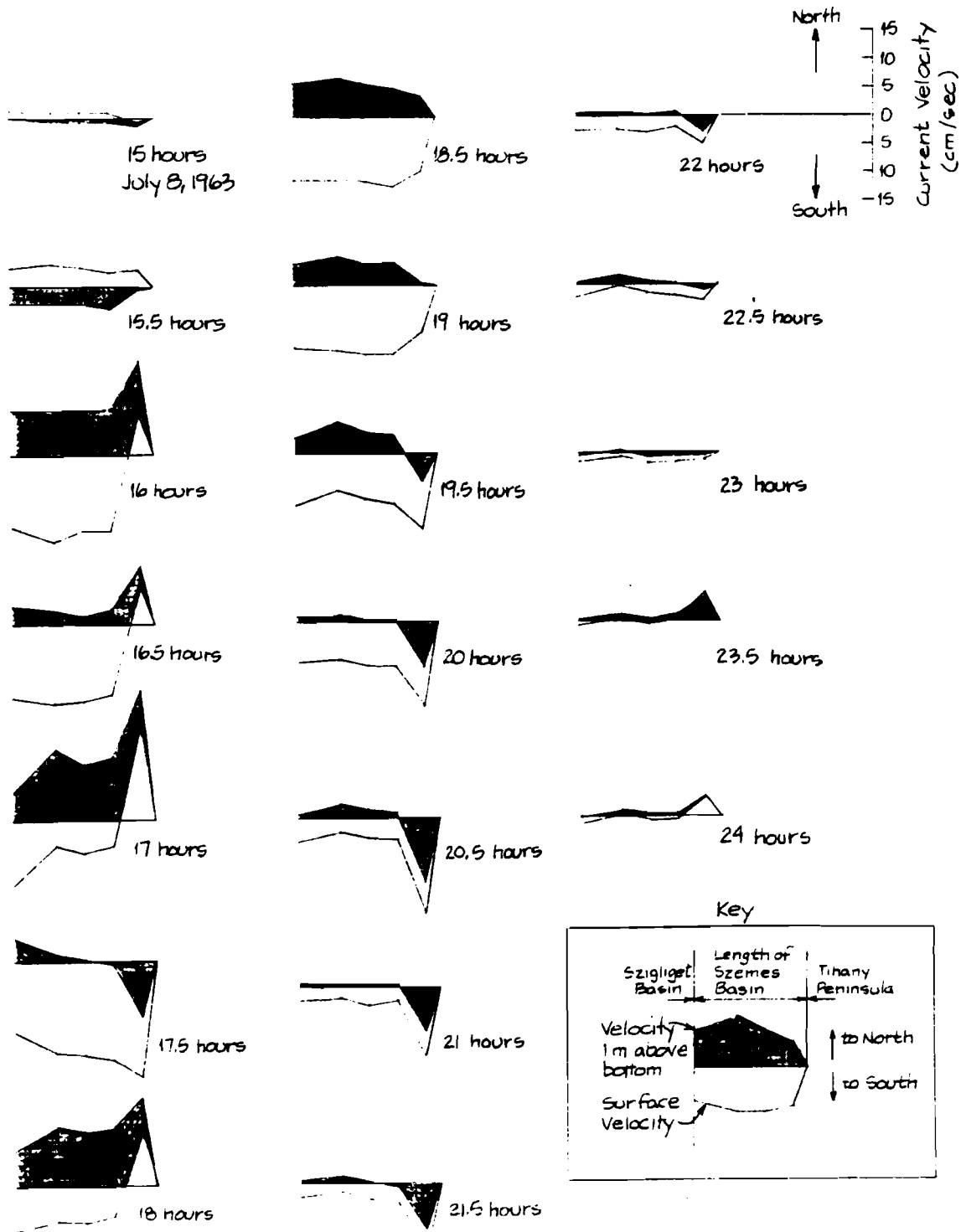
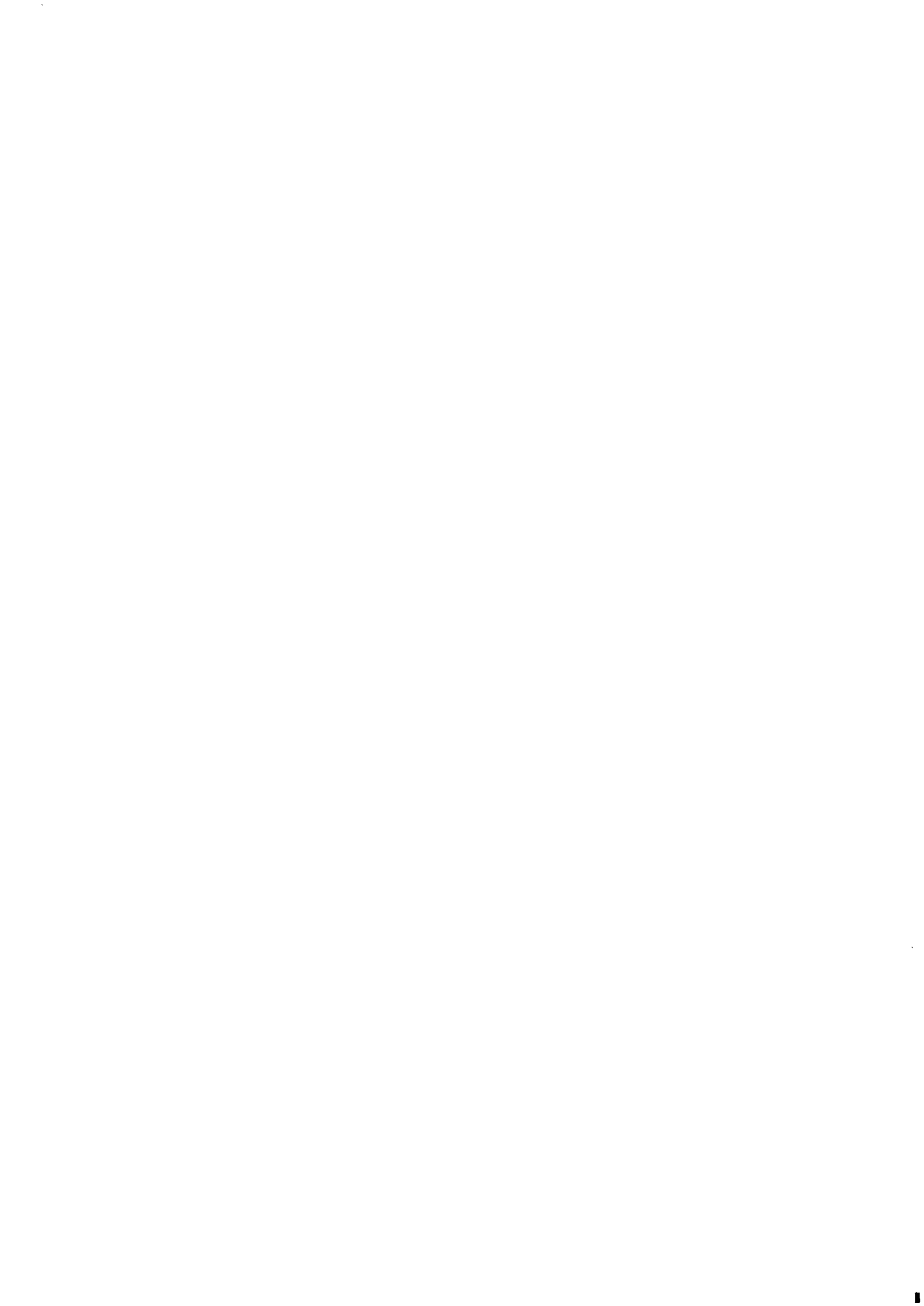


Figure 8.32

Longitudinal variation and vertical structure of transverse velocity within the Szemes basin
Simulation of July 8, 1963



9 CONCLUSION

9.1 Summary of Findings

Our analysis of wind-driven circulation in Lake Balaton has led to the following conclusions:

Although the basic aspects of modeling wind-driven circulation are relatively unambiguous in the literature, there is considerable uncertainty and disagreement over the form and value of certain key model inputs, particularly the vertical eddy viscosity and bottom and surface shear conditions.

The Galerkin model of wind-driven circulation is a relatively inexpensive means to predict the three-dimensional structure of water motion within the lake. An analysis of its assumptions and approximations confirms its validity for use in Lake Balaton.

Careful attention to matching the length and time scales of the processes of interest in the lake is required for both the hydrodynamic transport and biogeochemical components of a coupled water quality model.

The Galerkin model, with proper calibration, can reproduce the general behavior of Lake Balaton. The calibration parameters found successful for Balaton include a bi-linear eddy viscosity function, with a constant value of $20 \text{ cm}^2/\text{s}$ to the water column mid-depth, from where it decreases linearly to 0 at the lake bottom.

The model is unable to satisfactorily replicate the hydrodynamic behavior of the lake using a depth-constant vertical eddy viscosity.

The model is very sensitive to its input parameters, particularly the form and value of the vertical eddy viscosity and the magnitude and spatial variation of the wind shear stress.

The model predictions reveal that seiche motion is the dominant longitudinal transport mechanism in the lake. Laterally, the lake is well mixed by strong wind events.

9.2 Utility of the Galerkin Model for Lake Balaton

Chapter 8 has demonstrated that the Galerkin model can be properly calibrated and verified for Lake Balaton, and can therefore be used as a predictive tool in studies of the lake. Having succeeded in showing that it is feasible to use the model, we must now assess if it is practical to do so.

A first consideration must be cost. To simulate a 48 hour period with the coarse grid requires 60 CPU seconds of computer time on the M.I.T. IBM 370/168. This same task requires about 500 CPU seconds with the fine grid. These are substantial computation times, so that the model is hardly inexpensive, particularly when using the fine grid. In fact, it is probably much too expensive to be used in conjunction with a water quality model to simulate seasonal or yearly periods.

A second consideration is the accuracy of the model. The studies reported in Chapter 8 emphasize the influence of the wind data and other inputs upon the model predictions. Clearly, the model results are only as good as the data driving it, and diligence and care are required to develop input data which adequately represent the wind over the entire lake.

Other aspects of the model accuracy may be raised. The model incorporates the following assumptions and procedures which may not always be justified:

A linear bottom friction law is used.

The vertical eddy viscosity was assumed independent of the wind speed.

The Galerkin base functions, u_0 and v_0 , are biased towards capturing velocity gradients near the surface with less concern for those near the bottom.

The displacement of the water surface is assumed small relative to the water depth.

Convective accelerations and horizontal eddy transport are neglected.

These theoretical criticisms should be weighed against the apparent ability of the model to fairly represent the lake's behavior. Indeed, the model has shown a gratifying ability to model the unusual behavior of the very shallow lake despite approximations and parameter uncertainties.

We must further consider the prospects of additional verification of the model. Though our historical event simulations have yielded a good degree of verification, more could be done. One major problem is that while the model's determination of a vertical velocity distribution imposes an extra computational burden, the vertical information is difficult to verify. Our field studies suggest that the predicted profile shape may be accurate in a time-averaged sense, but a firm conclusion awaits further field data. Similarly, the detail of the predicted horizontal circulation patterns has only a remote chance of adequate verification. The synoptic measurement program needed to supply such verification data is not a practical possibility for Lake Balaton. Though data for other shallow lakes exist for independent verification, the unusual geometry of Lake Balaton demands an individual verification.

A final point to contemplate is the practicality of the model as a component of a coupled water quality model. The high cost factor for this model, mentioned above, derives from the burden created by computation in three dimensions. The vertical velocity profile, for example, is expensive to compute, but is far more information than could be effectively used as input to a linked water quality model. Even the transverse information may not be useful in this respect: a longitudinal one-dimensional water quality model may be perfectly adequate for Lake Balaton.

Though the criticisms raised above restrict the use of the model as a practical tool for water quality engineering and management, the model can nevertheless play a very valuable role as a research and exploration tool. Chapter 7 indicated the importance of the hydrodynamics as a factor in the lake's water quality. However, the interaction of water quality and hydrodynamics is only poorly understood in the lake, and the magnitude of mixing and transport fluxes is largely unknown. For example, our results have shown that the mass transports presently used in water quality models of the lake are far too small. A program of field measurements to fill this gap is impractical, leaving the three-dimensional computer model as the most attractive feasible means to detailed study of the lake hydrodynamics. The 3-D model can be particularly useful as a comparison standard for simpler models of the lake - for example, a transient one-dimensional longitudinal model. We explore these ideas further in the following section.

9.3 Extending the Capability to Model Lake Balaton's Water Quality

A basic rule of mathematical modeling is to use the simplest model adequate for the desired purpose. Though easily stated, this rule is perhaps not so easily implemented, since it is difficult to define "adequate for the desired purpose." In this section, we will elaborate on the nature of this definition for Lake Balaton, and suggest the role of the three-dimensional circulation model in the definition process.

The lake water quality modeler faces a broad spectrum of possible water quality models. At the most complex end of this spectrum lies the transient three-dimensional water quality and transport model. At the simplest is the lake modeled as a fully mixed tank, operated on very long time steps and neglecting completely all internal transport. Possible model alternatives for Lake Balaton are shown in such a spectrum in Figure 9.1. Working water quality models of the lake lie near the lower end of this spectrum since they use a four-box formulation (Leonov, 1980; Csaki and Kutas, 1980; and van Straten, 1980).

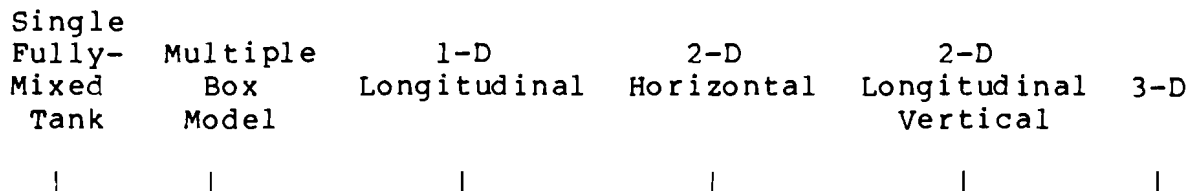


Figure 9.1

Water quality models possible for Lake Balaton

To place our discussion of model characteristics in the proper context, we must first define the purposes and goals of the water quality modeling program. Ultimately, the models must be able to compare and evaluate possible water quality control alternatives for Lake Balaton. Though the

root of Balaton's water quality problem is known to be the introduction of the algal nutrient phosphorus into the lake, there is less certainty over the most effective means to limit nutrient influx. Nutrients are carried into the lake by such disparate sources as the single large inflow of the Zala River and the many small stream, local runoff, and sewage inflows scattered around the lake. These inflow sources vary greatly in time - for example, sewage inflows change with the seasonal tourist population, while the Zala River fluctuates with the annual variation of streamflow, and local runoff and streams respond to the episodic occurrence of rainfall storms. The seasonality of farming leads to still more variation in the quantity of nutrients originating from agricultural fertilizers. These various nutrient sources, which differ so much in their spatial and temporal distribution, require very different control strategies. The water quality model must differentiate the mechanisms and consequences of these controls by recognizing their spatial and temporal character.

Another factor which governs the selection of the model is the availability of field data with which to verify the model results. Model predictions which cannot be substantiated by field observations are of little value; an unverified model cannot be used with confidence to design water quality controls. In Balaton, there are regular field measurements of water quality constituents at only nine stations along the lake ten times per year. (See van Straten et al, 1979.) And, these measurements do not evaluate concentration variations in the vertical or transverse directions. This effectively limits the model resolution to differences along the lake over time periods on the order of a few days.

To satisfy the goals set for the model, but observing the limitations imposed by the available data, we require a water quality model able to predict variations along the lake's long axis and over time periods as short as a few days. Such a model is congruent with the water quality problems identified by van Straten et al (1979); in particular, it can isolate the severe local problems of Keszthely Bay including such transient phenomena as algal blooms. These rough bounds on the model characteristics suggest a transient one-dimensional model of the circulation as our simplest possibility, but we must first consider the approximations and simplifications such a model entails.

Development of a one-dimensional transport model requires that the longitudinal velocity be integrated over the width and depth of the lake cross section. This process is also the basis to develop one-dimensional models of stream water quality, a field in which a substantial body of literature exists. For either the lake or stream, integration over the cross section causes all vertical and lateral variations in

velocity to be eliminated and leads to the longitudinal dispersion coefficient to capture the effects of such variations on longitudinal transport. The dispersion coefficient is defined as a function of the stream velocity, as well as geometrical and other properties. The literature of stream pollution modeling cites a number of problems in this approach, including lateral velocity variations which are greater than the theoretical, dead zones in the flow, secondary circulations due to lateral and vertical velocities, and multiple flow paths in braided streams. These stream characteristics all lead to large increases in the dispersion coefficient above the value predicted by theory.

Although the analogy with stream modeling is instructive, Lake Balaton has many striking differences from the stream situation. While stream flow is generally unidirectional throughout the cross section, our field studies and computer simulations have shown flow reversals in vertical and lateral space in Lake Balaton. Further, the common transverse winds lead to a significant lateral circulation in the lake. These flows, which correspond to secondary circulations in streams, can actually exceed the longitudinal flows in Balaton. Thus, the sectionally averaged longitudinal velocity will be far less representative for Balaton than it will be for streams. This requires a much larger longitudinal dispersion coefficient than would typically be found in stream modeling.

Variations of the longitudinal velocity with time are also important in Balaton due to the frequent and strong seiche motion. This type of motion is similar to that found in a tidal estuary, suggesting an analogy between our modeling task and that of estuarine water quality. Two types of estuarine water quality models exist: the real-time model, which considers the variation of longitudinal velocity over time scales much shorter than the tidal period, and the non-tidal model, which assumes a velocity due only to the net freshwater flow from the estuary. The non-tidal model depends upon averaging over the tidal period to simplify the velocity term, whose temporal variations must then be accounted for in the longitudinal dispersion coefficient. The consequent dispersion coefficient is much greater than the corresponding coefficient for the real-time estuary model. Harleman (1971) cites severe difficulties in defining the dispersion coefficient for non-tidal models and recommends the real-time model for all serious estuary modeling efforts.

The experience in estuarine modeling offers an important lesson for our study of Lake Balaton. Clearly, averaging over sufficient time periods to eliminate seiche motion is possible, but would create considerable difficulties in the determination of the proper longitudinal dispersion

coefficient. This recommends the real time solution of the seiche motion over time steps no longer than about an hour. (In fact, use of an explicit non-rigid-lid computation scheme will impose stability constraints limiting the time step to the order of minutes.) The output from this model may then be averaged in time if it is desired to reduce the time step frequency in a linked biogeochemical model.

With this, we have reasonably established the desired model for Lake Balaton: a one-dimensional longitudinal model able to simulate transient seiche motion. However, we have also disclosed a possible pitfall in this approach. Such a one-dimensional model would incorporate all the complexities due to lateral variations in the longitudinal velocity and transverse circulations into a single parameter, the longitudinal dispersion coefficient. Experiments with a four-box model of Lake Balaton have shown significant sensitivity in the predicted water quality to the magnitude of exchange flows between the boxes (van Straten, 1980). Though the exchange flows are not identical to the dispersion mechanism, they are sufficiently similar to suggest problems. We believe the dispersion coefficient will likely be a sensitive parameter of a one-dimensional water quality model as well. Clearly, it must be carefully defined and closely studied through sensitivity studies.

The results from our simulation of the July 1963 event, analysed in Section 8.5, allow us to identify major hydrodynamic influences upon the water quality. The back and forth motion due to the seiche is the most obvious influence. This motion is primarily translational: it moves parcels of water along the lake, first in one direction and then back. Though lateral and vertical velocity nonuniformities in this motion lead to some dispersion, longitudinal mixing is a secondary effect. In contrast, the motion which occurs when the current reverses direction over the water depth is a hydrodynamic influence which primarily mixes, rather than translates, water along the lake. This type of motion was found only occasionally in the simulation of July 1963, but it nevertheless is a major cause of mass exchange along the lake. Mixing of this type - that is, very strong, but intermittent, mixing - will be poorly captured by a dispersion coefficient dependent upon the average velocity in the lake cross-section.

It is at this point that the role of the three-dimensional model becomes clear. The 3-D model calculates directly the exchange flows which the 1-D model approximates obliquely through the longitudinal dispersion coefficient. Comparison of the fluxes predicted by these two models thus enables the 1-D hydrodynamic model to be checked and its adequacy evaluated. Sensitivity studies on the longitudinal dispersion in conjunction with the three-dimensional model could be particularly fruitful in this respect.

In summary, we see that the role of the three-dimensional model will be one of parameter estimation and calibration for a simpler, less expensive simulation model. In the following section we suggest a model to be developed from the three-dimensional model which strikes a middle ground between the 3-D and 1-D models. This model, we believe, offers an alternative which can operate as an essentially one-dimensional transport model for use in water quality simulation, but which preserves important characteristics discovered in our studies with the three-dimensional model.

9.4 Future Research

The findings reported in this paper suggest many avenues of future research. Areas of study currently contemplated are continuing verification studies, comparison and evaluation of the three-dimensional model with independent one and two-dimensional models, and further investigation of the model results for greater insight into transport and mixing within the lake. The most important goal of our future research is, of course, to develop a linked hydrodynamic-biogeochemical model of the lake water quality.

Currently, efforts are being made at IIASA to obtain the necessary water surface elevation data to test the model with events occurring in 1977. Wind records for 1977 at three stations on the lake have already been included in the IIASA Lake Balaton data bank, along with other meteorological and water quality data. (The wind records are shown in Figure 6.2 of this report.) Unfortunately, continuously recording current meters are no longer in place in the lake so that current velocities can not be a part of the data base. Nevertheless, the availability of three sources of wind data affords an opportunity to further explore the troublesome question of wind data sensitivity.

Evolution of the hydrodynamic model into a water quality model requires both simplification of the hydrodynamic computation and coupling with a biogeochemical component. In the previous section, we concluded that a one-dimensional longitudinal model was a practical and appropriate level of complexity for Lake Balaton. One-dimensional transport is already an output of the existing 3-D model, calculated by laterally summing the mass transports computed in each grid. This is an indirect and expensive route to the desired output, however - a strictly one-dimensional model would yield this information directly and at less cost.

Our calibration experiments and simulations with the three-dimensional model suggest possible problems with a simple 1-D model, however. Calibration experiments showed great sensitivity to the form of the vertical eddy viscosity, as well as the inability to properly model seiche motion with a vertically constant eddy viscosity. We fear that a 1-D model cannot do justice to the subtle dependencies upon this parameter and may fail to properly capture the seiche motion and dissipation. Moreover, a 1-D model cannot model the occurrence of vertical reversals in the longitudinal current. This important exchange mechanism must instead be captured in the dispersion coefficient - a treacherous procedure best avoided. Thus the computationally less expensive 1-D model will result in other costs: decreased accuracy and more difficult parameter estimation.

As a consequence of these difficulties, we propose an alternative to the strictly one-dimensional model. This model can be developed by restructuring the 3-D model to eliminate the lateral direction, leading to a two-dimensional longitudinal-vertical model. This change will reduce the model finite-difference grid to a simple one-dimensional discretization and considerably lessen the program's computational cost. It will retain, however, the potentially important abilities to vary the vertical eddy viscosity and to compute the opposing mass fluxes which occur when the current reverses in the vertical. Comparison of the behavior of this model with that of a simple one-dimensional model can evaluate the importance of the model formulation and eddy viscosity function to the model results.

The longitudinal-vertical model will, we expect, be sufficiently simple for coupling with an existing biogeochemical model. A number of approaches to the coupling mechanism are possible. For example, the four-box approach may be continued for water quality, while a finer grid for the hydrodynamics is employed. In this case, only the hydrodynamic predictions at the box interface sections would be employed. Or, the water quality model could be changed to correspond with the hydrodynamic model discretization, so that both transport and water quality parameters are computed in an essentially continuous fashion along the lake. A compromise between these two extremes is, of course, also possible. Still another alternative might be to use the water quality model independently of the hydrodynamic model, but with exchange flow functions or dispersion coefficients based upon the hydrodynamic results. For example, from an analysis of the three-dimensional hydrodynamic model results it may be possible to derive a unit function for exchange flow. Such a function could be convoluted with longitudinal wind speed histories to compute exchange flows for the water quality model. Examination of these and other possible coupling mechanisms to identify the most desirable will be a major goal of our continuing research.

APPENDIX A FIELD STUDIES OF LAKE BALATON CURRENTS

A.1 Introduction

Field studies were made as a part of this research on four different days, July 11, 1980 and August 11, 12 and 15, 1980. The measuring program sought a qualitative picture of the vertical velocity profile at various locations in the lake and under various wind conditions. A map showing the approximate locations of the measuring stations is included as Figure A.1.

The basic tool for the measurements was a Marsh-McBirney Model 201 Electromagnetic Current Meter. This instrument consists of a sensor probe which is attached by 12 meters of cable to an electronic processor with a visually read panel meter. The processor and panel meter are housed together in a portable electronics case. When the probe is immersed, water flowing past it interacts with the probe's magnetic field to induce a small voltage in the water about the probe. This voltage, which is related to the water velocity, is sensed by electrodes on the probe and then processed to produce a velocity read-out.

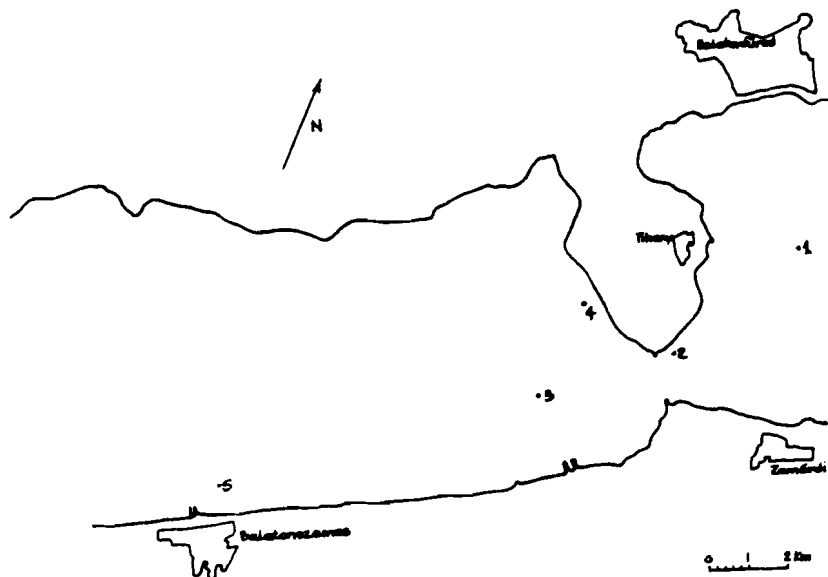


Figure A.1

Approximate location of measurement stations

A.2 Measurement Results

The following describes the conditions and results for each study day in chronological order. At the end of this Appendix, a list of all collected data is included as Table A.1.

July 11

These studies were made with the assistance of the Hungarian Academy of Sciences Biological Institute at Tihany. The Institute's research boat, the Loczy Lajos, was used to make measurements at Stations 1 through 4 about the peninsula of Tihany. Since this was the first use of the current meter in Lake Balaton the studies were intended to test the utility of the meter as well as gather some data.

Wind conditions were variable, but generally light during the morning. During the first two sets of measurements, the winds were from the east and quite light. Later, as we proceeded to Station 3, the winds shifted to the north and grew stronger, almost stormy. These winds died out by the time of our final measurements, however. Stations 3 and 4 were in the wind shadow of the hills on the western side of the Tihany Peninsula during the north winds.

The measurement apparatus consisted of a 5 meter iron pipe, roughly 2 cm in diameter, to which the current meter probe was attached at the end. Tape strips were positioned at one half meter intervals from the probe to mark the length of the pipe, and cross marks were also placed to show the direction in which the probe was pointed. The pipe was lowered into the water to various depths and the velocity was read from the read-out meter on the boat. Since the probe only senses current velocity in a single direction, the pipe was rotated until the direction of maximum velocity was found. The speed was then recorded, along with the direction as estimated by comparing the directional tape marks on the pipe with a compass. The meter velocity reading was quite steady and showed no large influence due to boat motion. The boat was anchored at each stop.

The single exception to this procedure was made at Station 4 during the readings beginning at 1215. Here, the probe was moved about two meters from the end of the pipe and the pipe was pushed into the lake bottom to remain stationary for about 15 minutes at a depth of 2.5 meters. During that time the current reading remained essentially constant. The readings at 2, 1.5 and 0.5 meters were then made in the fashion described above.

The data collected are shown in Figures A.2 through A.5 following the text of this Appendix. With the exception of the nearly constant profile in the Strait of Tihany (Station

2), the currents were variable in both speed and direction. At Station 3 at 1245 hours, for example, the current appeared particularly transient, shifting direction and varying speed considerably at the 2.5 meter depth.

August 11 and 12

These studies were made using the Biological Institute's research boat in the same fashion as reported above. The only significant change in procedure was the use of VITUKI's stream gaging rod rather than an iron pipe for holding the current meter velocity probe. The metal gaging rod was scored at 10 cm intervals, enabling more accurate depth placement of the probe.

The procedure used in these studies was to position the boat (with three anchors) and remain in place for repeated measurements. On the 11th the wind was very light at first, but accelerated by mid-afternoon to 3.5 m/s. Wind direction was generally from the east with the exception of a brief period around 1500 hours when the wind came from SSW. Six profiles at Station 1 and two at Station 3 are included as Figures A.6 and A.7.

One variation on the measurement procedure was employed at Station 1 to evaluate the steadiness of the current. The probe was aligned with the approximate wind direction (80 degrees) and held stationary at four depths for 2 or 3 minute durations. During these periods, readings were made continuously at an interval of about 3 seconds (the time to read aloud and write down a measurement). The results are shown in Figure A.8.

Measurements were made only on the morning on August 12 and, as we typically found in the morning, winds were light. Three profiles at Station 3 were taken and are included as Figure A.9.

August 15

Using the VITUKI research boat, Laszlo Somlyody made measurements off Balatonszemes on the 15th. The VITUKI boat is larger than the Biological Institute's and proved less suited for the measurements. Keeping the boat stationary was particularly troublesome and prevented taking useful measurements during the morning. By afternoon, a procedure was devised to collect useful data and three detailed profiles were made under fairly brisk onshore winds. The collected data are given in Figures A.10 and A.11.

A.3 Conclusions

The collected data lead to the following conclusions:

Strong, unidirectional currents were found in Tihany Strait, in agreement with Muszkalay's (1973) earlier measurements.

This conclusion is qualified by the fact that it is based upon a single measured profile.

Currents in other parts of the lake are highly transient, apparently responding to an unsteady turbulent transport of wind shear vertically into the water column, as well as to other apparently strong influences such as seiching.

The continuous measurements made at Station 1, shown in Figure A.8, are particularly revealing in this respect. Visual inspection of Figure A.8 indicates increasing unsteadiness with depth - compare, for example, the trace for 0.5 meter with that for 2.5 meters. This is confirmed by the statistics plotted in Figure A.9. The mean velocity falls more or less into the type of profile predicted by theory. The increasing standard deviation with depth confirms our observation that unsteadiness increases with depth. Significantly, these measurements indicate a fundamental difficulty in accurately the velocity profile with a single meter in the relatively slow procedure used in our studies.

The currents rarely, if ever, behave as predicted by theoretical arguments such as Plate's (1970).

Few of the profiles conform with classic theory in which the surface current aligns with the wind and in which there is a return current along the bottom in the reverse direction. The series of six consecutive profiles at Station 1 on August 11 under progressively stronger winds could be expected to show the development of such a flow profile. But, as seen in Figure A.6 such is not the case with any consistency. In general, the profiles show unidirectional flow, implying that seiche motion or horizontal flow gyres dominate the flow, preventing establishment of vertical return circulation. Only a synoptic measurement program would be able to prove or disprove this hypothesis, however.

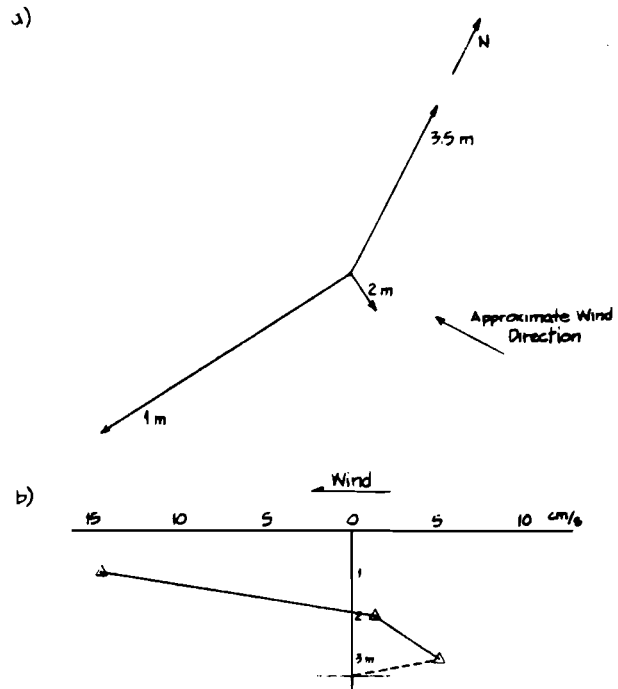


Figure A.2 Current measurements at Station 1, 11 July 1980
 a) Current vector diagram
 b) Velocity component along lake longitudinal axis versus depth

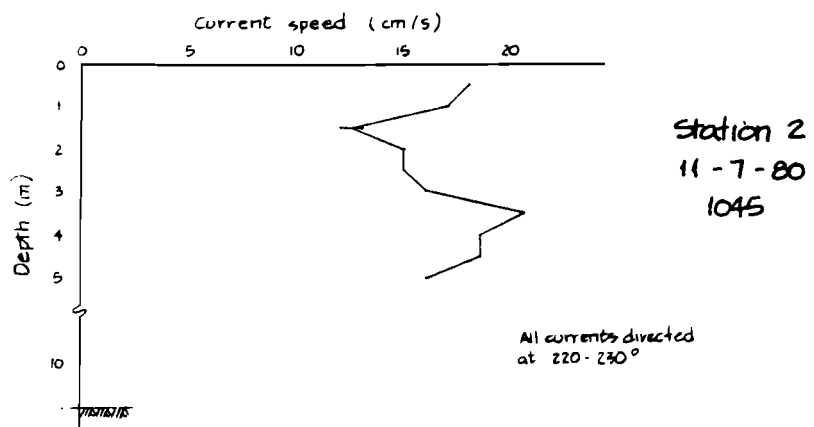


Figure A.3 Current measurements at Station 2, 11 July 1980
 Velocity profile in Tihany Strait

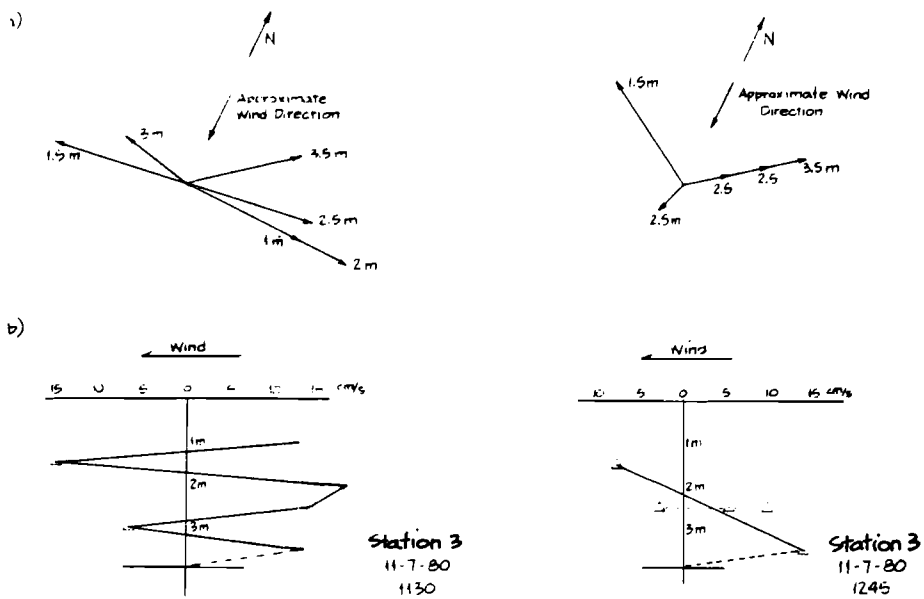


Figure A.4 Current Measurements at Station 3, 11 July 1980

- a) Current Vector Diagrams
- b) Longitudinal Velocity Profiles

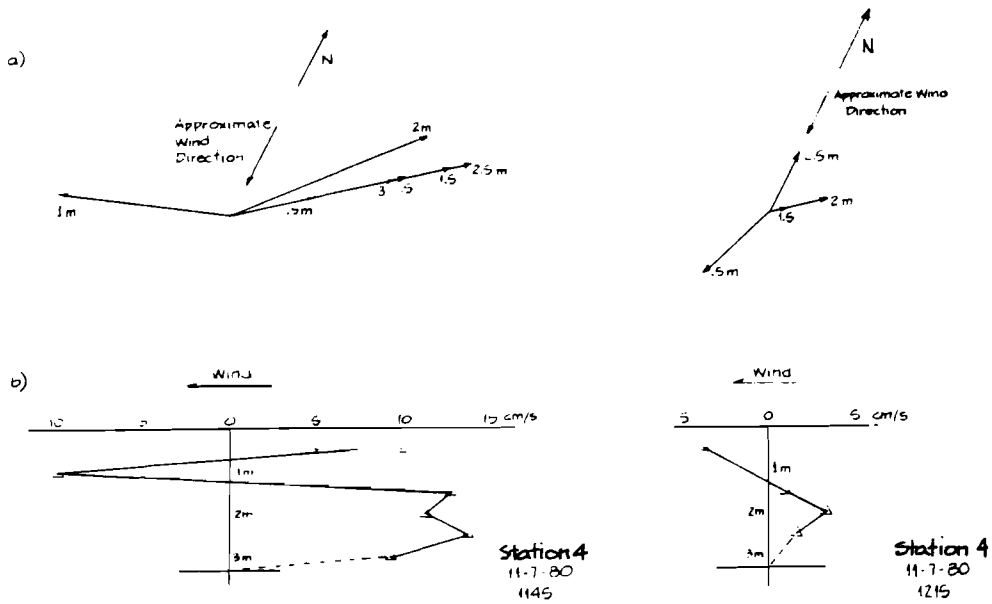


Figure A.5 Current Measurements at Station 4, 11 July 1980

- a) Current Vector Diagrams
- b) Longitudinal Velocity Profiles

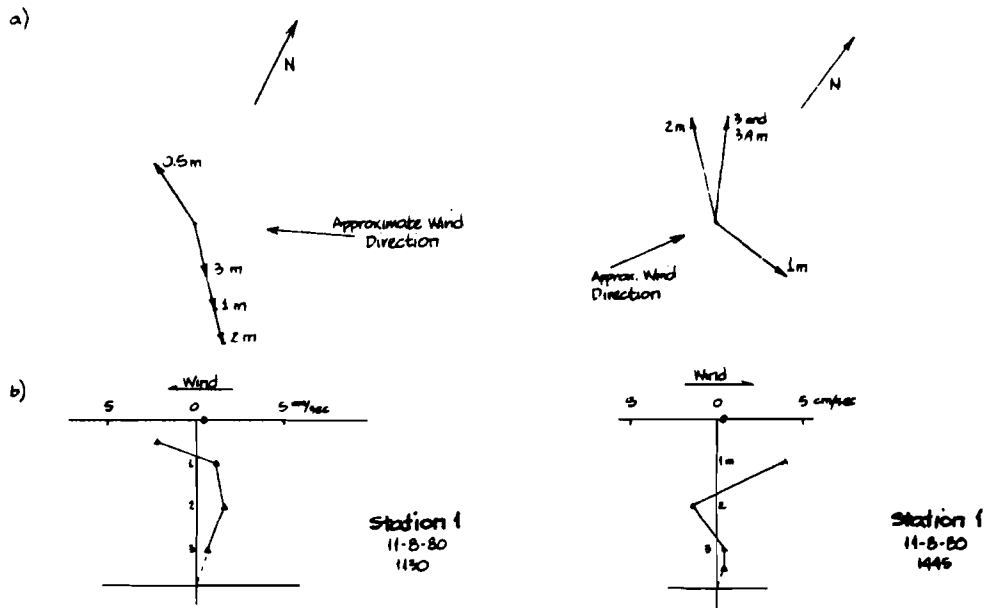


Figure A.6 Current Measurements at Station 1, 11 August 1980

- a) Current vector diagrams
- b) Longitudinal velocity profiles

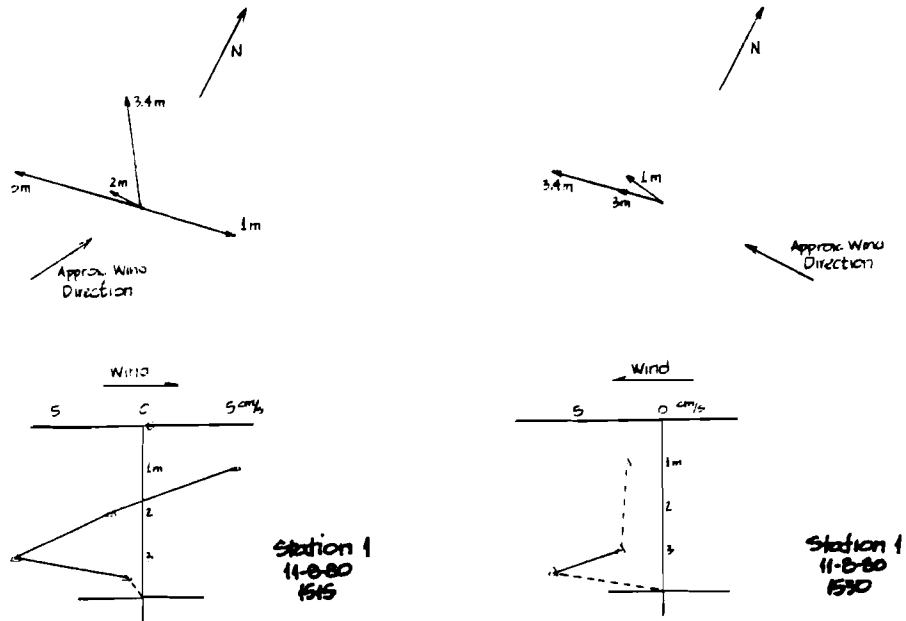


Figure A.6- Current Measurements at Station 1, 11 August 1980

continued

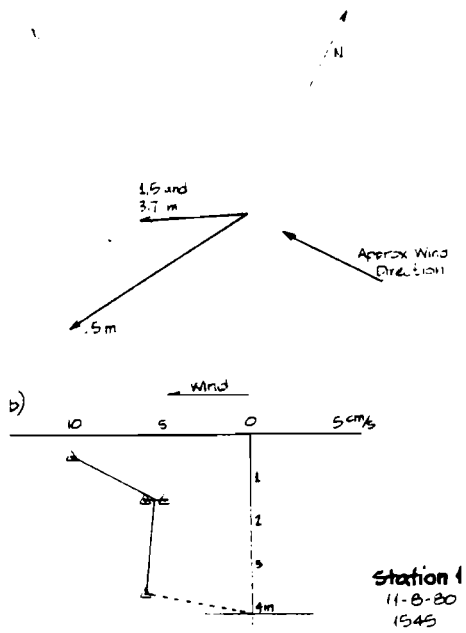


Figure A.6 Current measurements at Station 1, 11 August 1980
continued

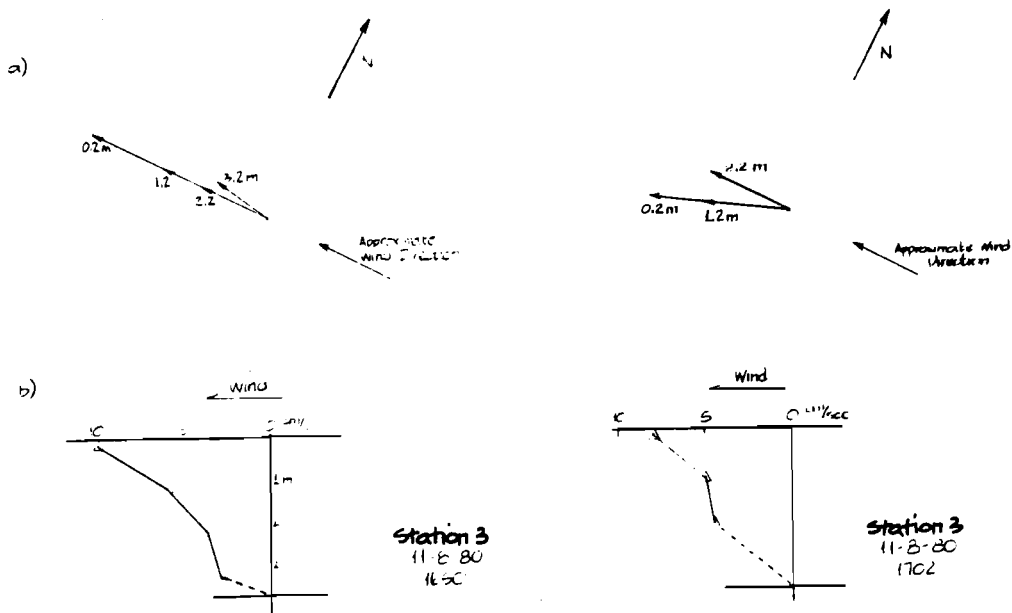


Figure A.7 Current Measurements at Station 2, 11 August 1980

- a) current vector magnitude
- b) longitudinal velocity profile

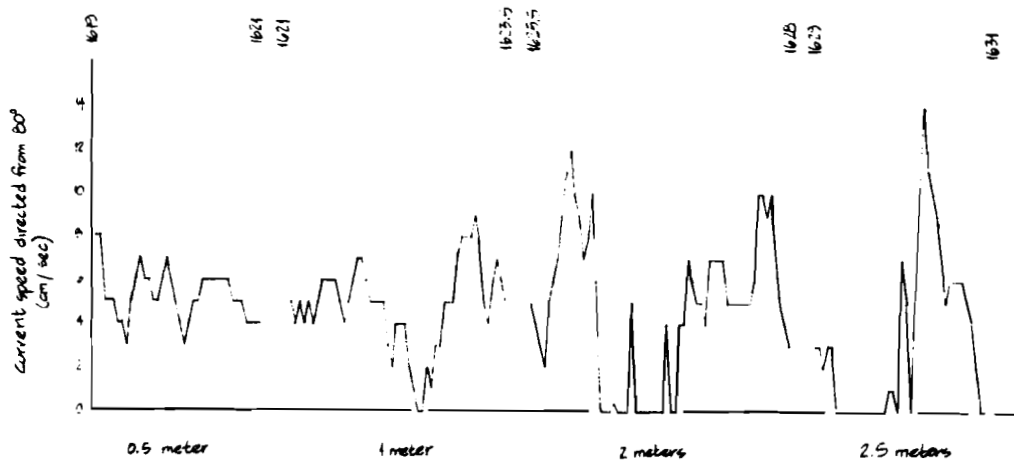


Figure A.8 Continuous measurements at Station 1
11 August 1980 1619 to 1631 hours
Measurement interval is
approximately 3 seconds

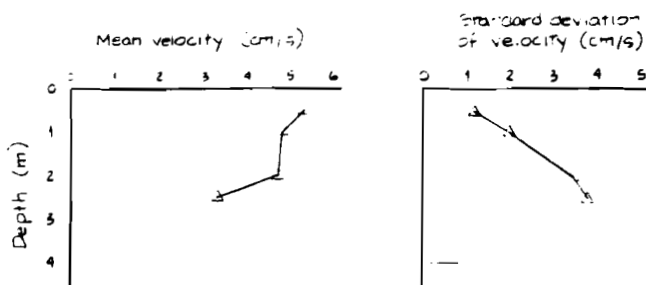


Figure A.9 Temporal statistics of continuous
measurements at Station 1 11 August 1980

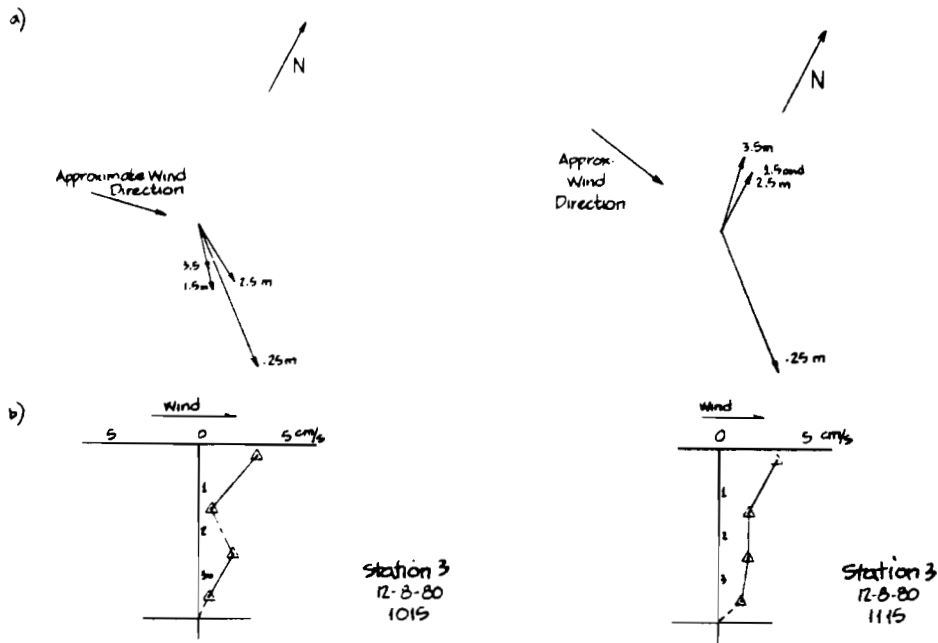


Figure A.10 Current Measurements at Station 3, 12 August 1980

- a) Current vector diagrams
- b) Longitudinal velocity profile

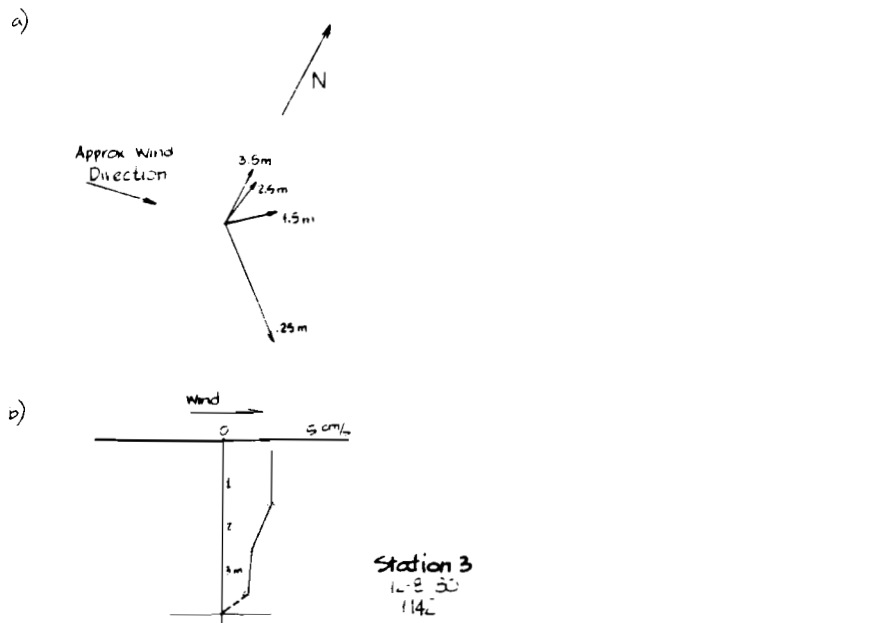
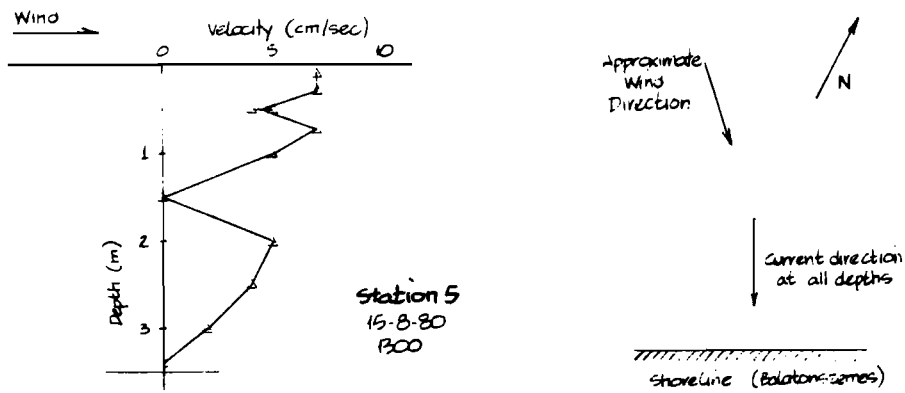


Figure A.10 Current measurements at Station 3, 12 August 1980

continued



Velocity Profile directed from 330°
(i.e. in onshore direction)

Figure A.11 Current measurements at Station 5, 15 August 1980, 1300 hours

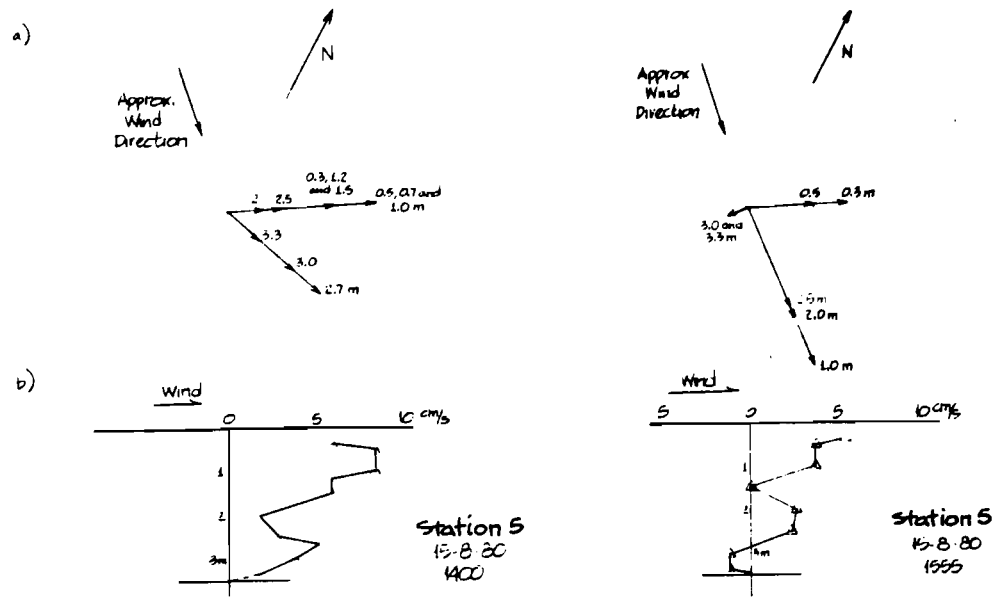


Figure A.12 Current measurements at Station 5, 15 August 1980

- a) current vector diagrams
- b) velocity profiles

Table A.1

Collected current data

<u>Date, Station</u>	<u>Hour</u>	<u>Depth (m)</u>	<u>Current Measurement Speed (cm/sec)</u>	<u>Direction * (degrees)</u>	<u>Wind at Szemes Speed (km/hr)</u>	<u>Direction</u>	<u>Comments</u>
<u>July 11, 1980</u>							
1 (depth 3.5 m)	1015	3	10.5	180			light wind from east
		2	2.5	300			
2 (depth 10.6 m)	1045	1	17	30			light wind from east
		5	16	230			
		4.5	18.5	230			
		4	18.5	230			
		3.5	20.5	230			
		3	16	230			
		2.5	15	230			
2	15	230					
3 (depth 3.9 m)	1130	1.5	12.5	230			north wind- increasing in speed during measurements
		1	17	230			
		0.5	18	220			
		3.5	13.5	230			
		3	8.5	100			
4 (depth 3.3 m)	1145	2.5	15	260			north wind- now decreasing
		2	20.5	270			
		1.5	15.5	80			
		1	14.5	270			
		0.5	variable 25 max.				
		3	9.5	230			
		2.5	14	230			
		2	12	230			
		1.5	13	230			
		1	10	70			
0.5	5 to 10	230					
4	1215	2.5	4	180			north wind
		2	3.5	230			
		1.5	1	230			
		0.5	5	20			

* Direction from which current flows in degrees counterclockwise from magnetic north

<u>Date, Station</u>	<u>Hour</u>	<u>Depth (m)</u>	<u>Current Measurement Speed (cm/sec)</u>	<u>Current Measurement Direction * (degrees)</u>	<u>Wind at Szemes Speed (km/hr)</u>	<u>Wind at Szemes Direction</u>	<u>Comments</u>
3	1245	3.5	14.5	230			north wind
		2.5	10	230			sequential readings made in roughly ten minutes
		2.5	3-5	20			
		2.5	5-6	230			
		1.5	14	120			
<u>August 11, 1980</u>							
1 (depth 3.8 m)	1130	3.5	0	-	0.5	S	observed wind from east to northeast
		3	3	320	at 1100		
		2	7	320			
		1	5	320			
		0.5	4	120			
1 (depth 3.8 m)	1155	3.5	0	-	3.0	S	
		3	0	-	at 1200		
		2	0	-			
		1	0-4	180			
		0.5	7	180			
1 (depth 3.9 m)	1445	3.4	6	130	10.5	-	observed wind from approx. 210 deg.
		3	5	130	at 1500		
		2	6	150			
		1	5	270			
1 (depth 3.9 m)	1515	3.4	6.5	145	10.5	-	
		3	7.5	80	at 1500		
		2	2.0	90			
		1	5.5	260			
1 (depth 3.9 m)	1530	3.4	6.5	80	13.0	-	observed wind from east increasing wind speed
		3	2.5	80	at 1600		
		2	variable	-			
		1	2.5	100			
1 (depth 4.2 m)	1545	3.7	variable-	60	13.0	-	
		1.5	approx. 6	60	at 1600		
		0.5	5-6	60			
			12	30			
3 (depth 3.7 m)	1650	3.2	3.5	100	7.0	-	observed wind from east
		2.2	4	90	at 1700		
		1.2	6.5	90			
		0.2	11	90			

<u>Date, Station</u>	<u>Hour</u>	<u>Depth</u> (m)	<u>Current Measurement</u> Speed (cm/sec) Direction * (degrees)	<u>Wind at Szemes</u> Speed (km/hr) Direction	<u>Comments</u>
3 (depth 3.7 m)	1702	3.2	variable 7 max.	-	-
		2.2	5	90	7.0 at 1700
		1.2	5	70	
		0.2	8	70	
<u>August 12, 1980</u>					
3 (depth 4 m)	1015	3.5	2	320	-
		2.5	3	300	1.5 at 1000
		1.5	3	320	
		0.25	7	310	
3 (depth 4 m)	1115	3.5	3.5	170	-
		2.5	3	180	5.0 at 1100
		1.5	3	180	
		0.25	7	310	
3 (depth 4 m)	1142	3.5	3.5	180	-
		2.5	3	190	5.5 at 1200
		1.5	3	230	
		0.25	7.5	310	
<u>August 15, 1980</u>					
5 (depth 3.5 m)	1300	0.1	7	330	-
		0.3	7	330	18.0 at 1300
		0.5	4-5	330	
		0.7	7	330	
		1.0	5	330	
		1.5	0	-	
		2.0	5	330	
		2.5	4	330	
		3.0	2	330	
		3.3	0	-	

observed wind
from 280 deg.

observed wind
from NNW

<u>Date, Station</u>	<u>Hour</u>	<u>Depth (m)</u>	<u>Current Measurement Speed (cm/sec)</u>	<u>Current Measurement Direction * (degrees)</u>	<u>Wind at Szemes Speed (km/hr)</u>	<u>Wind at Szemes Direction</u>	<u>Comments</u>
5 (depth 3.5 m)	1425	0.3	6	285	17.0	-	
		0.5	8	285	at 1400		
		0.7	8	285			
		1.0	8	285			
		1.2	6	285			
		1.5	6	285			
		2.0	2	285			
		2.5	3	285			
		2.7	7	240			
		3.0	5	240			
		3.3	2.5	240			
5 (depth 3.5 m)	1555	0.3	4.5	310	7.0	-	
		0.5	3	310	at 1600		
		1.0	8	240			
		1.5	0	-			
		2.0	5-6	240			
		2.5	5	240			
		3.0	1	40			
		3.3	1	40			



APPENDIX B DERIVATION OF THE GALERKIN MODEL

B.1 Formulation of the Galerkin Equations

In the lake circulation problem, we seek functions u and v which satisfy the momentum equations 7.2 and 7.3. For convenience, we will express these equations using operator notation. The equations then become:

$$L_x(u) = \frac{\partial u}{\partial t} - \frac{\partial}{\partial z} (A_v \frac{\partial u}{\partial z}) = fv - g \frac{\partial \eta}{\partial x} \quad (B.1a)$$

$$L_y(v) = \frac{\partial v}{\partial t} - \frac{\partial}{\partial z} (A_v \frac{\partial v}{\partial z}) = -fu - g \frac{\partial \eta}{\partial y} \quad (B.1b)$$

where L_x and L_y are differential operators. Equations B.1 are satisfied by u and v exactly, but the approximation functions defined in Equations 7.9, \hat{u} and \hat{v} , can satisfy these relations only approximately. Nevertheless, we can still determine the approximations to achieve a solution in some best fit manner. The error in the approximations is defined by the residuals, R_x and R_y :

$$R_x = L_x(\hat{u}) - L_x(u) \quad (B.2a)$$

$$R_y = L_y(\hat{v}) - L_y(v) \quad (B.2b)$$

The best fit solution determines the values of \hat{u} and \hat{v} which minimizes these residuals.

There are many possible ways in which to minimize the residuals. One method, which includes the Galerkin technique, is the method of weighted residuals. This method

achieves a best fit solution over some domain by considering the weighted integral of the residual. When the value of the integral is zero, the residual is taken to be minimized over the domain. In the circulation problem, the domain of interest is the water depth, $z=0$ to h , so that the integrals formed are:

$$\int_0^h R_x W dz = 0 \quad (B.3a)$$

$$\int_0^h R_y W dz = 0 \quad (B.3b)$$

The term W in the integrals is the weighting function. The Galerkin method is distinguished from other weighted residual methods by the use of the expansion functions, Ω_j , as the weighting functions also:

$$\int_0^h R_x \Omega_i dz = 0 \quad i = 1, 2, \dots, n \quad (B.4a)$$

$$\int_0^h R_y \Omega_i dz = 0 \quad i = 1, 2, \dots, n \quad (B.4b)$$

Equation B.4a produces a set of n algebraic equations which may be solved for the n unknown c_j ; similarly, B.4b yields equations in the unknown d_j . A particularly convenient choice of the Ω_i are functions which are orthogonal. That is, functions for which

$$\int_0^h \Omega_j \Omega_i dz = 0 \quad \text{for } i \neq j$$

The use of orthogonal functions considerably simplifies Equations B.4 by eliminating all but a few terms.

B.2 Derivation of Nelson's Model

Nelson (1979), in her derivation of the wind circulation model, builds upon previous work by Cooper and Pearce (1977) with the Galerkin technique. Cooper and Pearce had employed orthogonal cosine expansion functions,

$$\Omega_j = \cos \frac{a_j z}{h} \quad (\text{B.5})$$

and sine functions for the leading terms of the Galerkin expansion,

$$u_o = - \frac{h\tau_s^x}{\pi\rho A_v} \sin \frac{\pi z}{h} \quad (\text{B.6a})$$

$$v_o = - \frac{h\tau_s^y}{\pi\rho A_v} \sin \frac{\pi z}{h} \quad (\text{B.6b})$$

The expressions for u_o and v_o satisfy the surface shear condition (Equation 7.5) and a no-slip condition. Cooper and Pearce had employed a no-slip boundary condition instead of the linear friction law (Equation 7.7) used by Nelson. Unfortunately, Cooper and Pearce found this model to be unsatisfactory, requiring many terms in the cosine expansion series to converge to a reasonable result. They attributed this difficulty to the steep velocity gradients near the no-slip bottom and suggested a modified formulation. The modifications, implemented by Nelson, include the substitution of the linear friction law for the bottom boundary condition and the consequent reformulation of the leading functions of the expansion.

Nelson's reformulation of the Galerkin statement

continues the use of cosine expansion functions, but employs new leading functions:

$$u_o = \frac{\tau_s^x z^2 (z-h)}{\rho h^2 (\alpha_1 h + \beta_1)} + \frac{\tau_s^x}{\rho \alpha_1} \ln \left(\frac{\alpha_1 h + \beta_1}{\alpha_1 z + \beta_1} \right) \quad (\text{B.7a})$$

$$v_o = \frac{\tau_s^y z^2 (z-h)}{\rho h^2 (\alpha_1 h + \beta_1)} + \frac{\tau_s^y}{\rho \alpha_1} \ln \left(\frac{\alpha_1 h + \beta_1}{\alpha_1 z + \beta_1} \right) \quad (\text{B.7b})$$

where α_1 and β_1 are the coefficients of the eddy viscosity formula (Equation 7.8) for the linear segment at the water surface. (See Figure 7.1.) This functional form is selected in order to capture the shape of the velocity profile near the bottom, particularly the troublesome steep velocity gradient. The second terms in Equations B.7 are the analytical solution for a 1-D infinite channel with linear eddy viscosity variation, while the first terms are included to simplify satisfaction of the bottom boundary conditions. The complete trial functions are thus:

$$\begin{aligned} \hat{u} &= u_o + \sum_{j=1}^n c_j \Omega_j \\ &= \frac{\tau_s^x z^2 (z-h)}{\rho h^2 (\alpha_1 h + \beta_1)} + \frac{\tau_s^x}{\rho \alpha_1} \ln \left(\frac{\alpha_1 h + \beta_1}{\alpha_1 z + \beta_1} \right) + \sum_{j=1}^n c_j \cos \frac{a_j z}{h} \end{aligned} \quad (\text{B.8a})$$

$$\begin{aligned} \hat{v} &= v_o + \sum_{j=1}^n d_j \Omega_j \\ &= \frac{\tau_s^y z^2 (z-h)}{\rho h^2 (\alpha_1 h + \beta_1)} + \frac{\tau_s^y}{\rho \alpha_1} \ln \left(\frac{\alpha_1 h + \beta_1}{\alpha_1 z + \beta_1} \right) + \sum_{j=1}^n d_j \cos \frac{a_j z}{h} \end{aligned} \quad (\text{B.8b})$$

The values of a_j are determined so as to satisfy the bottom boundary conditions. They are defined implicitly by the expression:

$$a_j \tan a_j = \frac{c_b h}{A_v(h)} \quad (\text{B.9})$$

where $A_v(h)$ is the value of the eddy viscosity at the bottom.

Formulation of the Galerkin statement requires the substitution of the series expressions for u and v into the equations of motion and calculating the weighted residual integrals. A detailed derivation of these integrals is given by Nelson (1979), and only a short review will be included here. The Galerkin statement is given by the expansion of Equations B.4, however, since Equations B.4a and B.4b are so similar, only the first will be treated here. For each term in the expansion function (that is, for $i=1,2,3,\dots,n$) a Galerkin expansion is completed:

$$\int_0^h R_{x_i} \Omega_i dz = \langle R_{x_i}, \Omega_i \rangle = 0$$

where the notation $\langle A, B \rangle = \int_0^h AB dz$ has been introduced to simplify the equations. Substituting for R :

$$\begin{aligned} & \langle \left(\frac{\partial \hat{u}}{\partial t} - \frac{\partial}{\partial z} \left(A_v \frac{\partial \hat{u}}{\partial z} \right) - f \hat{v} + g \frac{\partial \eta}{\partial x} \right), \Omega_i \rangle = \\ & = \frac{\partial}{\partial t} \langle \hat{u}, \Omega_i \rangle - \left\langle \frac{\partial A_v}{\partial z} \frac{\partial \hat{u}}{\partial z}, \Omega_i \right\rangle - \left\langle A_v \frac{\partial^2 \hat{u}}{\partial z^2}, \Omega_i \right\rangle \\ & - \langle f \hat{v}, \Omega_i \rangle - g \frac{\partial \eta}{\partial x} \langle 1, \Omega_i \rangle = 0 \end{aligned} \quad (\text{B.10})$$

Owing to the orthogonality of the expansion function, each integral above will reduce to but a few terms. For example, since $\langle \Omega_i, \Omega_j \rangle = 0$,

$$\langle \hat{u}, \Omega_i \rangle = \langle u_0, \Omega_i \rangle + c_i \langle \Omega_i, \Omega_i \rangle$$

Generally, the integrals are solved analytically as far as possible, with numerical integration employed for those few which evade solution. The resulting final expressions have the form:

$$\frac{\partial c_i}{\partial t} = D_i + E_i d_i + \sum_{j=1}^n F_{ij} c_j$$

or, in matrix notation:

$$\frac{\partial \underline{c}}{\partial t} = \underline{D} + \underline{E} \underline{d} + \underline{F} \underline{c} \tag{B.11a}$$

where a single underbar denotes a vector and a double bar denotes a matrix. The vector \underline{D} includes the dependencies on wind shear and water surface slope, \underline{E} contains the Coriolis influence, and \underline{F} arises from the vertical viscosity term. The final expression for the d_i is entirely analogous:

$$\frac{\partial \underline{d}}{\partial t} = \underline{G} + \underline{H} \underline{c} + \underline{I} \underline{d} \tag{B.11b}$$

The vectors \underline{c} and \underline{d} contain the n expansion coefficients for each grid location and thus are functions of x , y and t . Similarly, the coefficient matrices, \underline{D} , \underline{E} , \underline{F} , \underline{G} , \underline{H} and \underline{I} , vary in space and time according to the variation of the lake's geometry and properties and the forces upon the lake.

The continuity equation (7.4), since it depends upon vertically integrated mass transports, does not require a Galerkin solution. However, it must be recast in a form compatible with the representations of \hat{u} and \hat{v} . Repeating

Equation 7.4,

$$\frac{\partial U}{\partial x} + \frac{\partial V}{\partial y} = \frac{\partial \eta}{\partial t} \quad (7.4)$$

it can be seen that U and V must be determined from u and v.
From the definition of U:

$$\begin{aligned} U &= \int_0^h \hat{u} dz = \langle 1, \hat{u} \rangle \\ &= \langle 1, u_0 \rangle + \sum_{i=1}^n c_i \langle 1, \Omega_i \rangle \\ &= J_x + \sum_{i=1}^n k_i c_i \end{aligned} \quad (B.12a)$$

Similarly,

$$V = J_y + \sum_{i=1}^n k_i d_i \quad (B.12b)$$

After substitution into the Equation 7.4, and changing to vector notation,

$$\frac{\partial}{\partial x} (\underline{k} \underline{c}) + \frac{\partial}{\partial y} (\underline{k} \underline{d}) = \frac{\partial \eta}{\partial t} - \frac{\partial J_x}{\partial x} - \frac{\partial J_y}{\partial y}$$

or, more concisely,

$$\frac{\partial}{\partial x} (\underline{k} \underline{c}) + \frac{\partial}{\partial y} (\underline{k} \underline{d}) = P \quad (B.13)$$

where c, d, K and P vary in time and horizontal space.

B.3 Solution of the Equations

B.3.1 Finite Difference Solution

The circulation model must solve the two momentum equations,

$$\frac{\partial \underline{c}}{\partial t} = \underline{E} + \underline{F} \underline{d} + \underline{G} \underline{c}$$

$$\frac{\partial \underline{d}}{\partial t} = \underline{H} + \underline{I} \underline{c} + \underline{J} \underline{d}$$

and the continuity equation,

$$\frac{\partial}{\partial x} (\underline{k} \underline{c}) + \frac{\partial}{\partial y} (\underline{k} \underline{d}) = P$$

as functions of time and horizontal space. This is accomplished in Nelson's model using an explicit finite difference scheme, alternately solving the momentum equations and the continuity equation.

Application of the finite difference scheme requires the division of the lake into a grid of discrete rectangular areas. A square grid, or more precisely, two square grids is used in Nelson's model. The two grids arise from the use of a staggered grid scheme on which velocity components are determined on the grid mid-sides, while water surface displacements are found at the grid center points. (See Figure 7.2.)

An explicit solution technique is employed by Nelson, first solving the momentum equations for the current velocities at full time steps, then using those velocities in the continuity equation to solve for the water surface elevation at half time steps. From the surface elevations, surface slopes can be determined for substitution into the momentum equation, which is solved at the next time step. This cycle is repeated until the simulation period is completed.

In solving the momentum equations, the solution proceeds along the rows from left to right, solving for all columns

in a row before moving up to the next row. The values of c and d_i are determined in turn by the expressions:

$$\begin{aligned}
 c_i(\ell, m, n+1) &= c_i(\ell, m, n) + \Delta t \{ E_{i1}(\ell, m, n) \eta_x(\ell, m, n + \frac{1}{2}) \\
 &+ E_{i2}(\ell, m, n) \tau^x(\ell, m, n) + F_i(\ell, m, n) d_i(\ell, m, n) \\
 &+ \sum_{j=1}^n G_{ij}(\ell, m, n) c_j(\ell, m, n) \} \quad \text{for } i = 1, 2, \dots, n \quad (\text{B.14a})
 \end{aligned}$$

$$\begin{aligned}
 d_i(\ell, m, n+1) &= d_i(\ell, m, n) + \Delta t \{ H_{i1}(\ell, m, n) \eta_y(\ell, m, n + \frac{1}{2}) \\
 &+ H_{i2}(\ell, m, n) \tau^y(\ell, m, n) + I_i(\ell, m, n) c_i(\ell, m, n) \\
 &+ \sum_{j=1}^n J_{ij}(\ell, m, n) d_j(\ell, m, n) \} \quad \text{for } i = 1, 2, \dots, n \quad (\text{B.14b})
 \end{aligned}$$

where the indexing notation uses ℓ as the x grid coordinate, m as the y grid coordinate and n as the time index. The E and H terms of Equations B.11 have been expanded here to show the dependence on wind shear stress in the x and y directions:

$$\tau^x \text{ and } \tau^y$$

and on the surface slope:

$$\eta_x = \frac{\partial n}{\partial x} \quad \text{and} \quad \eta_y = \frac{\partial n}{\partial y}$$

Nelson (1979) gives a detailed derivation of these

equations, including a definition of the coefficient terms, E_1 , E_2 , F , G , H_1 , H_2 , I and J .

B.3.2 Stability Criteria

The explicit solution scheme employed by Nelson is conditionally stable, requiring two criteria to be met in order to achieve a solution. The first criterion is the well-known Courant condition, which limits the solution time step to the time required for a surface gravity wave to traverse a grid square:

$$\Delta t < \frac{\Delta x}{\sqrt{gH}}$$

This limit arises since the model employs a free surface formulation, rather than the rigid lid approximation.

A second criterion is due to the time limit imposed by vertical diffusion. The criterion is similar to those specified for multi-layer models (for example, Sheng et al, 1978), but it is in a less straightforward form owing to the absence of a defined vertical grid spacing, Δz , in the Galerkin method. The criterion is:

$$\Delta t < \frac{2}{[a_j^2 \frac{A_v}{h^2}]_{\max}}$$

The exact magnitude stated was determined by Cooper and Pearce (1978) by trial and error.

The criterion to be used in any particular application is the smaller of these two. In very shallow lakes, the vertical diffusion time was found to be severely restrictive.

B.3.3 Modification of the Solution Procedure

A major change in the model solution technique was dictated by the severe restriction on time step size imposed by the diffusion time limit in shallow water. Depths as small as one meter in the application lake imposed time limits on the order of a few seconds. Practical simulation would be prohibitively expensive with this restriction, so a means to circumvent the diffusion time limit was necessary.

A change in the solution scheme from completely explicit to one which was implicit in the vertical (but still explicit in the horizontal) was made to remove the restrictive time limit. The alterations, which do not eliminate the Courant condition, affect the solution for the c_i and d_i coefficients at each grid square.

Returning to the matrix notation of Equation B.11a:

$$\frac{\partial \underline{c}}{\partial t} = \underline{D} + \underline{E} \underline{d} + \underline{F} \underline{c}$$

the explicit solution scheme of Nelson can be shown as:

$$\frac{\underline{c}^{t+\Delta t} - \underline{c}^t}{\Delta t} = \underline{D}^t + \underline{E}^t \underline{d}^t + \underline{F}^t \underline{c}^t \quad (\text{B.15})$$

where the superscript indicates the time at which a variable is determined. Since $\underline{c}^{t+\Delta t}$ appears only on the left of this equation, it is possible to solve for each individual c_i explicitly. For an implicit solution, the following finite difference representation is substituted:

$$\frac{\underline{c}^{t+\Delta t} - \underline{c}^t}{\Delta t} = \underline{D}^t + \underline{E}^t \underline{d}^t + \underline{F}^t \frac{1}{2} (\underline{c}^t + \underline{c}^{t+\Delta t}) \quad (\text{B.16})$$

This equation must be solved implicitly, that is, simultaneously for all c_i . The implicit equation has the general form:

$$\underline{A} \underline{c}^{t+\Delta t} = \underline{B} \underline{c}^t + \underline{C} \quad (\text{B.17})$$

Fortunately, as long as the vertical eddy viscosity does not change with time, the A matrix remains the same and requires inversion only at the simulation start. A, B and C must be determined for each grid square, and B and C must be recomputed each time step. This change in the solution technique eliminates the diffusion time condition as a limit on the computation, leaving the many times larger Courant condition as the sole stability limit.

REFERENCES

Abbott, M.B., "Computational Hydraulics: A Short Pathology," Journal of Hydraulic Research, 14:4, 271, 1976.

Abbott, M.B. and C.H. Rasmussen, "On the Numerical Modeling of Rapid Expansions and Contractions that are Two-Dimensional in Flow," Hydraulic Engineering for Improved Water Management, 17th Congress, International Association for Hydraulic Research, Baden-Baden, Germany, August, 1977.

Babajimopoulos, C. and K.W. Bedford, "Formulating Lake Models which Preserve Spectral Statistics," ASCE, Journal of the Hydraulics Division, 106:HY1, 1, January 1980.

Banks, R.B., "Some Features of Wind Action on Shallow Lakes," ASCE, Journal of the Environmental Engineering Division, 101:EE5, 813, October 1975.

Bedford, K.W. and I.S. Rai, "Efficient Pressure Solutions for Circulation Prediction," ASCE, Journal of the Hydraulics Division, 104: HY6, 899, June 1978.

Bengtsson, L., "Mathematical Models of Wind Induced Circulation in a Lake," Hydrology of Lakes Symposium, IAHS-AISH Publication 109, Helsinki, 1973.

Bhomik, N.G. and J.B. Stall, "Circulation Patterns in the Fox Chain of Lakes in Illinois," Water Resources Research, 14:4, 633, August 1978.

Bonham-Carter, G. and J.H. Thomas, "Numerical Calculation of Steady Wind-Driven Currents in Lake Ontario and Rochester Embayment," Proceedings of the 16th Conference on Great Lakes Research, 640, 1973.

Brown, R.T., "Effects of Data Variability and Model Structure on Reservoir Ecosystem Simulation," PhD Thesis, Department of Civil Engineering, Massachusetts Institute of Technology, Cambridge, Massachusetts, April 3, 1978.

Bryan, K., "A Numerical Method for the Circulation of the World Ocean," Journal of Computational Physics, 4:3, 347, October 1969.

Bye, J.A.T., "Wind-Driven Circulation in Unstratified Lakes," Limnology and Oceanography, 10, 451, 1975.

Cheng, R.T., T.M. Powell and T.M. Dillon, "Numerical Models of Wind-Driven Circulation in Lakes," Applied Mathematical Modeling, 1, 141, December 1976.

Cheng, R.T. and C. Tung, "Wind Driven Circulation by the Finite Element Method," Proceedings of the 13th Conference on Great Lakes Research, 891, 1970.

Cooper, C.K. and B.R. Pearce, "A Three-Dimensional Model to Calculate Currents in Coastal Waters Utilizing a Depth Varying Vertical Eddy Viscosity," Report Number 226, Ralph M. Parsons Laboratory for Water Resources and Hydrodynamics, Department of Civil Engineering, Massachusetts Institute of Technology, Cambridge, Massachusetts, August 1977.

Csaki, P. and T. Kutas, "The BEM Modeling Approach II: Model Development in the Lake Balaton Ecosystem," Proceedings of the Second Joint MTA/IIASA Task Force Meeting on Lake Balaton Modeling, Held August 27-30, 1979, Veszprem, Hungary, 1980.

Dronkers, J.J., Tidal Computations in Rivers and Coastal Waters, John Wiley and Sons, New York, 1964.

Engelund, F., "Effect of Lateral Wind on Uniform Channel Flow," Progress Report 45, Institute of Hydrodynamic and Hydraulic Engineering, Technical University of Denmark, page 33, April 1978.

Entz, B., "Regional and Circadian Oxygen Determination in Lake Balaton Concerning the Eutrophication of the Lake," Annales Instituti Biologici (Tihany), 43, 69, 1976.

Fisher, I., "Representation of Hydrophysical and Ecological Processes in the Simulation of Water Quality of Shallow Lakes," Personal communication, The University of New England, Armidale, N.S.W., Australia, 1980.

Gallagher, R.H., J.A. Liggett and S.T.K. Chan, "Finite Element Shallow Lake Circulation," ASCE, Journal of the Hydraulics Division, 99:HY7, 1083, July, 1973.

Gedney, R.T. and W. Lick, "Wind-Driven Currents in Lake Erie," Journal of Geophysical Research, 77:15, 2714, May 20, 1972.

Hamblin, P. F. and J.R. Salmon, "On the Vertical Transfer of Momentum in a Lake," Memoires Societe Royale des Sciences de Liege, 6e serie, tome VII, 211, 1975.

Hamvas, F., "Investigations into the Erosion of Shore at Lake Balaton," Hydrology of Lakes and Reservoirs, Symposium of Garda, IAHS-AISH Publication No. 70, 473, October 1966.

Haq, A. and W. Lick, "On the Time-Dependent Flow in a Lake,"

Journal of Geophysical Research, 80:3, 431, January 20, 1975.

Harleman, D.R.F., "One-Dimensional Models," in Estuarine Modeling: An Assessment, edited by G.H. Ward and W.H. Espey, Report 16070 DZV 02/71, U.S. Environmental Protection Agency, February 1971.

Harleman, D.R.F. and P. Shanahan, "Aspects of Wind-Driven Circulation and Mixing in Eutrophication Studies of Lake Balaton," Proceedings of the Second Joint MTA/IIASA Task Force Meeting on Lake Balaton Modeling, held August 27-30, 1979, Veszprem, Hungary, 1980.

Hicks, B.B., R.L. Drinkrow, and G. Grauze, "Drag and Bulk Transfer Coefficients Associated with a Shallow Water Surface," Boundary Layer Meteorology, 6, 287, 1974.

Hollan, E. and T.J. Simons, "Wind-Induced Changes of Temperature and Currents in Lake Constance," Archiv für Meteorologie, Geophysik und Bioklimatologie, Series A, 27, 333, 1978.

Hsu, S.A., "Wind Stress on Nearshore and Lagoonal Waters of a Tropical Island," Limnology and Oceanography, 20:1, 113, January 1975.

Hutchinson, G.E., A Treatise on Limnology, Volume 1, Part 1 - Geography and Physics of Lakes, John Wiley and Sons, Inc., New York, 1975.

Kenney, B.C., "Lake Surface Fluctuations and the Mass Flow Through the Narrows of Lake Winnipeg," Journal of Geophysical Research, 84:C3, 1225, March 20, 1979.

Kizlauskas, A.G. and P.L. Katz, "A Two-Layer Finite-Difference Model for Flows in Thermally Stratified Lake Michigan," Proceedings of the 16th Conference on Great Lakes Research, 743, 1973.

Koutitas, C.G., "Numerical Solution of the Complete Equations for Nearly Horizontal Flows," Advances in Water Resources, 1:4, 213, 1978.

Lean, G.H. and T.J. Weare, "Modeling Two-Dimensional Circulating Flow," ASCE, Journal of the Hydraulics Division, 105:HY1, 17, January 1979.

Leenderste, J.J., "A Water-Quality Simulation Model for Well-Mixed Estuaries and Coastal Seas: Volume I, Principles of Computation," Memorandum RM-6230-RC, Rand Corporation, Santa Monica, California, February 1970.

Leonov, A. "Mathematical Modeling of Phosphorus

Transformation in Relation to Eutrophication of Lake Balaton," Proceedings of the Second Joint MTA/IIASA Task Force Meeting on Lake Balaton Modeling," held August 27-30, 1979, Veszprem, Hungary, 1980.

Lick, W., "Numerical Modeling of Lake Currents." Annual Review of Earth and Planetary Sciences, 4, 49, 1976.

Lien, S.L. and J.A. Hoopes, "Wind Driven, Steady Flows in Lake Superior," Limnology and Oceanography, 23:1, 91, January 1978.

Liggett, J.A., "Cell Method for Computing Lake Circulation," ASCE, Journal of the Hydraulics Division, 96:HY3, 725, March 1970.

Lindijer, G.J.H., "Three-Dimensional Circulation Models for Shallow Lakes and Seas; General Formulation and Stationary Models," Report R 900-I, Delft Hydraulics Laboratory, Netherlands, July 1976.

Lindijer, G.J.H., "Three-Dimensional Circulation Models for Shallow Lakes and Seas; Semi-Analytical Steady State Analysis of Wind-Driven Current Including the Effect of a Depth-Dependent Turbulent Exchange Coefficient," Report R 900-II, Delft Hydraulics Laboratory, Netherlands, March 1979.

Liu, H. and H.J. Perez, "Wind-Induced Circulation in Shallow Water," ASCE, Journal of the Hydraulics Division, 97:HY7, 923, July 1971.

Madsen, O.S., "A Realistic Model of the Wind-Induced Ekman Boundary Layer," Journal of Physical Oceanography, 7:2, 248, March 1977.

Murray, S.P., "Trajectories and Speeds of Wind-Driven Currents near the Coast," Journal of Physical Oceanography, 5, 347, April 1975.

Murty, T.S. and D.B. Rao, "Wind-Generated Circulations in Lakes Erie, Huron, Michigan and Superior," Proceedings of the 16th Conference on Great Lakes Research, 927, 1970.

Muszkalay, L., "La Mesure des Denivellations Longitudinales et Transversales de la Nappe D'Eau du Lac Balaton," ("Measurement of Longitudinal and Transverse Water Surface Denivellations in Lake Balaton" - in French), Hydrology of Lakes and Reservoirs, Symposium of Garda, Volume 1, IAHS-AISH Publication Number 70, 100, October 1966.

Muszkalay, L., "A Balaton Vizenek Jellemzo Mozgasai," ("Characteristic Water Motions in Lake Balaton" - in Hungarian), VITUKI (Research Center for Water Resources

Development), Budapest, Hungary, 1973.

Nelson, S.M., "Application of a Numerical Model for Three-Dimensional Sheared Flows," M.S. Thesis, Department of Civil Engineering, Massachusetts Institute of Technology, Cambridge, Massachusetts, September 1979.

Neumann, G. and W.J. Pierson, Principles of Physical Oceanography, Prentice-Hall Incorporated, Englewood Cliffs, New Jersey, 1966.

Ottesen-Hansen, N.-E., "Effect of Wind Stress on Stratified Deep Lake," ASCE, Journal of the Hydraulics Division, 101:HY8, 1037, August 1975.

Paskausky, D.F., "Winter Circulations in Lake Ontario," Proceedings of the 14th Conference on Great Lakes Research, 593, 1971.

Paul, J.F., W.L. Richardson, A.B. Gorstko, and A.A. Matveyev, "Results of a Joint U.S.A./U.S.S.R. Hydrodynamic and Transport Modeling Project," Report EPA-600/3-79-015, U.S. Environmental Protection Agency, February 1979.

Plate, E.J., "Water Surface Velocities Induced by Wind Shear," ASCE, Journal of the Engineering Mechanics Division, 96:EM3, 295, June 1970.

Platzman, G.W., "The Dynamical Prediction of Wind Tides on Lake Erie," Meteorological Monographs, 4:26, September 1963.

Ruggles, K.W., "The Vertical Mean Wind Profile Over the Ocean for Light to Moderate Winds," Journal of Applied Meteorology, 9:3, 389, June 1970.

Seki, H., M. Takahashi, Y. Hara and S. Ichimura, "Dynamics of Dissolved Oxygen During Algal Bloom in Lake Kasumigaura, Japan," Water Research, 14, 170, 1980.

Shemdin, O.H., "Modeling of Wind Induced Current," Journal of Hydraulic Research, 11:3, 281, 1973.

Sheng, Y.P., W. Lick, R.T. Gedney and F.B. Molls, "Numerical Computation of Three-Dimensional Circulation in Lake Erie: A Comparison of a Free-Surface Model and a Rigid-Lid Model," Journal of Physical Oceanography, 8:4, 713, July 1978.

Sibul, O., "Laboratory Study of Wind Tides in Shallow Water," Technical Memorandum No. 61, Beach Erosion Board, U.S. Army Corps of Engineers, August 1955.

Simons, T.J., "Development of Numerical Models of Lake Ontario," Proceedings of the 14th Conference on Great Lakes Research, 654, 1971.

Simons, T.J., "Development of Numerical Models of Lake Ontario: Part II," Proceedings of the 15th Conference on Great Lakes Research, 655, 1972.

Simons, T.J., "Hydrodynamic Models of Lakes and Shallow Seas," Unpublished Draft Report, Canada Centre for Inland Waters, Burlington, Ontario, Canada, February 1979.

Simons, T.J. and D.C.L. Lam, "Some Limitations of Water Quality Models for Large Lakes: A Case Study of Lake Ontario," Water Resources Research, 16:1, 105, February 1980.

Somlyody, L., "Hydrodynamical Aspects of the Eutrophication Modeling in the Case of Lake Balaton," Collaborative Paper CP-79-1, International Institute for Applied Systems Analysis, Laxenburg, Austria, February 1979.

Stolzenbach, K.D., O.S. Madsen, E.E. Adams, A.M. Pollack and C.K. Cooper, "A Review and Evaluation of Basic Techniques for Predicting the Behavior of Surface Oil Slicks," Report Number 222, Ralph M. Parsons Laboratory for Water Resources and Hydrodynamics, Massachusetts Institute of Technology, Cambridge, Massachusetts, February 1977.

Su, C.-L., J.H. Pohl and G. Shih, "Wind-Driven Circulations in Lake Okeechobee," Finite Elements in Water Resources, Proceedings of the First International Conference on Finite Elements in Water Resources held at Princeton University, edited by W.G. Gray, G.F. Pinder and C.A. Brebbia, Pentech Press, London, page 4.113, July 1976.

Sundermann, J. "Numerical Modeling of Circulation in Lakes," Hydrodynamics of Lakes, Proceedings of a Symposium 12-13 October, 1978, Lausanne, Switzerland, edited by W.H. Graf and C.H. Mortimer, Elsevier Scientific Publishing Company, New York, page 1, 1979.

Thomas, J.H., "A Theory of Steady Wind-Driven Current in Shallow Water with Variable Eddy Viscosity," Journal of Physical Oceanography, 5:1, 136, January 1975.

van Straten, G., "Analysis of Model and Parameter Uncertainty in Simple Phytoplankton Models of Lake Balaton," Second ISEM Meeting, Liege, Belgium, April 1980.

van Straten, G., G. Jolankai and S. Herodek, "Review and Evaluation of Research on the Eutrophication of Lake Balaton -- A Background Report for Modelling," Collaborative Paper CP-79-13, International Institute for Applied Systems Analysis, Laxenburg, Austria, August 1979.

van Straten, G. and L. Somlyody, "Lake Balaton

Eutrophication Study: Present Status and Future Program," Working Paper, International Institute for Applied Systems Analysis, Laxenburg, Austria, 1980.

Wilson, B.W., "Note on Surface Wind Stress over Water at Low and High Wind Speeds," Journal of Geophysical Research, 65:10, 3377, October 1960.

Witten, A.J. and J.H. Thomas, "Steady Wind-Driven Currents in a Large Lake with Depth-Dependent Eddy Viscosity," Journal of Physical Oceanography, 6:1, 85, January 1976.

Wu, J. "Wind Stress and Surface Roughness at Air-Sea Interface," Journal of Geophysical Research, 74:2, 444, January 15, 1969.